UNIVERSITÉ PARIS-SUD

ÉCOLE DOCTORALE : Science et Technologie de l'Information des Télécommunications et des Systèmes (STITS)
Laboratoire des Systèmes Communicants au CEA-List

DISCIPLINE *PHYSIQUE*

THÈSE DE DOCTORAT

soutenue le 10 Février 2014 par

Sinda SMIRANI

Étude du Codage Réseau au Niveau de la Couche Physique pour les Canaux Bidirectionnels à Relais

Directeur de thèse:	Pierre Duhamel	Directeur de recherche (LSS, Supélec)

Composition du Jury:

Rapporteurs	Didier LE RUYET	Président du jury, Professeur (CNAM)
	Deniz GUNDUZ	Assistant-Professor (Imperial College London)
Examinateurs	Jean-Claude BELFIORE	Professeur (Telecom ParisTech)
	Benoit GELLER	Professeur (ENSTA)
	Mohamed KAMOUN	Ingénieur de recherche (CEA-List)
	Raymond KNOPP	Enseignant-chercheur (EURECOM)
	Abdellatif ZAIDI	Maître de conférences (Univ. Marne la Valée)
Membre invité	Mireille SARKISS	Ingénieur de recherche (CEA-List)

PARIS-SUD UNIVERSITY

DOCTORAL SCHOOL : Science and Technologies of Information,
Telecommunications and Systems (STITS)
Communicating Systems Laboratory in CEA-List

DISCIPLINE *PHYSICS*

Ph.D. THESIS

defended on 10 February, 2014 by

Sinda SMIRANI

Physical-Layer Network Coding for Two-Way Relay Channels

Thesis Supervisor: Pierre Duhamel — Senior Researcher (LSS, Supélec)

Jury Members:

Referees	Didier LE RUYET	Jury president, Professor (CNAM)
	Deniz GUNDUZ	Assistant-Professor (Imperial College London)
Examiners	Jean-Claude BELFIORE	Professor (Telecom ParisTech)
	Benoit GELLER	Professor (ENSTA)
	Mohamed KAMOUN	Research Engineer (CEA-List)
	Raymond KNOPP	Professor (EURECOM)
	Abdellatif ZAIDI	Assistant-Professor(Univ. Marne la Valée)
Invited Member	Mireille SARKISS	Research Engineer (CEA-List)

to my parents who taught me to go ahead,
to my husband who gives me hope to move forward,
to my daughter who lights up my life..

Abstract

Network coding has emerged as an alternative technique to routing that enhances the throughput at the network layer. Recently, network coding has been applied at the physical layer to take advantage of the natural signal superposition that occurs in the radio link. In this context, the physical-layer network coding can be seen as an in-network processing strategy for which multiple forwarding schemes can be proposed. This thesis investigates a set of processing schemes tailored to the network coding at the physical layer with various compromises between performance and complexity.

We consider a two-way relay channel (TWRC), a typical communication system in cooperative networks, where two terminals communicate with each other via a relay node. This communication occurs during two transmission phases, namely a multiple-access phase and a broadcast phase. For TWRC scenario, we first analyze a decode-and-forward strategy with finite size alphabets. We calculate the end-to-end average error probabilities based on random coding error exponents. Then, we derive the achievable rate regions with respect to a maximal probability of error allowed at each terminal.

Next, we propose two low-complexity and practical schemes based on compress-and-forward relaying strategy. The first scheme employs nested lattice coding. The second is an improved version which enables higher data rates for the user experiencing the best channel conditions. We present an information-theoretic framework to reconstruct the achievable rate regions of both schemes by considering optimal time division between both transmission phases.

After the asymptotic regime analysis, we study single-layer lattice coding scheme with finite dimension lattices. We focus on the analog transmission problem where the distortion is optimized.

Finally, we investigate single-layer lattice coding scheme for parallel Gaussian two-way relay channel. We present two achievable rate regions based on whether the relay processes all the sub-channels jointly or separately.

Résumé

Le codage réseau est apparu comme une technique alternative au routage au niveau de la couche réseau permettant d'améliorer le débit et d'optimiser l'utilisation de la capacité du réseau. Récemment, le codage réseau a été appliqué au niveau de la couche physique des réseaux sans-fil pour profiter de la superposition naturelle des signaux effectuée par le lien radio. Le codage réseau peut être vue comme un traitement interne du réseau pour lequel différentes techniques de relayage peuvent être utilisées. Cette thèse étudie un ensemble de traitements ayant des compromis variés en terme de performance et complexité.

Nous considérons le canal bidirectionnel à relais [1], un modèle de canal de communication typique dans les réseaux coopératifs, où deux terminaux s'échangent mutuellement des messages par l'intermédiaire d'un relais. La communication se déroule en deux phases, une phase à accès multiple et une phase de broadcast. Pour ce scénario, nous analysons, dans une première partie, une stratégie de "decode-and-forward". Nous considérons, pour cette étude, des alphabets de taille finie et nous calculons les probabilités moyennes d'erreur de bout-en-bout en se basant sur la métrique d'exposant d'erreur du codage aléatoire [2]. Puis, nous dérivons les régions des débits atteignables par rapport à une probabilité d'erreur maximale tolérable au niveau de chaque nœud.

Dans une deuxième partie de la thèse, nous proposons deux schémas de codage réseau pratiques, avec complexité réduite, qui se basent sur la stratégie de relayage "compress-and-forward" (CF). Le premier schéma utilise un codage en réseau de points imbriqués (nested lattices). Le deuxième schéma est une version améliorée qui permet d'atteindre des débits de données supérieurs pour l'utilisateur qui a les meilleures conditions canal. Nous construisons les régions des débits atteignables par les deux schémas proposés tout en optimisant la répartition du temps alloué à chacune des deux phases de transmission.

Après l'étude du régime asymptotique, nous analysons le schéma de codage CF avec des réseaux de points de dimension finie. Nous nous concentrons sur le problème de la transmission analogique où la distorsion est optimisée. Enfin, nous étudions l'application d'un schéma de codage, basé sur la stratégie CF avec des réseaux de points imbriqués, pour le canal bidirectionnel à canaux parallèles.

[1] Two-Way Relay Channel

[2] Random Coding Error Exponent

Ainsi, nous présentons deux régions de débits atteignables selon la technique de traitement, conjoint ou séparé, des sous-canaux par le relais.

Acknowledgements

Here come, finally, the moment to write the acknowledgements. The part I dreamt writing for months. It is a pleasure to thank the many people that shared with me this unforgettable experience.

First, I would like to express my gratitude to my thesis director Prof. Pierre Duhamel for his clever presence during my Ph.D development. I have beneficed form the quality of his guidance, his continuous support of my Ph.D study and research, and for the choice of the scientific direction of the thesis.

I am deeply grateful to my advisor Mohamed Kamoun, for giving me first the opportunity to start this thesis in the Communicating Systems Laboratory in the French Atomic Energy Commission. I thank him for his enthusiasm, support and invaluable advices during the course of my Ph.D. I thank him for being always available.

My gratitude extends to my co-advisors Abdellatif Zaidi and Mireille Sarkiss for the last two years. The insightful remarks of Abdellatif and his wealth of knowledge in information theory and lattice coding made possible to go through the second and important part of this thesis. I thank Mireille for her motivation, moral support and encouragement. She was their with helping hand, when I definitely needed.

I would like to thank all my PhD commitee members: Professors Didier Le Ruyet, Jean-Claude Belfiore, Deniz Gunduz, Raymond Knopp and Benoit GELLER, for having kindly accepted to serve at my PhD defence. Special thanks go to my two thesis referees Prof. Deniz Gunduz and Prof. Didier Le Ruyet for their constructive comments and suggestions to improve the manuscript.

I also thank all the LSCiens, the past and current colleagues in LSC, with whom I spend three of my best years. I thank especially Christophe Janneteau, the lab manager, for offering to us all the facilities in the lab. I thank him for his great efforts lately that permitted for me to defence my PhD in the best conditions.

Words cannot express my gratitude to my parents, my brother and sister for their support and unconditional love throughout my life. I thank my parents for their constant encouragement. The insistence of my father on working towards the best one could hope for has been instrumental to what I have accomplished.

I thank my husband Foued for his presence, patience and encouragements. I thank him for having faith on me and motivating me to forge ahead. I dedicate this thesis to my baby Ecile, who come to this life in the last year of my PhD. We have surpassed together many difficult moments. I apologize for all the stress you have lived with me during your first year. I wish for you a life without stress, with lots of love and success.

Sinda Smirani

Contents

List of Figures **xiii**

List of Tables **xv**

Abbreviations **xvii**

1 Introduction **1**
1.1 Motivations 2
1.2 Thesis Outline 4

2 Physical-Layer Network Coding Schemes for Two-Way Relay Channel **7**
2.1 Introduction 7
2.2 System Model and Assumptions 10
2.3 Physical-Layer Network Coding based Relaying Schemes 13
2.3.1 Decode-and-Forward 14
2.3.1.1 Multiple Access Channel Capacity 14
2.3.1.2 Broadcast Channel with Side Information 15
2.3.1.3 End-to-End Achievable Rate Region 16
2.3.2 Amplify-and-Forward 17
2.3.3 Compress-and-Forward 19
2.3.4 Comparison between Relaying Strategies for TWRC 23
2.4 Conclusion 23

3 Finite Dimension Decode-and-Forward Scheme for Two-Way Relay Channel **25**
3.1 Random Error Exponent Motivation 26
3.2 End-to-End Error Probabilities for Discrete Memoryless Channel . . 28
3.3 End-to-End Error Probabilities for AWGN Channel 33
3.3.1 Gaussian Error Exponents 33
3.3.2 Rate Region Maximization 35
3.4 Numerical Results 36
3.4.1 Achievable Rate Regions for Fixed Transmit Power Allocation 36
3.4.2 Achievable Rate Regions with Transmit Power Optimization 39
3.5 Conclusion 40

4 Compress-and-Forward Schemes for Two-Way Relay Channel 45
4.1 Introduction . . . 46
4.2 Preliminaries on Lattice Coding . . . 48
4.3 Achievable Rate Region for TWRC . . . 50
4.3.1 Lattice-based Source Coding . . . 51
4.3.1.1 Encoding . . . 51
4.3.1.2 Decoding . . . 52
4.3.2 Rate Analysis . . . 52
4.3.3 Achievable Rate Region . . . 54
4.3.4 Analog Signal Transmission . . . 55
4.4 Improved Achievable Rate Region for TWRC . . . 57
4.4.1 Doubly Nested Lattices for Source Coding . . . 58
4.4.1.1 Encoding . . . 59
4.4.1.2 Decoding . . . 61
4.4.2 Rate Analysis . . . 61
4.4.3 Achievable Rate Region . . . 64
4.4.4 Analog Signal Transmission . . . 65
4.5 Numerical Results . . . 66
4.6 Conclusion . . . 74

5 Finite Dimension Compress-and-Forward Scheme for Two-Way Relay Channel 75
5.1 Introduction . . . 75
5.2 Achievable Rate Region for TWRC . . . 76
5.3 Proof of Theorem 5.1 . . . 77
5.3.1 Lattice-based Source Coding . . . 77
5.3.1.1 Encoding . . . 78
5.3.1.2 Decoding . . . 79
5.3.2 Rate Analysis . . . 79
5.4 Numerical Implementation . . . 83
5.5 Conclusion . . . 88
5.6 Appendix : Proof of Proposition 5.2 . . . 89

6 Application: Compress-and-Forward Scheme for Parallel Gaussian Two-Way Relay Channel 91
6.1 Introduction . . . 92
6.2 System Model . . . 92
6.3 Achievable rate region for Joint Lattice Coding Scheme . . . 95
6.3.1 Lattice-based source coding . . . 96
6.3.1.1 Encoding . . . 96
6.3.1.2 Decoding . . . 97
6.3.2 Rate analysis . . . 97
6.3.3 Achievable rate region . . . 99
6.4 Achievable Rate Region for Separate Lattice Coding Scheme . . . 100
6.5 Numerical Results . . . 102

6.5.1 Optimization problem . . . 103
6.5.2 Simulations . . . 103
6.6 Conclusion . . . 105

7 Conclusion **107**
7.1 Thesis Summary . . . 107
7.2 Perspectives . . . 109

Bibliography **111**

Résumé des travaux de la thèse **120**

List of Figures

2.1 Two-Way relay Channel (TWRC) 8
2.2 Four-phase transmission with conventional routing in TWRC 8
2.3 Three-phase transmission with classical network coding in TWRC . 9
2.4 Two-phase transmission with PNC in TWRC 9
2.5 Two-phase transmission in TWRC: MAC and Broadcast phases . . 10

3.1 Achievable rate regions of DF and AF under average and peak transmit power for equal SNRs, $SNR_1 = SNR_2 = 10$dB 37
3.2 Illustrative example of the border rates dependence as function of the ray direction 38
3.3 Optimal α with DF strategy for $\theta \in [0, \pi/2]$ under average and peak transmit power for equal SNR=10dB 39
3.4 Maximum achievable rate regions for $P_{e,1}, P_{e,2} \leq 10^{-6}$, n = 500, $\text{SNR}_1 = 10$dB, $\text{SNR}_2 = \delta\ \text{SNR}_1$. 40
3.5 Optimal α for $P_{e,1}, P_{e,2} \leq 10^{-6}$, n = 500, SNR_1 =10dB, $\text{SNR}_2 = \delta$ SNR_1. 41
3.6 Achievable rate regions under fixed and optimized power allocations, SNR = 15dB, n= 500 42
3.7 Power allocation for symmetric static channels, SNR = 15dB, n= 500 43

4.1 Lattice encoding at the relay and decoding at terminals T_i, $i = 1, 2$ 51
4.2 Layered Lattice encoding at the relay 60
4.3 Lattice source decoding at the Terminal T_1 61
4.4 Achievable rate regions and the outer bound capacity of the Gaussian TWRC. In the left, T_1 has the best transmit power and the worst channel, in the right, T_2 has the best transmit power and the worst channel. 68
4.5 Equal rates $R_{12} = R_{21}$ for symmetric channels: $\text{SNR} = \text{SNR}_{1R} = \text{SNR}_{R1} = \text{SNR}_{2R} = \text{SNR}_{R2}$. LCF1 outperforms AF and DF for SNR > 11 dB 69
4.6 Achievable rate regions of LCF1 and LCF2. LCF2 achieves greater end-to-end rates at T_1 71
4.7 Achievable rate regions of DF, AF, LCF1 and LCF2 in different channel and power settings 72
4.7 Achievable rate regions of DF, AF, LCF1 and LCF2 in different channel and power settings (cont.) 73

5.1 Lattice coding scheme for TWRC 84
5.2 Achievable rate region of different finite dimension lattice pairs compared to the high dimension achievable region for $SNR_1 = SNR_2 = SNR_r = 10$ dB. A difference of 0.15 bit/dimension between infinite and finite dimension lattices 87
5.3 Achievable rate region of different finite dimension lattice pairs compared to the high dimension achievable region for $P_1 = 8$ dB, $P_2 = 5$ dB, $P_r = 10$ dB, $|h_1| = 2$ and $|h_2| = 1$ 87

6.1 Multiple access phase of parallel Gaussian TWRC 93
6.2 Broadcast phase of parallel Gaussian TWRC 93
6.3 Achievable rate regions of Joint-LCF and Separate-LCF for equal powers, P = 10 dB 104
6.4 Achievable rate regions of Joint-LCF and Separate-LCF rates for $P_1 = 15$ dB, $P_2 = 5$ dB and $P_R = 10$ dB 104

7.1 Canal bidirectionnel à relais 121
7.2 Régions de débits atteignables maximums pour $P_{e,1}, P_{e,2} \leq 10^{-6}$, n = 500, $RSB_1 = 10$dB, $RSB_2 = \delta$ RSB_1. 127
7.3 Région de débits atteignables maximums pour une allocation de puissance fixe et optimisée, RSB = 15 dB, n= 500. 128
7.4 Régions de débits atteignables de DF, AF, LCF1 et LCF2 pour $P_1 = 20$ dB, $P_2 = 18$ dB, $P_R = 17$ dB, $|h_1|^2 = 4$, $|h_2|^2 = 0.5$ 131
7.5 Régions des débits atteignables pour Joint-LCF and Separate-LCF pour des puissances é gales, $P_1 = P_2 = P_R = 10$ dB 136

List of Tables

5.1 Some important binary lattices and their useful properties 86

Abbreviations

AF	Amplify-and-Forward
ANC	Analog Network Coding
AWGN	Additive White Gaussian Noise
BC	Broadcast channel
BCSI	Broadcast Channel with Side Information
CF	Compress-and-Forward
CSI	Channel State Information
DF	Decode-and-Forward
DNF	Denoise-and-Forward
i.i.d	independent identically distributed
LCF	Lattice based Compress-and-Forward
LSD	Lattice Source Decoder
LSE	Lattice Source Encoder
MAC	Multiple Access Channel
NC	Network Coding
NSM	Normalized Second Moment
OFDM	Orthogonal Frequency-Division Multiplexing
OFDMA	Orthogonal Frequency-Division Multiple Access
TWRC	Two-Way Relay Channel
pDF	partial Decode-and-Forward
PNC	Physical Layer Network coding
RV	Random Variable
SC-FDMA	Single-Carrier Frequency-Division Multiple Access
SNR	Signal-to-Noise Ratio

TD	Time Division
TDMA	Time-Division Multiple-Access
VNR	Volume-to-Noise Ratio
WZ	Wyner-Ziv
XOR	Exclusive OR

Chapter 1

Introduction

Wireless communication has evolved from a niche technology in the 90's into an indispensable part of life. In 2013, there are almost as many cell phone subscribers as people in the world [31]. This spectacular growth is still occurring with many new wireless applications that are emerging over the years. The increasing demand of users for high-speed wireless data services become the major driver for the research in the wireless industry. These services include mobile Internet with video applications, interactive gaming, file sharing, shipping high definition multimedia to entertainment devices in homes, to name few. These growing demands pose a challenge as the available spectrum is limited and the future systems will turn to higher frequencies than those used nowadays. At higher frequencies, wireless communication will become subject to more radio propagation impairments especially multipath and attenuation. These effects contribute to the difficulty of establishing reliable information transmissions and of providing satisfactory services for the users anywhere, at any time.

Diversity techniques play an important role in combating transmission failures caused by fading and interference. With the increasing size of communication networks, cooperative diversity, established by implementing a multi-hop communication, can increase data rates and improve reliability. Due to the broadcast nature of the wireless channel, the transmitted message from a node is received not only by its intended receiver, but also by other neighbouring nodes. Those

nodes can act as relays and forward their received signals over independent paths to their intended users. In this manner, they introduce spatial diversity gains and help the end-to-end transmissions.

Relaying strategies are promising technological advancements for future wireless networks. These systems can take advantage of ad-hoc deployments which exploit cooperative communications. Without substantial infrastructure, the nodes in ad-hoc networks communicate with each other using peer-to-peer links. In such systems, end-to-end information delivery is performed by conventional routing schemes where the router nodes store and forward their received data. Recently, network coding has been proposed as a promising technique to replace the conventional routing in these networks. It allows a relay to process its received data from multiple sources and generate new packets containing data for other nodes. When applied to the physical layer, network coding can leverage the broadcast properties of the wireless channel to allow a more efficient use of the wireless spectrum.

The basic model to study network coding in wireless communication is the two-way relay channel (TWRC) where two nodes exchange data via a relay. It is encountered in various wireless scenarios like ad-hoc and cellular networks. Recently, this model has became a high priority research topic in multi-user information theory, and many studies have been interested in characterizing its capacity.

1.1 Motivations

This thesis deals with the problem of communicating over TWRC. For this problem, various network coding strategies have been studied in the literature. In some strategies, the relay decodes the message of each user separately and then computes a function of the two concurrently transmitted messages. In others, the relay computes a function of the two messages directly from the channel output without intermediate decoding. We call these strategies physical-layer network coding (PNC) techniques when the network coding is applied to the physical layer. PNC schemes take advantage of the superposition property of the radio link that is con-

sidered usually as an interference nuisance to the system. These schemes rely on two phases, namely a multiple Access (MAC) phase and a Broadcast (BC) phase. In the first time slot, the communicating nodes simultaneously send their messages to the relay. Then, the relay broadcasts a message that has been computed from the mixture of signals sent by both nodes. This PNC technique offers a significant spectral efficiency improvement compared to classical network coding applied at the network layer.

Several PNC schemes have been proposed for TWRC. Some of them have high complexity but advantageous performance while others sacrifice performance for low complexity. The main contribution of this work is to provide PNC schemes that present a tunable trade-off between performance and complexity.

The principal performance metric analyzed throughout this work is the achievable rate region. This metric permits to establish the rate limits of a coding scheme. These limits are useful to benchmark practical schemes and to assess the gap with respect to the best achievable performance. In addition, the capacity of TWRC is unknown in general. Thus, the principal performance difference between the coding schemes for this channel is the set of rate pairs that can be achieved in specific conditions. In particular, the coding scheme that approaches the outer bound capacity has the best performance. Random coding tools has been extensively used to determine the achievable rates. However, these codes are impractical for real systems. This has motivated us to focus on structured codes which are close to realistic implementations. Furthermore, the studies on the achievable rate region are valid for high dimension assumptions in order to ensure a vanishing error probability. Such assumption can not be realized in practice. That's why, we provide analyses of the end-to-end transmission rates when finite dimensions are assumed. These analyses can be used for the design of a practical system.

1.2 Thesis Outline

In this thesis work, we propose PNC schemes for TWRC where the end-to-end transmission takes two time slots. We consider time division optimization between both phases, i.e MAC and BC. This can only enlarge the derived achievable rate regions.

In Chapter 2, we define our system model and the basic assumptions considered in this thesis. Then, we present a brief overview of the PNC schemes proposed for TWRC in the literature. We detail, in particular, the coding schemes based on cooperative relaying strategies, basically Decode-and-Forward (DF), Amplify-and-Forward (AF) and Compress-and-Forward (CF). We review their achievable rate regions for discrete and Gaussian memoryless channels. For CF based scheme, we provide a new derivation of the achievable rates for Gaussian channel using results from rate-distortion theory and Wyner-Ziv coding [85]. Finally, we present a brief comparison between the achievable rates of the presented relaying schemes. This comparison will be illustrated in Chapter 4. The results presented in Chapter 2 will be used as a baseline for performance comparison with new proposed schemes in the next chapters of this document.

In Chapter 3, we consider DF relaying strategy at the relay. The study of achievable rate regions presented in Chapter 2 gives only the transmission rates that can be achieved using large codewords length. In this case, it is assumed that the sources have unlimited data to send in order to meet arbitrarily small error probability. However, the error probability cannot be avoided when a finite block length is used. A traditional approach to assess the reliability-rate trade-off in a point-to-point scenarios consists in deriving error exponent metric [22]. In this chapter, we consider the extension of this concept to TWRC by investigating the end-to-end error probabilities at each terminal as a function of the codewords' length and by considering DF strategy at the relay. Then, we derive a DF rate region by taking into account finite-length codewords and average error probability constraints. Through simulations, we present both the asymptotic rate region and finite block length rate regions when fixed and optimal allocations are considered.

In Chapter 4, we consider CF relaying strategy at the relay. We derive two achievable rate regions for TWRC where the proposed PNC schemes are based on lattice coding. The relay considers its received signal from both terminals as a source to be compressed. Thus, it uses a Wyner-Ziv encoding by taking into account that each terminal has a partial knowledge of this source, called side information, which is its own signal that has been transmitted during the first phase. First, we develop a coding scheme in which the relay broadcasts the same signal to both terminals. We show that this scheme offers the same performance as random coding based CF protocol. Then, we propose, and analyze the performance of, an improved coding scheme in which the relay sends not only a common description of its output, but also an individual description that is destined to be recovered only by the user who experiences better channel conditions and transmit power. Through simulations, we show that the new scheme provides substantial gains in rates. It also outperforms AF strategy for all SNR values, and DF strategy for certain SNR regimes.

While high dimension lattices have been used in the previous chapter to guarantee an error free decoding, in Chapter 5, we are interested in finite dimension lattices. In this case, the decoding error probability cannot be arbitrarily small. Based on this observation, we investigate the proposed CF lattice coding scheme with finite dimension lattices. In particular, we focus, in this work, on the analog transmission problem where the distortion at the receiving terminals is optimized. In fact, by carefully choosing source coding factors, the results match with the optimum forward test channel with minimum distortion. We characterize the transmission rate regions allowed by our coding scheme under non vanishing yet constrained decoding error probabilities. Then, we discuss its design criteria using practical finite dimension lattices. Finally, we illustrate our results with some numerical examples.

In Chapter 6, we investigate our CF lattice coding scheme in practical modern communication scenarios such as multi-carrier systems, multi-stream transmission with multiple antennas, spread spectrum with multiple sequences. In this case, the channel can be modeled by a parallel Gaussian channel. For these systems,

two-way relaying offers a competitive solution for range extension. In this chapter, we consider a parallel Gaussian TWRC where two communicating terminals exchange their messages over independent parallel Gaussian channels. The relay jointly processes all the sub-channels together. We characterize the rate region allowed by this coding scheme. We compare it to a "separate processing approach" that is the direct extension of the CF lattice coding scheme where the same strategy is repeated for each sub-channel. Finally, we assess through simulations the performance penalty of the separate processing compared to the joint processing approach.

In Chapter 7, we conclude this thesis and present some possible future research directions.

Chapter 2

Physical-Layer Network Coding Schemes for Two-Way Relay Channel

2.1 Introduction

Network coding has been proposed as a promising technique at the network layer to improve the network capacity [2, 18]. In fact, unlike conventional routing approaches, where the relay stores the received information and forwards it to its neighbour nodes, network coding allows the relay to process incoming data from multiple sources. In this way, the amount of information transmitted through the network can be reduced and hence the network throughput can be increased. For instance, for multicast problems in lossless wired networks, it has been shown that the max-flow min-cut upper bound can be achieved with network coding while it is not possible with traditional store-and-forward techniques [2].

The application of network coding to wireless networks was first considered in [49, 84, 83, 10]. In these contributions, the interest of network coding for unicast and multicast traffic in mobile ad-hoc networks has been proven. Since then, various works have been interested in employing network coding in wireless protocols

to improve their throughput or reliability [82, 35, 34, 4]. The authors in [82] considered information exchange in wireless networks. In this paper, multi-hop wireless routing is considered where the traffic between the two end-nodes is bidirectional. Whenever a transmission opportunity arises, a relay router combines two packets, one for each direction, with a simple exclusive-OR (XOR) operation and broadcasts it to its neighbours. Both receiving routers already know one of the packets, they can decode the new packet. Hence, each broadcast opportunity allows two routers to receive a new packet, effectively doubling the capacity of the path. The authors show that network coding along with the physical layer broadcast property offered by the wireless medium, improve the resources utilization.

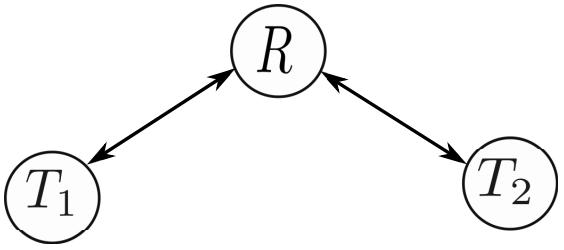

Figure 2.1: Two-Way relay Channel (TWRC)

The basic network setting that illustrates the significant advantage of network coding over conventional routing is the two-way relay channel (TWRC) presented in Fig.2.1. In half-duplex scenarios where the nodes cannot transmit and receive in the same time, the conventional routing scheme requires four transmission time slots as illustrated in in Fig. 2.2. In classical network coding, each user transmits

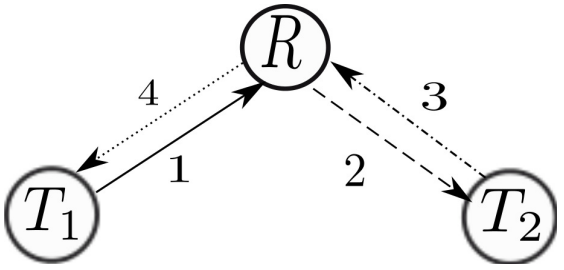

Figure 2.2: Four-phase transmission with conventional routing in TWRC

data to the relay in a time-division multiple-access (TDMA) manner. The relay then computes the XOR of the two incoming packets from the two user nodes before forwarding the resulting message during the third time slot (c.f. Fig. 2.3).

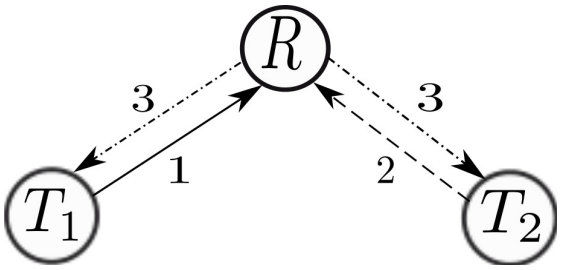

FIGURE 2.3: Three-phase transmission with classical network coding in TWRC

Recently, there have been many efforts to further improve the spectral efficiency in the TWRC. In [92], physical-layer network coding (PNC) was proposed where network coding is performed on the baseband signals at the physical layer. In particular, with PNC, both users transmit at the same time slot. The relay decodes directly from the received signal the XOR of the transmitted packets and broadcasts the result of this operation during the second time slot. Compared to conventional routing and classical network coding, PNC offers a significant spectral efficiency improvement since it requires only two transmission times as depicted in Fig. 2.4. More generally, while network coding combines raw bits or packets

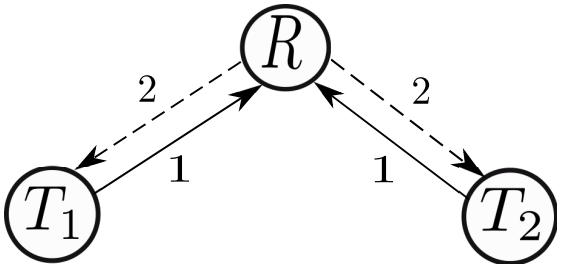

FIGURE 2.4: Two-phase transmission with PNC in TWRC

at the network layer, physical-layer network coding strategies combine symbols at the physical layer to produce new symbols. Several types of relaying strategies can be applied in the same network setting and require all two transmission times. We can distinguish three known cooperative protocols: AF, DF and CF. Throughout this thesis, we call a PNC strategy any coding technique applied to TWRC where the overall communication occurs during two phases, namely a multiple Access (MAC) phase and a Broadcast (BC) phase.

The remainder of this chapter is organized as follows. In Section 2.2, we introduce our system model and the principle assumptions considered in this thesis. In

Section 2.3, we present the coding strategies of the basic relaying strategies for TWRC, namely DF, AF and CF and we present an overview of their achievable rate regions. We give also a brief comparison between the protocols.

Notations: Throughout this document, random variables (r.v.) are indicated by capital letters while the realizations are written in lowercase letters. Vector of r.v. or a sequence of realizations are indicated by bold fonts.

2.2 System Model and Assumptions

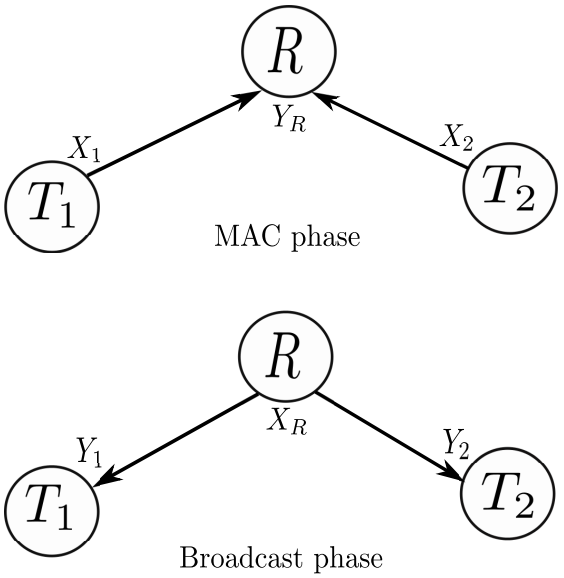

Figure 2.5: Two-phase transmission in TWRC: MAC and Broadcast phases

Consider the communication system described in Fig. 2.5 in which two source nodes, T_1 and T_2, exchange two individual messages m_1 and m_2, with the help of a relay R. For this model, we have the following assumptions:

a.1 There is no direct link between T_1 and T_2.

a.2 The relay and the source nodes operate in half-duplex mode which means that a node cannot transmit and receive at the same time using the same frequency.

a.3 The bidirectional communication takes n channel uses that are split into two orthogonal phases: MAC phase and BC phase, with lengths $n_1 = \alpha n$ and $n_2 = (1-\alpha)n$, $\alpha \in [0,1]$ respectively.

The protocol starts with the multiple access phase where terminal T_i, $i \in \{1,2\}$, draws uniformly a message m_i from the set $\mathcal{M}_1 = \{1, 2, \cdots, 2^{nR_{i\bar{i}}}\}$ and sends it to the other terminal $\mathrm{T}_{\bar{i}}$ where $R_{i\bar{i}}$ denotes the message rate of node T_i destined to $\mathrm{T}_{\bar{i}}$. $\bar{i}$ refers to the other terminal index. Let $\mathbf{x}_i(m_i) \in \mathbb{R}^{n_1}$ be the channel codeword of length n_1 sent by node T_i and P_i be the transmit power constraint of T_i. $\mathbf{x}_i(m_i)$ is sent according to the following assumptions:

a.4 $$\frac{1}{n_1}\sum_{k=1}^{n_1}|x_{i,k}|^2 \leq P_i;$$

The messages are transmitted through a memoryless Gaussian channel and the relay R receives a signal $\mathbf{y}_R \in \mathbb{R}^{n_1}$.

During the BC phase, the relay generates a message m_R which is a function of the received messages depending on the PNC scheme that is employed. Then, m_R will be mapped to an n_2-dimensional codeword $\mathbf{x}_R(m_R) \in \mathbb{R}^{n_2}$. The average power constraint at the relay P_R verifies

a.5 $$\frac{1}{n_2}\sum_{k=1}^{n_2}|x_{R,k}|^2 \leq P_R;$$

The signal $\mathbf{x}_R$ is transmitted through a broadcast memoryless channel and the received signal at node T_i is $\mathbf{y}_i \in \mathbb{R}^{n_2}$, $i \in \{1,2\}$. Since each terminal already knows a part of the received message, sent during the MAC phase, it will use this side information to decode the unknown message.

In this thesis, there is no cooperation between the two phases. This means that no feedback is used for cooperation between the encoders. From Shannon's two-way channel [68], this is known as the restricted two-way channel. The following assumptions are further considered:

a.6 A block flat fading channel is assumed. Let h_1, the channel gain between terminal T_1 and the relay R and h_2, the channel gain between terminal T_2 and the relay R. Channel reciprocity between both transmission' phases (MAC and BC) is assumed i.e. $h_{i\to R} = h_{R\to i} = h_i$, $i \in \{1, 2\}$. Perfect channel state information (CSI) is available to all nodes.

a.7 Let $\mathbf{Z}_i$,$i \in \{1, 2, R\}$, the noise random vectors where the components are i.i.d additive white Gaussian noise (AWGN) at each receiver with variance σ_i^2 i.e. $\sim \mathcal{N}(0, \sigma_i^2)$ for $i \in \{1, 2, R\}$. We assume that the noise components are independent from the channel inputs.

Since both channels are memoryless, the received signal at the relay can be written as:

$$\mathbf{y}_R = h_1\mathbf{x}_1 + h_2\mathbf{x}_2 + \mathbf{z}_R \tag{2.1}$$

and the received signal at terminals T_1 and T_2 are

$$\mathbf{y}_i = h_i\mathbf{x}_R + \mathbf{z}_i \ , \ i \in \{1, 2\}. \tag{2.2}$$

We define the signal-to-noise ratio (SNR) for the link $i \to R$ as $SNR_{iR} := \dfrac{|h_i|^2 P_i}{\sigma_R^2}$, $i \in \{1, 2\}$ and the SNR for the link $R \to i$ as $SNR_{Ri} := \dfrac{|h_i|^2 P_R}{\sigma_i^2}$, $i \in \{1, 2\}$.

Let $(\lceil 2^{nR_{12}} \rceil, \lceil 2^{nR_{21}} \rceil, n)$ a code for the TWRC that consists of both sets $\mathcal{M}_1$ and $\mathcal{M}_2$ and the set of the following coding functions:

- Encoding functions $f_{i,j}, j \in [1, n_1]$ and $f_{R,k}, k \in [1, n_2]$ at the both terminals and the relay respectively:

$$\begin{aligned} f_{i,j}: \quad & \mathcal{M}_1 \to \mathbf{X}_i \\ & m_i \longmapsto\to x_{i,j}(m_i) \end{aligned}$$

$$\begin{aligned} f_{R,k}: \quad & \mathcal{M}_R \to \mathcal{X}_R \\ & m_R \longmapsto x_{R,k}(m_R) \end{aligned}$$

- Decoding functions $g_{i,k}, k \in [1, n_2]$ such that:

$$g_{i,k}: \quad (\mathcal{Y}_i, \mathcal{M}_i) \rightarrow \mathcal{M}_{\bar{i}}$$
$$(y_{R,k}, m_i) \longmapsto m_{\bar{i}}$$

  where $\bar{i}$ refers to the other terminal.

The individual error probabilities for this system are defined as follows:

$$P_{e,1} = Pr(g_1(m_1, y_R) \neq m_2)$$

$$P_{e,2} = Pr(g_2(m_2, y_R) \neq m_1)$$

Definition 2.1. For the aforementioned TWRC, a rate pair (R_{12}, R_{21}) is said to be achievable if there exists a sequence $(\lceil 2^{nR_{12}} \rceil, \lceil 2^{nR_{21}} \rceil, n)$ codes such that the decoding error probability at both terminals approaches zero for n sufficiently large $(n \rightarrow \infty)$.

2.3 Physical-Layer Network Coding based Relaying Schemes

Various PNC schemes have been proposed for TWRC scenarios. A PNC strategy refers to the process of computing a message to be sent by the relay node during the BC phase based on the the signals received from the two terminals during the MAC phase. In [92], the authors presented a technique where the base-band signals are mapped to the XOR operation of the binary messages in the relay in order to emulate classical network coding. Another XOR mapping strategy was proposed in [60] introducing Denoise-and-forward (DNF) scheme. With DNF, the relay maps the received signals into symbols or codewords from a discrete constellation. In [59], information-theoretical approach was considered to derive an upper bound on the achievable rate with DNF scheme employed at the relay. In [41, 42], the authors designed and optimized the denoising mapping and constellations for DNF.

Independently, a related scheme was proposed in [87] where after estimating both transmitted packets, the relay employs a channel code to protect the XORed bits against channel noise. In the aforementioned references, the signals are represented by finite fields. In [93], the authors classify PNC mappings according to whether the adopted network-code field is finite or infinite. In this section, we are interested in real field PNC-based schemes. We outline in the sequel different PNC schemes that we group into three relaying categories.

2.3.1 Decode-and-Forward

With DF strategy, the relay jointly decodes both messages before re-encoding them for transmission in the BC phase. This protocol was extended from classical relay channel [8, 43] to TWRC in [63] for half duplex and in [64] for full duplex cases. In these works, the relay after decoding both messages re-encodes them using superposing coding. In [56, 55], the two-phase achievable rate region of TWRC based on DF relaying protocol was derived. The same achievable rate region was determined independently in [39, 38] where optimal coding schemes based on network coding and random binning techniques are employed at the relay after decoding both messages.

In fact, the DF achievable rate region is the combination of the individual capacities of the two channels i.e. MAC and BC with side information. We review it in the next sections.

2.3.1.1 Multiple Access Channel Capacity

In a multiple access channel, two or more terminals transmit independent messages to a common receiver over a shared channel. In TWRC scenario, the uplink phase corresponds to a MAC. The capacity region of this channel for the discrete memoryless case was derived in [1, 46]. Let R_{1R} and R_{2R} denote the rates from terminal T_1 to the relay and from T_2 to the relay respectively. A jointly reliable communication can be met from the two source nodes to the relay as long as

the rates (R_{1R} and R_{2R}) are in the MAC capacity. Let $\mathcal{C}_{\text{MAC}}$ denotes the MAC capacity, it is given by all rate pairs (R_{1R}, R_{2R}) satisfying:

$$R_{1R} \leq I(X_1; Y_R|X_2) \tag{2.3}$$

$$R_{2R} \leq I(X_2; Y_R|X_1) \tag{2.4}$$

$$R_{1R} + R_{2R} \leq I(X_1, X_2; Y_R) \tag{2.5}$$

for random variables $[X_1, X_2, Y_R]$ with values in $\mathcal{X}_1 \times \mathcal{X}_2 \times \mathcal{Y}_R$ and joint distribution $q_1(x_1)q_2(x_2)p(y_R|x_1, x_2)$ [6].

For the channel model described in Section 2.2,

$$\begin{aligned} R_{1R} &\leq \log_2\left(1 + \frac{P_1|h_1|^2}{\sigma_R^2}\right) \\ R_{2R} &\leq \log_2\left(1 + \frac{P_2|h_2|^2}{\sigma_R^2}\right) \\ R_{1R} + R_{Rr} &\leq \log_2\left(1 + \frac{P_1|h_1|^2 + P_2|h_2|^2}{\sigma_R^2}\right) \end{aligned} \tag{2.6}$$

2.3.1.2 Broadcast Channel with Side Information

The downlink phase in the TWRC can be modeled by a Broadcast channel with side information (BCSI) at the receivers. The broadcast channel is a channel involving simultaneous communication from the relay to both receivers [7]. Moreover, in our case, both terminals have *a priori* knowledge of their messages which have been sent in the first phase. The receivers use this information to decode their intended message. The capacity region $\mathcal{C}_{\text{BCSI}}$ of this channel was fully characterized in [79, 55]. It is given by the set of all rate pairs (R_{R1}, R_{R2}) satisfying:

$$R_{R1} \leq I(X_R; Y_1) \tag{2.7}$$

$$R_{R2} \leq I(X_R; Y_2) \tag{2.8}$$

for random variables $[X_R, Y_1, Y_2]$ with values in $\mathcal{X}_R \times \mathcal{Y}_1 \times \mathcal{Y}_2$ and joint distribution $q_R(x_R)p(y_1, y_2|x_R)$.

The link between the relay and each terminal is equivalent to a single user interference free channel. For channel model described in Section 2.2, the achievable rate region of BCSI is

$$R_{R1} \leq \log_2\left(1+\frac{P_R|h_1|^2}{\sigma_1^2}\right) \tag{2.9}$$

$$R_{R2} \leq \log_2\left(1+\frac{P_R|h_2|^2}{\sigma_2^2}\right). \tag{2.10}$$

A coding strategy for BCSI based on modulo lattice addition [13] was used in [44]. It was shown also in [15], that the individual link capacities in BCSI can be achieved using bitwise XOR. This operation is applied on the codewords that have been received by the relay in the uplink phase. The resulting codeword transmitted with a signal level that is limited with the transmit power constraints of the relay. At each node, the received signal is demodulated and bit-wise XORed with the side information codeword. Then soft-decision decoding is performed for the resulting signal with specific log-likelihood functions. Similar encoding and decoding strategies are presented in [66] where the relay performs joint channel and network coding. In these strategies, the modulation addition operation is performed on the codeword symbols rather on the bits.

2.3.1.3 End-to-End Achievable Rate Region

Total achievable region is limited by both uplink and downlink capacities. Hence, based on the cut-set bounds, it is given by the set of all rate pairs (R_{12}, R_{21}) satisfying:

$$nR_{12} \leq \min\{n_1 R_{1R}, n_2 R_{R2}\} \tag{2.11}$$

$$nR_{21} \leq \min\{n_1 R_{2R}, n_2 R_{R1}\} \tag{2.12}$$

where $(R_{1R}, R_{2R}) \in \mathcal{C}_{\text{MAC}}$ and $(R_{R2}, R_{R1}) \in \mathcal{C}_{\text{BCSI}}$.

Let $\alpha \in [0,1]$ be the time division coefficient defined in assumption a.3 in Section 2.2 such that $n_1 = \alpha n$ and $n_2 = (1-\alpha)n$. Replacing α by its value, we can

rewrite (2.11) and (2.12) for a fixed α as follows:

$$R_{12} \leq \min\{\alpha R_{1R}, (1-\alpha)R_{R2}\} \tag{2.13}$$

$$R_{21} \leq \min\{\alpha R_{2R}, (1-\alpha)R_{R1}\} \tag{2.14}$$

An achievable rate region of TWRC with DF, $\mathcal{R}_{\mathrm{DF}}$, is the union over $\alpha \in [0,1]$ of all achievable rates for a fixed time division coefficient between both links.

$$\mathcal{R}_{\mathrm{DF}} = \bigcup_{0\leq\alpha\leq 1} \{\alpha\mathcal{C}_{\mathrm{MAC}} \bigcap (1-\alpha)\mathcal{C}_{\mathrm{BCSI}}\} \tag{2.15}$$

Equivalently $\mathcal{R}_{\mathrm{DF}}$ is written as the set of all rate pairs (R_{12}, R_{21}) satisfying for $\alpha \in [0,1]$:

$$R_{12} \leq \min\left\{\frac{\alpha}{2}\log_2\left(1+\frac{P_1|h_1|^2}{\sigma_R^2}\right), \frac{1-\alpha}{2}\log_2\left(1+\frac{P_R|h_2|^2}{\sigma_2^2}\right)\right\} \tag{2.16}$$

$$R_{21} \leq \min\left\{\frac{\alpha}{2}\log_2\left(1+\frac{P_2|h_2|^2}{\sigma_R^2}\right), \frac{1-\alpha}{2}\log_2\left(1+\frac{P_R|h_1|^2}{\sigma_1^2}\right)\right\} \tag{2.17}$$

$$R_{12}+R_{21} \leq \frac{\alpha}{2}\log_2\left(1+\frac{P_1|h_1|^2+P_2|h_2|^2}{\sigma_R^2}\right). \tag{2.18}$$

2.3.2 Amplify-and-Forward

AF strategy is a linear relaying protocol where the signal sent by the relay during the BC phase is a scaled version of the signal received during the MAC phase. The transmitted signal level at the relay is limited by its transmit power constraint. Since nodes T_1 and T_2 know their own transmitted signals, they can subtract them before decoding. This strategy was proposed in the context of satellite communication for one-way relay channel in [51, 9]. For TWRC, this protocol was evaluated in [63, 62, 64]. Analog network coding (ANC), introduced in [34], is an amplify-and-forward based PNC scheme that works at the signal level and represents a simpler implementation than DF based schemes. ANC have been studied for different modulation and channel settings in many references [76, 80,

19, 50]. In [61], a similar AF based scheme called AF-BAT[1] relaying was proposed independently.

We can summarize the AF protocol for real Gaussian TWRC as follows: the relay amplifies the received signal with a scaling factor ω to satisfy the relay power budget P_R where

$$\omega = \left(\frac{P_R}{P_1|h_1|^2 + P_2|h_2|^2 + \sigma_R^2} \right)^{\frac{1}{2}}.$$

Therefore, the transmitted signal at the relay is $\mathbf{X}_R = \omega \mathbf{Y}_R$. Prior to decoding the desired message, each terminal T_i substructs the self-interfering signal (side information) from the received signal $\mathbf{Y}_i$ defined in (2.2). The effective received signals at terminals T_1 and T_2 can be written as respectively as:

$$\tilde{\mathbf{Y}}_1 = h_1 \omega h_2 \mathbf{X}_2 + h_1 \omega \mathbf{Z}_R + \mathbf{Z}_1,$$

and equivalently the effective received signal at terminal T_2 is

$$\tilde{\mathbf{Y}}_2 = h_2 \omega h_1 \mathbf{X}_1 + h_2 \omega \mathbf{Z}_R + \mathbf{Z}_2.$$

Both channels are equivalent to additive direct Gaussian channels where the capacity is given by $\frac{1}{2}\log_2(1 + SNR)$. The relay only amplifies its received signal. Therefore, to ensure that there is no data loss between MAC and BC transmission phases, the time division α with AF relaying scheme is always equal $\frac{1}{2}$. Thus, a total factor of $\frac{1}{4}$ is pre-log added for the achievable rates.
We conclude that the achievable rates for the link from T_1 to T_2 and from T_2 to T_1, R_{12} and R_{21}, respectively satisfy:

$$R_{12} \leq \frac{1}{4}\log_2\left(1 + \frac{|h_2|^2\omega^2|h_1|^2 P_1}{\sigma_2^2 + |h_2|^2\omega^2\sigma_R^2}\right),$$

$$R_{21} \leq \frac{1}{4}\log_2\left(1 + \frac{|h_1|^2\omega^2|h_2|^2 P_2}{\sigma_1^2 + |h_1|^2\omega^2\sigma_R^2}\right)$$

[1]Bi-directional Amplification of Throughput

and the achievable rate region of AF, $\mathcal{R}_{\mathrm{AF}}$, is given by the set of all rate pairs (R_{12}, R_{21}) satisfying:

$$R_{12} \leq \frac{1}{4}\log_2\left(1+\frac{|h_2|^2|h_1|^2P_RP_1}{\sigma_2^2\sigma_R^2+\sigma_2^2|h_1|^2P_1+\sigma_2^2|h_2|^2P_2+\sigma_R^2|h_2|^2P_R}\right) \tag{2.19}$$

$$R_{21} \leq \frac{1}{4}\log_2\left(1+\frac{|h_1|^2|h_2|^2P_RP_2}{\sigma_1^2\sigma_R^2+\sigma_1^2|h_1|^2P_1+\sigma_1^2|h_2|^2P_2+\sigma_R^2|h_1|^2P_R}\right). \tag{2.20}$$

2.3.3 Compress-and-Forward

Cover and El Gamal proposed in [8, Theorem 6] a relaying strategy for the one-way relay channel where the relay sends a compressed and quantized version of its channel output to the destination. The destination decodes by combining the relay signal with its own received signal from the direct link. The relay applies Wyner-Ziv (WZ) source coding [86] to exploit side information at the destination. Nowadays, this strategy is often called compress-and-forward [43]. This scheme was extended to TWRC in [64]. CF for TWRC have been widely investigated with random coding in [64, 65, 36, 26]. An achievable rate region was first proved in [64]. The achievable rates presented in [65, 36, 26] present only slight differences related to a time sharing parameter.

In [36], an achievable rate region of random coding CF for TWRC with time division optimization has been derived. It is given by the convex hull of all rate pairs (R_{12}, R_{21}):

$$R_{12} \leq \alpha I(X_1; \hat{Y}_R|X_2, Q) \tag{2.21}$$

$$R_{21} \leq \alpha I(X_2; \hat{Y}_R|X_1, Q) \tag{2.22}$$

subject to:

$$\alpha I(\hat{Y}_R; Y_R|X_1, Q) \leq (1-\alpha) I(X_R; Y_1|Q) \tag{2.23}$$

$$\alpha I(\hat{Y}_R; Y_R|X_2, Q) \leq (1-\alpha) I(X_R; Y_2|Q) \tag{2.24}$$

where the joint probability distribution verify:

$$p(q)p(x_1|q)p(x_2|q)p(y_R|x_1,x_2)p(\hat{y}_R|y_R)p(x_R|q).$$

$\hat{Y}_R$ represents a quantized and compressed version of Y_R at the relay and Q denotes a discrete time-sharing random variable with distribution $p(q)$.

The forwarding strategy at the relay relies on WZ encoding with random codewords. The relay quantizes the received signal and broadcasts the quantized signal to both terminals T_1 and T_2. By exploiting their correlated side information and the quantized received signal from the relay, each terminal decodes the other user' message. CF achievable rate region for Gaussian TWRC has been evaluated in [36, 26].
In the following, we give a detailed evaluation of the CF rate region in the Gaussian case presented in Section 2.2. Note that this evaluation is not given in the aforementioned references and it has been partially published in [73]. We consider for this evaluation a different test channel model with results from the rate distortion theory.

Compress-and-Forward for Gaussian TWRC

In the classical Wyner-Ziv coding [86, 85], the reconstruction of Y_R at decoder T_i, $\hat{Y}_{R,i}$, $i = 1, 2$, is a function of the compressed source $\hat{Y}_R$ and the side information X_i i.e. $\hat{Y}_{R,i} = f(\hat{Y}_R, X_i)$. We denote the distortion at each receiver T_i by D_i, defined as

$$D_i = \frac{1}{n_2}\sum_{k=1}^{n_2} |Y_{R,k} - \bar{Y}_{R,i,k}|^2. \tag{2.25}$$

The relay performs a single quantization scheme which is adapted to the worst terminal (the one which has the weakest side information). Without loss of generality, we assume that $|h_2|^2P_2 \leq |h_1|^2P_1$. In this case, terminal T_2 has the weakest side information. The relation between $\hat{Y}_R$ and Y_R is given by the forward test

channel [85]:

$$\hat{Y}_R = \beta^2(Y_R + \Psi) \tag{2.26}$$

where $\beta^2 = \dfrac{\mathrm{VAR}(Y_R|X_2) - D_2}{\mathrm{VAR}(Y_R|X_2)}$. $\mathrm{VAR}(Y_R|X_2)$ is the conditional variance of Y_R given X_2. $\Psi \sim \mathcal{N}\left(0, \dfrac{\mathrm{VAR}(Y_R|X_2)D_2}{\mathrm{VAR}(Y_R|X_2) - D_2}\right)$.
Note that $\mathrm{VAR}(\Psi) = \dfrac{D_2}{\beta^2}$ and $\hat{Y}_R = \beta^2 Y_R + \beta^2\Psi$. Thus, we can rewrite the rates according to this Gaussian model as:

$$\begin{aligned}
R_{12} &\leq \alpha I(X_1; \hat{Y}_R|X_2) \\
&= \alpha I(X_1; \beta^2 Y_R + \beta^2\Psi|X_2) \\
&= \alpha I(X_1; \beta^2(h_2X_2 + h_1X_1 + Z_R + \Psi)|X_2) \\
&= \alpha I(X_1; \beta^2(h_1X_1 + Z_R + \Psi)) \\
&= \alpha h(\beta^2(h_1X_1 + Z_R + \Psi)) - h(\beta^2(Z_R + \Psi)) \\
&= \frac{\alpha}{2}\log_2\left(\frac{|h_1|^2P_1 + \sigma_R^2 + \dfrac{D_2}{\beta^2}}{\sigma_R^2 + \dfrac{D_2}{\beta^2}}\right) \\
&= \frac{\alpha}{2}\log_2\left(1 + \frac{\beta^2|h_1|^2P_1}{\beta^2\sigma_R^2 + D_2}\right).
\end{aligned}$$

R_{21} is computed similarly. Moreover, limited by the worst receiver T_2,

$$\max(I(\hat{Y}_R; Y_R|X_1), I(\hat{Y}_R; Y_R|X_2)) = I(\hat{Y}_R; Y_R|X_2)$$

Thus the constraints (2.23) and (2.24) reduce to

$$\alpha I(\hat{Y}_R; Y_R|X_2) \leq (1-\alpha)\min\{I(X_R; Y_1), I(X_R; Y_2)\} \tag{2.27}$$

The left-hand side of the inequality can be computed as:

$$\begin{aligned} I(\hat{Y}_R; Y_R|X_2) &= I(\beta^2 Y_R + \beta^2\Psi; Y_R|X_2) \\ &= I(\beta^2(h_1X_1 + Z_R + \Psi); h_1X_1 + Z_R) \\ &= h(\beta^2(h_1X_1 + Z_R + \Psi)) - h(\beta^2\Psi) \\ &= \frac{1}{2}\log_2\left(\frac{|h_1|^2P_1 + \sigma_z^2 + \frac{D_2}{\beta^2}}{\frac{D_2}{\beta^2}}\right) \\ &= \frac{1}{2}\log_2\left(1 + \beta^2\frac{|h_1|^2P_1 + \sigma_z^2}{D_2}\right) \\ &= \frac{1}{2}\log_2\left(\frac{|h_1|^2P_1 + \sigma_z^2}{D_2}\right) \\ &= R(D_2). \end{aligned}$$

$R(D_2)$ is the WZ rate distortion function of the Gaussian source Y_R with side information X_2 at T_2, defined as the minimum source coding rate for distortion D_2. It is given by:

$$R(D_2) = \frac{1}{2}\log_2^+\left(\frac{\mathrm{VAR}(Y_R|S_2)}{D_2}\right), 0 \le D_2 \le \mathrm{VAR}(Y_R|S_2)$$

Finally, an achievable rate region of CF, $\mathcal{R}_{\mathrm{CF}}$, is given as the set of all rate pairs (R_{12}, R_{21}) satisfying for $\alpha \in [0,1]$:

$$R_{12} \le \frac{\alpha}{2}\log_2\left(1 + \frac{|h_1|^2P_1(|h_1|^2P_1 + \sigma_R^2 - D_2)}{\sigma_R^2(|h_1|^2P_1 + \sigma_R^2) + D_2|h_1|^2P_1}\right) \tag{2.28}$$

$$R_{21} \le \frac{\alpha}{2}\log_2\left(1 + \frac{|h_2|^2P_2(|h_1|^2P_1 + \sigma_R^2 - D_2)}{\sigma_R^2(|h_1|^2P_1 + \sigma_R^2 - D_2) + D_2|h_1|^2P_1}\right) \tag{2.29}$$

subject to:

$$\alpha\log_2\left(\frac{|h_1|^2P_1 + \sigma_R^2}{D_2}\right) \le (1-\alpha)\min\left\{\log_2\left(1 + \frac{|h_2|^2P_R}{\sigma_2^2}\right), \log_2\left(1 + \frac{|h_1|^2P_R}{\sigma_1^2}\right)\right\} \tag{2.30}$$

for $\alpha \in [0,1]$.

In [47], the authors propose another CF protocol called noisy network coding based on message repetition coding and simultaneous decoding. In this scheme,

the relay compression indices are sent directly without using WZ coding as in the previous CF schemes. Then each decoder performs simultaneous joint typicality decoding on the received signals from all the blocks without explicitly decoding the compression indices.

2.3.4 Comparison between Relaying Strategies for TWRC

The presented strategies ie DF, AF and CF perform differently for different SNR regimes and channel conditions. It was shown in [36, 37] that, in general, DF schemes outperforms the other terminals specially at low SNR regimes while AF and CF outperforms DF for high SNR regime. For instance, AF strategy, although its simplicity, suffers from noise amplification especially at low SNRs. In fact, since the relay does not remove its additive noise, the noise is forwarded along with the useful signals. As a result, AF performance is not as good as DF in which the relay "tries to clean up the noise". Though, the effect of the noise is neglected for high SNR regimes.

CF strategy outperforms AF for symmetric channels. Its performance are close to AF for high SNR regime since in both strategies the relay does not decode the transmitted messages from terminals T_1 and T_2 like in DF. DF strategy is limited for high SNR regime by the multiple access sum-rate (2.18) which is affected by the interference of transmitted signals from both nodes.

2.4 Conclusion

In this chapter, we reviewed physical-layer network coding schemes proposed for TWRC where the end-to-end communication occurs in two time slots. We presented the basic coding schemes of AF, DF and CF strategies and presented their achievable rate regions for TWRC. We also detailed the Gaussian version of these rates according to our system model. Finally, we gave a brief comparison be-

tween the presented strategies based on the literature results. These results will be illustrated in details in Chapter 4.

As a conclusion, it is expected that when the relay does not know the full codebooks of both nodes, and hence DF strategy cannot be applied, it rather chooses CF strategy than AF. This will justify our choice of CF strategy in our proposed PNC schemes in the next chapters.

Chapter 3

Finite Dimension Decode-and-Forward Scheme for Two-Way Relay Channel

In the previous chapter, we addressed the fundamental limits on achievable rates for the Two-Way Relay Channel. We presented achievable rate regions for a select of PNC relaying schemes based on random coding. From an information-theoretic perspective, the derived rate regions are achieved by sufficiently large codewords. In such case, the sources are assumed to have unlimited data to send in order to meet an arbitrarily small error probability, at the expense of increasing the complexity at the encoder and the decoder. These schemes cannot be implemented in practice. We need to assess the error probability performance when finite length codeword are employed.

In a point-to-point channel setting, the reliability-rate trade-off has been studied in the literature by analyzing the bit error probability using error exponent metric, representing the reliability function of the channel [22]. A straightforward extension of this concept can be achieved in a multi-user setting by deriving the individual error probabilities at each receiver or the error probability of the system. A system is considered to be in error if at least one user's codeword is decoded

erroneously. Therefore, in order to study the capacity region of a multi-user channel, it is sufficient to show that the system error probability approaches zero as the block-length increases.

This chapter focuses on the individual error probabilities as a function of the codewords' length for decode-and-forward relaying strategy in TWRC scenario. The maximum transmission rates are determined as a function of the block length and the maximum tolerated error probability.

The content of this chapter has been partially published in [71].

3.1 Random Error Exponent Motivation

Consider a discrete single-user memoryless channel of capacity C. Let $P_e(n, R)$ be the smallest average error probability after block decoding on this channel. It is defined for any code of block length n and a given data rate $R < C$. It was shown in [17, 67, 16, 20] that for this channel, block coding schemes exist for which $P_e(n, R)$ approaches zero exponentially with increasing block length. It has been shown that $P_e(n, R)$ is upper-bounded by an exponentially decreasing function of n. The error exponent is then defined as the rate of the exponential decay and is so-called the channel reliability function. It is expressed as

$$E(R) \triangleq \lim_{n\to\infty} -\frac{P_e(n, R)}{n} \tag{3.1}$$

and so the probability of error can be written as $P_e(n, R) \approx e^{-nE(R)}$, where the rate R is in bits per channel use. Note that the limit in (3.1) can be also read as the inferior limit or superior limit of the function.

Error exponents offer a quantitative indicator of the complexity required to achieve a certain level of reliability in communication at a rate below the channel capacity. They have been studied in details for discrete memoryless channels and additive white Gaussian noise (AWGN) channels [17, 67, 16, 20, 69]. Lower and upper

bounds have been defined for $E(R)$ since it is difficult to derive the exact error exponent.

The classical lower bound is given by Fano [16] and Gallager [22]; it is known as the random coding error exponent or Gallager's exponent. This quantity provides an upper bound for the error probability of the best encoding/decoding strategy for a given rate and block length. It is used to estimate the codeword length required to achieve a prescribed error probability [3].

The random coding bound $E_{rd}(R)$ is derived based first on maximum likelihood (ML) decoding, i.e., decoding the user source message $k \in [1, K]$ that maximizes the conditional probability $P(j|k)$, where $j \in [1, J]$ is in the output alphabet. Then, an upper-bound is taken on the average error probability over a set of block codes of length n with arbitrary chosen input distribution $\mathbf{q}(\mathbf{x})$, where $\mathbf{x}$ is the channel input sequence.

Using this approach, Gallager [22] showed that:

$$P_e(n, R) \leq \exp(-nE_{rd}(R))$$

where

$$E_{rd}(R) = \max_{0 \leq \rho \leq 1} \max_{\mathbf{q}} (E_o(\rho, \mathbf{q}) - \rho R)$$

and

$$E_o(\rho, \mathbf{q}) = -\ln \sum_{0 \leq j \leq 1} \left(\sum_{0 \leq k \leq 1} q(k) P(j|k)^{\frac{1}{1+\rho}} \right)^{1+\rho},$$

$E_{rd}(R)$ is the tightest bound obtained by choosing ρ and the input probability distribution $\mathbf{q}$ that maximize $(E_o(\rho, \mathbf{q}) - \rho R)$.

It has been shown that the random coding exponent performs well at high rates close to the channel capacity. Gallager proved in this case that this bound is the exact error exponent for the set of random codes [21]. However, at low rates, Gallager tightened this bound by expurgating the poor codewords from the set of codes [22]. In fact, $E_{rd}(R) = E(R)$ at high rates; thus, the weakness of the bound, at low rates, is not due to upper-bounding the average error probability over the

set of codes, but it results from the fact that the best codes perform much better than the average, especially at low rates [21].

Studies on error exponents have been extended to multi-access channels in [23, 24]. For instance, let consider a multiple access channel where two source nodes are transmitting codewords of length n at rates R_1 and R_2 respectively to a single receiver. The smallest average error probability at the decoder is denoted by $P_{e,\mathrm{MAC}}(n, R_1, R_2)$, and the error exponent for this multiple access channel is defined as

$$E_{\mathrm{MAC}}(R_1, R_2) \triangleq \lim_{n\to\infty} -\log \frac{P_{e,\mathrm{MAC}}(n, R_1, R_2)}{n}. \tag{3.2}$$

Random coding bounds for MAC were studied by many authors: Slepian and Wolf [70], Dyachkov [11], Gallager [23], Pokorny and Wallmeier [57], Liu and Hughes [48].

In this chapter, the universal Gallager random coding exponent is adopted to derive the upper-bounds on the system error probabilities when decode-and-forward relaying strategy is used at the relay. Performing at rates near the capacity has motivated us to choose this random coding exponent metric. In the following, the individual error probabilities will be derived for TWRC.

3.2 End-to-End Error Probabilities for Discrete Memoryless Channel

Based on the random coding rule, upper bounds on the average error probabilities at each transmitter can be derived. We consider the system model presented in Section 2.2 with DF strategy used at the relay. The channel is assumed to be discrete memoryless with finite size input and output alphabets. We denote the probabilities of successful and erroneous decoding of information sent by node T_i to node T_j: $P_{s,i\to j}$ and $P_{e,i\to j}$, respectively. Since we suppose DF relaying scheme,

the relay decodes both messages m_1 and m_2 sent by T_1 and T_2 respectively. Let denote $\hat{m}_i$, $i \in \{1, 2\}$ the message of node T_i decoded by the relay. $\hat{\hat{m}}_{\bar{i}}$ is the message decoded by node T_i coming from $T_{\bar{i}}$ through the signal received from the relay.

We will derive the end-to-end error probability from user node T_2 to node T_1, $P_{e,1}$. $P_{e,2}$ can be calculated similarly. $P_{e,1}$ is the error probability between the data transmitted by node T_2 and the data decoded at node T_1, it is given by

$$\begin{aligned} P_{e,1} &= P(\hat{\hat{m}}_2 \neq m_2) \\ &= 1 - P(\hat{\hat{m}}_2 = m_2) \\ &= 1 - (P_{s,2\to R} P_{s,R\to 1}) \\ &= 1 - (1 - P_{e,2\to R})(1 - P_{e,R\to 1}) \\ &= P_{e,2\to R} + P_{e,R\to 1} + P_{e,2\to R} P_{e,R\to 1} \\ &\simeq P_{e,2\to R} + P_{e,R\to 1}. \end{aligned} \tag{3.3}$$

A successful decoding occurs when the relay and the final receiver T_1 decode successfully the message m_2 as stated in the third equation. The probability of error $P_{e,1}$ is approximated by the last equation (3.3) since the product of sufficiently two low probabilities is negligible relative to their sum. Finally, $P_{e,1}$ is obtained as the sum of two terms:

- $P_{e,2\to R}$ represents the probability of erroneous decoding of message m_2 at the relay. Since MAC decoding is performed at the relay, the message pair (m_1, m_2) is jointly estimated. After decoding, the messages $(\hat{m}_1, \hat{m}_2)$ are obtained. Decoding error in m_2 happens when $(\hat{m}_1, \hat{m}_2) \neq (m_1, m_2)$ i.e. both messages are in error or when $\hat{m}_1 = m_1$ and $\hat{m}_2 \neq m_2$. In other words,

$\hat{m}_1$ can be any index in $\mathcal{M}_1$ and $P_{e,2\to R}$ is calculated as follows,

$$
\begin{aligned}
P_{e,2\to R} &= P(\hat{m}_2 \neq m_2) && \text{(3.4a)}\\
&= P\left(\bigcup_{j\in\mathcal{M}_1} (\hat{m}_1 = j, \hat{m}_2 \neq m_2)\right) && \text{(3.4b)}\\
&= P\left((\hat{m}_1 = m_1, \hat{m}_2 \neq m_2)\bigcup\left\{\bigcup_{j\in\mathcal{M}_1\setminus\{m_1\}} (\hat{m}_1 = j, \hat{m}_2 \neq m_2)\right\}\right) && \text{(3.4c)}\\
&= P(\hat{m}_1 = m_1, \hat{m}_2 \neq m_2) + P(\hat{m}_1 \neq m_1, \hat{m}_2 \neq m_2) && \text{(3.4d)}
\end{aligned}
$$

where

$$
\begin{aligned}
P(\hat{m}_1 \neq m_1, \hat{m}_2 \neq m_2) &= P\left(\bigcup_{j\in\mathcal{M}_1\setminus\{m_1\}} (\hat{m}_1 = j, \hat{m}_2 \neq m_2)\right) && \text{(3.5a)}\\
&= \sum_{j\in\mathcal{M}_1\setminus\{m_1\}} P(\hat{m}_1 = j, \hat{m}_2 \neq m_2) && \text{(3.5b)}
\end{aligned}
$$

Equation (3.4c) follows from the fact that the events $\{\hat{m}_1 = m_1, \hat{m}_2 \neq m_2\}$ and $\{\hat{m}_1 \neq m_1, \hat{m}_2 \neq m_2\}$ are mutually exclusive since the messages in the sets $\mathcal{M}_1$ and $\mathcal{M}_2$ are generated i. i. d. according to uniform distribution. Equation (3.5b) follows also from the fact that the events $E_j = \{\hat{m}_1 = j, \hat{m}_2 \neq m_2\}$ for $j \in \mathcal{M}_1$ are mutually exclusive.

The input sequences at terminals T_1 and T_2 are chosen independently according to a fixed probability distribution.

$$
\begin{aligned}
q_1(\mathbf{x}_1) &= \prod_{k=1}^{n_1} q_1(x_{1,k}), \quad x_1 = \{x_{1,1}, x_{1,2}, \cdots, x_{1,n_1}\}\\
q_2(\mathbf{x}_2) &= \prod_{k=1}^{n_1} q_2(x_{2,k}), \quad x_2 = \{x_{2,1}, x_{2,2}, \cdots, x_{2,n_1}\}
\end{aligned}
\qquad (3.6)
$$

We consider the two cases to derive (3.4c):

1. both m_1 and m_2 are decoded erroneously;
2. only m_2 is decoded wrongly.

Using the results in [23, Theorem 2], the error probabilities are bounded respectively by:

$$P(\hat{m}_1 \neq m_1, \hat{m}_2 \neq m_2) \leq 2^{-n_1[-\rho_R(R_{1R}+R_{2R})+E_{0R}(\rho_R,\mathbf{q}_1,\mathbf{q}_2)]} \tag{3.7}$$

where $\rho_R \in [0,1]$ and

$$\begin{array}{l} E_{0R}(\rho_1,\mathbf{q}_1,\mathbf{q}_2) = \\ -\log_2\left(\sum_{y_R}\left[\sum_{x_1,x_2} q_1(x_1)q_2(x_2)P(y_R|x_1x_2)^{\frac{1}{(1+\rho_1)}}\right]^{1+\rho_1}\right) \end{array} \tag{3.8}$$

and

$$P(\hat{m}_1 = m_1, \hat{m}_2 \neq m_2) \leq 2^{-n_1[-\rho_2 R_{2R}+E_{02R}(\rho_2,\mathbf{q}2)]} \tag{3.9}$$

where $\rho_2 \in [0,1]$ and

$$E_{02R}(\rho_2,\mathbf{q}_2) = -\log_2 \sum_{y_R}\left[\sum_{x_2} q(x_2).p(y_R|x_2)^{\frac{1}{(1+\rho_2)}}\right]^{(1+\rho_2)} \tag{3.10}$$

- $P_{e,R\to 1}$ in (3.3) is the probability of erroneous decoding at T_1 of the message sent from the relay given that the latter is successfully decoded. $P_{e,R\to 1} = P(\hat{\hat{m}}_2 \neq \hat{m}_2)$. As indicated in Section 2.3.1, the coding theorems for the broadcast channel with side information indicate that the capacity of the link between the relay and any receiver is equivalent to a single-user channel capacity. Equivalently, the average error probability for the link $R \to T_1$ can be approximated to the single-user channel error probability.
  The input sequence at the relay is chosen independently according to a fixed probability distribution.

$$q_R(\mathbf{x}_R) = \prod_{k=1}^{n_2} q_R(x_{R,k}), \quad x_R = \{x_{R,1}, x_{R,2}, \cdots, x_{R,n_2}\} \tag{3.11}$$

The error probability is bounded by:

$$P_{e,R\to 1} \leq 2^{-n_2[-\rho_{R1}R_{R1}+E_{0R1}(\rho_{R1},\mathbf{q}_R)]} \tag{3.12}$$

with $0 \leq \rho_{R1} \leq 1$ and

$$E_{0R1}(\rho_{R1}, \mathbf{q}_R) = -\log_2 \sum_{y_1} \left[\sum_{x_R} q(x_R).p(y_1|x_R)^{\frac{1}{(1+\rho_{R1})}} \right]^{(1+\rho_{R1})}. \quad (3.13)$$

To obtain the tightest bounds on (3.7), (3.9) and (3.12), the upper bounds are maximized over all input distributions and for all ρ_R, ρ_{2R} and ρ_{R1} respectively. We obtain the following random error exponents:

$$E_{rd,R}(R_{1R} + R_{2R}) = \max_{\mathbf{q}_1.\mathbf{q}_2} \max_{\rho_R} E_{0R}(\rho_R, \mathbf{q}_1, \mathbf{q}_2) - \rho_R(R_{1R} + R_{2R}), \quad (3.14)$$

$$E_{rd,2R}(R_{2R}) = \max_{\mathbf{q}_2} \max_{\rho_{2R}} E_{02R}(\rho_{2R}, \mathbf{q}_2) - \rho_{2R} R_{2R}, \quad (3.15)$$

$$E_{rd,R1}(R_{R1}) = \max_{\mathbf{q}_R} \max_{\rho_{R1}} E_{0R1}(\rho_{R1}, \mathbf{q}_R) - \rho_{R1} R_{R1}, \quad (3.16)$$

where $E_{rd,R}(R_{2R} + R_{1R})$ is the random error exponent that accounts for the MAC error at the relay when both messages are decoded wrongly; $E_{rd,2R}(R_{2R})$ is the random error exponent that accounts for the MAC error at the relay when only m_2 is in error; $E_{rd,R1}(R_{R1})$ is the random error exponent that accounts for BC error at terminal T_1. Finally, the total average error probability seen by node T_1 is given by:

$$P_{e,1} \leq 2^{-n_1 E_{rd,2R}(R_{2R})} + 2^{-n_1 E_{rd,R}(R_{2R} + R_{1R})} + 2^{-n_2 E_{rd,R}(R_{R1})}. \quad (3.17)$$

Similarly, the average error probability at node T_2 is given by:

$$P_{e,2} \leq 2^{-n_1 E_{rd,1R}(R_{1R})} + 2^{-n_1 E_{rd,R}(R_{2R} + R_{1R})} + 2^{-n_2 E_{rd,R2}(R_{R2})} \quad (3.18)$$

where $E_{rd,R}(R_{2R} + R_{1R})$ is given in (3.14). $E_{rd,1R}(R_{1R})$ is the random error exponent that accounts for the MAC error at the relay when only m_1 is in error; $E_{rd,R2}(R_{R2})$ is the random error exponent that accounts for BC error at terminal T_2. The random error exponents have the same form:

$$E_{rd,1R}(R_{1R}) = \max_{q_1} \max_{\rho_{1R}} E_{01R}(\rho_{1R}, q_1) - \rho_{1R} R_{1R} \quad (3.19)$$

with

$$E_{01R}(\rho_{1R}, q_1) = -\log_2 \sum_{y_R} \left[\sum_{x_1} q(x_1).p(y_R|x_1)^{\frac{1}{(1+\rho_{1R})}} \right]^{(1+\rho_{1R})}$$

and

$$E_{rd,R2}(R_{R2}) = \max_{q_R} \max_{\rho_{R2}} E_{0R2}(\rho_{R2}, q_R) - \rho_{R2} R_{R2} \tag{3.20}$$

with

$$E_{0R2}(\rho_{R2}, q_R) = -\log_2 \sum_{y_2} \left[\sum_{x_R} q(x_R).p(y_2|x_R)^{\frac{1}{(1+\rho_{R2})}} \right]^{(1+\rho_{R2})}.$$

The individual end-to-end average error probabilities are characterized here for discrete memoryless channel. In the next section, we derive them for AWGN channel and Gaussian distributions. In general to maximize the error exponents, choosing the distributions to be Gaussian is not the optimal choice [23], nevertheless this option helps to obtain a valid upper bound on error probabilities.

3.3 End-to-End Error Probabilities for AWGN Channel

3.3.1 Gaussian Error Exponents

Consider now the system model presented in Section 2.2 where Gaussian TWRC is detailed. We assume transmission under peak power P_i for each link and the SNRs are $SNR_{iR} = \frac{P_i|h_i|^2}{\sigma_R^2}$ and $SNR_{Ri} = \frac{P_R|h_i|^2}{\sigma_i^2}$ for $i \in \{1, 2\}$. We evaluate for this channel the random coding error exponents i.e. $E_{rd,R}$, $E_{rd,1R}$, $E_{rd,2R}$, $E_{rd,R1}$ and $E_{rd,R2}$ presented in (3.14), (3.19), (3.15), (3.16) and (3.20). Since continuous distributions are considered, sums are replaced with integrals. Thus, the error exponents values can be easily calculated as

$$E_{rd,R}(R_{1R} + R_{2R}) = \max_{0 \le \rho_R \le 1} \rho_R \left[\frac{1}{2} \log_2 \left(1 + \frac{SNR_{1R} + SNR_{2R}}{1 + \rho_R} \right) - (R_{1R} + R_{2R}) \right]. \tag{3.21}$$

All the other error exponents have the same general form,

$$E_{rd,ij}(R_{ij}) = \max_{0\leq\rho_{ij}\leq 1} \rho_{ij}\left[\frac{1}{2}\log_2\left(1+\frac{SNR_{ij}}{1+\rho_{ij}}\right) - R_{ij}\right] \tag{3.22}$$

where the indices i and j refer to the transmitting and receiving nodes respectively, $i, j \in \{1, 2, R\}$. ρ_{ij} is the corresponding optimization factor.

Considering this last form, $E_{rd,R}(R_{1R}+R_{2R})$ can be obtained by replacing the rate R_{ij} with $R_{1R} + R_{2R}$ and the signal-to-noise ratio SNR_{ij} with $SNR_{1R} + SNR_{2R}$. We maximize the error exponents over ρ_{ij}, for $0 \leq \rho_{ij} \leq 1$. We find that the optimal $\rho_{ij}^\star \in [0, 1]$ should verify the following equation

$$R_{ij} = \frac{1}{2}\log_2\left(1+\frac{SNR_{ij}}{1+\rho_{ij}^\star}\right) - \frac{\rho_{ij}^\star SNR_{ij}}{2(1+\rho_{ij}^\star)(1+\rho_{ij}^\star+SNR_{ij})}. \tag{3.23}$$

Since R_{ij} is supposed to be fixed, we should verify if the equation (3.23) has always a solution. Let $R_{ij}^{ref}(\rho_{ij}^\star)$ be a reference rate equal to the right hand side of (3.23). $R_{ij}^{ref}(\rho_{ij}^\star)$ is a decreasing function of $\rho_{ij}^\star$ thus $R_{ij}^{ref}(1) \leq R_{ij}^{ref}(\rho_{ij}^\star) \leq R_{ij}^{ref}(0)$. We have then:

$$\frac{1}{2}\log_2\left(1+\frac{SNR_{ij}}{2}\right) - \frac{SNR_{ij}}{4(2+SNR_{ij})} \leq R_{ij}^{ref}(\rho_{ij}^\star) \leq \frac{1}{2}\log_2(1+SNR_{ij}) \tag{3.24}$$

We notice that the upper bound on $R_{ij}^{ref}(\rho_{ij}^\star)$ represents the capacity of the single-user link between node i and node j, which is always verified for the rate R_{ij}. Thus, if $R_{ij} \geq \frac{1}{2}\log_2(1+\frac{SNR_{ij}}{2}) - \frac{SNR_{ij}}{4(2+SNR_{ij})}$, the optimal solution of (3.23) can be found and

$$E_{ij}(R_{ij}) = \frac{(\rho_{ij}^\star)^2 SNR_{ij}}{2(1+\rho_{ij}^\star)(1+\rho_{ij}^\star+SNR_{ij})}. \tag{3.25}$$

In the other case, we choose $\rho_{ij}^\star = 1$ and

$$E_{ij}(R_{ij}) = \frac{1}{2}\log_2\left(1+\frac{SNR_{ij}}{2}\right) - R_{ij}. \tag{3.26}$$

The derived error exponents are integrated in the expressions (3.17) and (3.18) to give an upper-bound on the end-to-end error probabilities between both terminals T_1 and T_2 via the relay R.

3.3.2 Rate Region Maximization

The achievable rate region of DF relaying scheme in TWRC has been presented in the previous chapter in section 2.3.1, equations (2.16), (2.17) and (2.18). The defined region is convex, hence the boundary points are determined by maximizing the weighted sum of both rates R_{12} and R_{21} at each $\eta \in [0,1]$ and by optimizing the time division α between MAC and BC phases:

$$\begin{aligned} \max_{0\leq\alpha\leq 1} \quad & \eta R_{12} + (1-\eta) R_{21} \\ \text{s.t.} \quad & (R_{12}, R_{21}) \in \mathcal{R}_{\text{DF}}. \end{aligned} \tag{3.27}$$

This optimization problem can be solved using convex optimization methods such as interior-point methods.

Operating in the border of that region assumes infinite-length codewords. This introduces more complexity at the encoder/decoder and prohibitive decoding delays. Therefore, to study the problem of rate optimization under practical and realizable constraints, we shall consider finite-length codewords and fixed target on error probabilities. In this context, for simplicity, we will employ the term "achievable rate region" to designate the region of rates where the error probability at the decoder does not exceed a predefined threshold.

A fixed block of n channel uses is considered. It is divided into the two phases MAC and BC such that $n_1 + n_2 = n$, thus $n_1 = \alpha n$ and $n_2 = (1-\alpha)n$ for $\alpha \in [0,1]$, as mentioned in the system model in Section 2.2. We derive valid upper bounds on the average end-to-end error probabilities as a function of n_1, n_2 and the intermediate rates between the nodes T_i and the relay R for $i \in \{1,2\}$. Let c_1 and c_2, two fixed targets on $P_{e,1}$ and $P_{e,2}$. Then, the error exponent upper-bounds verify

$$2^{-n_1 E_{rd,2R}(R_{2R})} + 2^{-n_1 E_{rd,R}(R_{2R}+R_{1R})} + 2^{-n_2 E_{rd,R1}(R_{R1})} \leq c_1 \tag{3.28}$$

$$2^{-n_1 E_{rd,1R}(R_{1R})} + 2^{-n_1 E_{rd,R}(R_{2R}+R_{1R})} + 2^{-n_2 E_{rd,R2}(R_{R2})} \leq c_2 \tag{3.29}$$

The end-to-end transmission rates should be included in DF achievable rate region $\mathcal{R}_{\mathrm{DF}}$ (2.15). Taking into account the new constraints (3.28) and (3.29), the new transmission rate region can be defined as follows,

$$\begin{aligned} \max_{0\leq\alpha\leq 1} \quad & \eta R_{12} + (1-\eta) R_{21} \\ \text{s.t.} \quad & (R_{12}, R_{21}) \in \mathcal{R}_{DF} \\ \text{and} \quad & P_{e,1} \leq c_1 \\ \text{and} \quad & P_{e,2} \leq c_2 \\ \text{for all} \quad & \text{values of } \eta \in [0,1]. \end{aligned} \tag{3.30}$$

3.4 Numerical Results

In this section, we evaluate the rate region with constrained error probabilities for fixed number of channel uses compared to the achievable rate region with infinite number of channel uses. We discuss the results with and without power optimization.

3.4.1 Achievable Rate Regions for Fixed Transmit Power Allocation

We assume, first, symmetric static channel and equal SNRs at both MAC and BC links. We consider $SNR_{1R} = SNR_{R1} = SNR_1$ and $SNR_{2R} = SNR_{R2} = SNR_2$. Two approaches are considered for the power limitation: peak power constraint and average power constraint. For the first approach, the power budget is consumed for each channel use. For the second approach, the transmit power averaged over the total transmission time does not exceed the power budget. In this case, the instantaneous transmit power at nodes T_i, $i \in \{1,2\}$ is scaled by the time division α, it is equal to $\dfrac{P_i}{\alpha}$ and the transmit power at the relay is $\dfrac{P_R}{(1-\alpha)}$.

Fig. 3.1 draws the achievable rate regions under average and peak transmit power for equal $SNR_i = 10\text{dB}$, $i \in \{1,2\}$ with AF and DF strategies. The achievable

rate regions have been defined by equations (2.16), (2.17) and (2.18) for DF and equations (2.19) and (2.19) for AF in Chapter 2, Section 2.3.1.

For a fixed power budget, average power constraint leads to an increase of the region area which has been extended by 35% (DF) and 30% (AF). This can be explained by the fact that average power transmission offers an additional degree of freedom that can be optimized with the time division coefficient α. With AF relaying, α is always equal to $\frac{1}{2}$, while with the considered DF, we have optimized the time division as shown in Fig.3.3. Thus, in both cases (peak and average power constraints) the DF outperforms the AF strategy as observed in Fig.3.1. When $R_{12} = R_{21}$ the rate difference is minimal between the two strategies for both cases and it is equal to 0.25 bit/channel use.

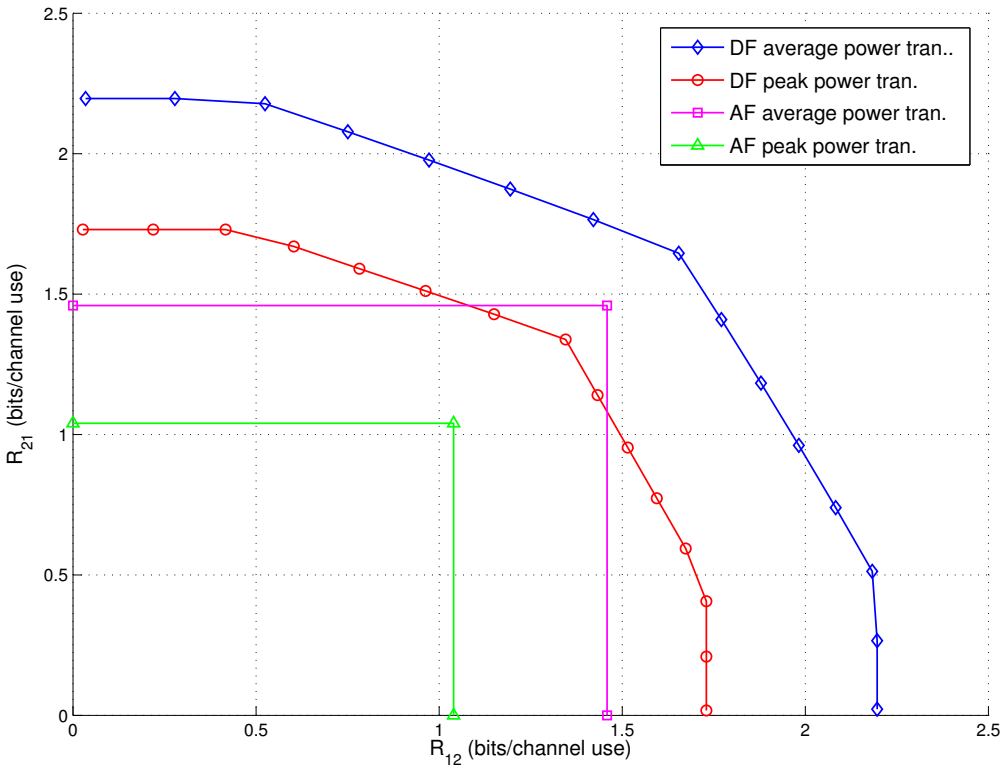

FIGURE 3.1: Achievable rate regions of DF and AF under average and peak transmit power for equal SNRs, $SNR_1 = SNR_2 = 10$dB

For $\theta \in [0, \frac{Pi}{4}]$, we consider the set of rates defined by $R_{21} = \tan(\theta)R_{12}$ as shown in Fig.3.2.

Fig.3.3 draws the optimal time division α for DF strategy under average and peak

transmit power for equal $SNR_i = 10$dB as function of θ. Fig.3.4 shows the

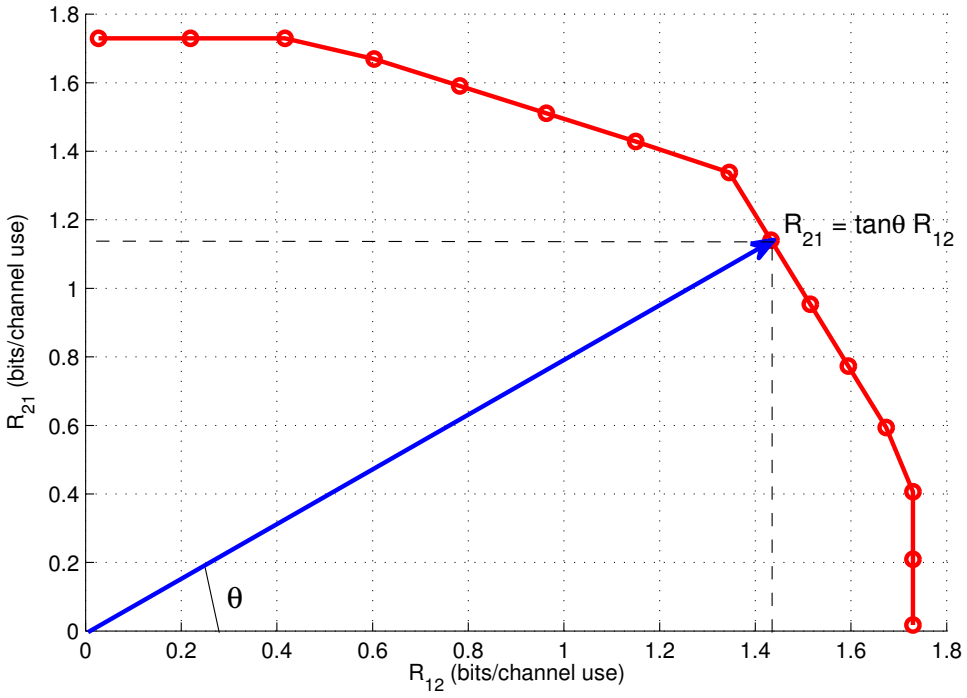

FIGURE 3.2: Illustrative example of the border rates dependence as function of the ray direction

achievable rate regions for the first optimization problem in (3.27) (dashed lines) and the second optimization problem in (3.30) (solid lines) with constrained error probabilities $c_i = 10^{-6}$ for each direction and a block length $n = 500$. We suppose that all nodes transmit under peak power with equal power budgets. We consider $SNR_1 = 10$ dB, and $SNR_2 = \delta SNR_1$ where $\delta \in [0, 1]$. In order to show the impact of the SNR asymmetry between T_1 and T_2, Fig 3.4 draws the achievable rates for different values of δ ranging from 0.25 to 1. Fig.3.5 shows the impact of the SNR asymmetry on the optimal α. The optimal α between the uplink and the downlink depends on the SNR values: when the SNRs are equal for all links, the optimal α is close (but not equal) to $\frac{1}{2}$. A peak for the direction $\theta = \frac{\pi}{4}$ is found i.e. when $R_{12} = R_{21}$. For the case of asymmetric SNRs ($\text{SNR}_2 \leq \text{SNR}_1$), the achievable rate region is limited by the weak link (T_2-relay) in both phases. The optimal α become an increasing function of $\tan(\theta)$ as the asymmetry between both links increases. In this case, more time is allocated to the MAC phase.

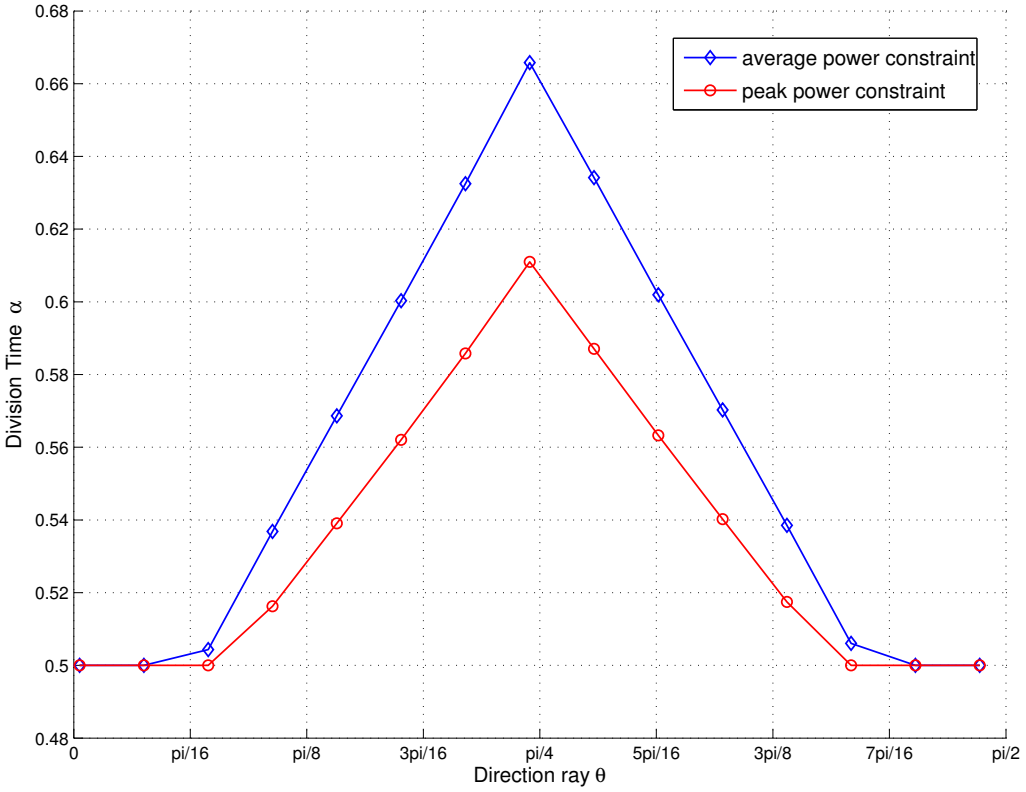

FIGURE 3.3: Optimal α with DF strategy for $\theta \in [0, \pi/2]$ under average and peak transmit power for equal SNR=10dB

3.4.2 Achievable Rate Regions with Transmit Power Optimization

Fig.3.6 shows the achievable rate regions for the problems in (3.27) and (3.30) when the transmit powers are optimized. A total power budget $P_{tot} = P_1 + P_2 + P_R$ should be satisfied for rates' maximization. This new constraint is added to the convex optimization problems. We suppose, here, that total $SNR = \frac{P_{tot}|h_i|^2}{\sigma_i^2} = 15$dB and $|h_1| = |h_2|$. The transmission rates are improved by using the optimal power allocation.

Fig.3.7 draws the power allocated at all nodes for the problem in (3.30) in the symmetric scenario. In this case, the powers allocated to the nodes T_1 and T_2 are identical. However, the relay transmits the composite signal with almost half of the power budget.

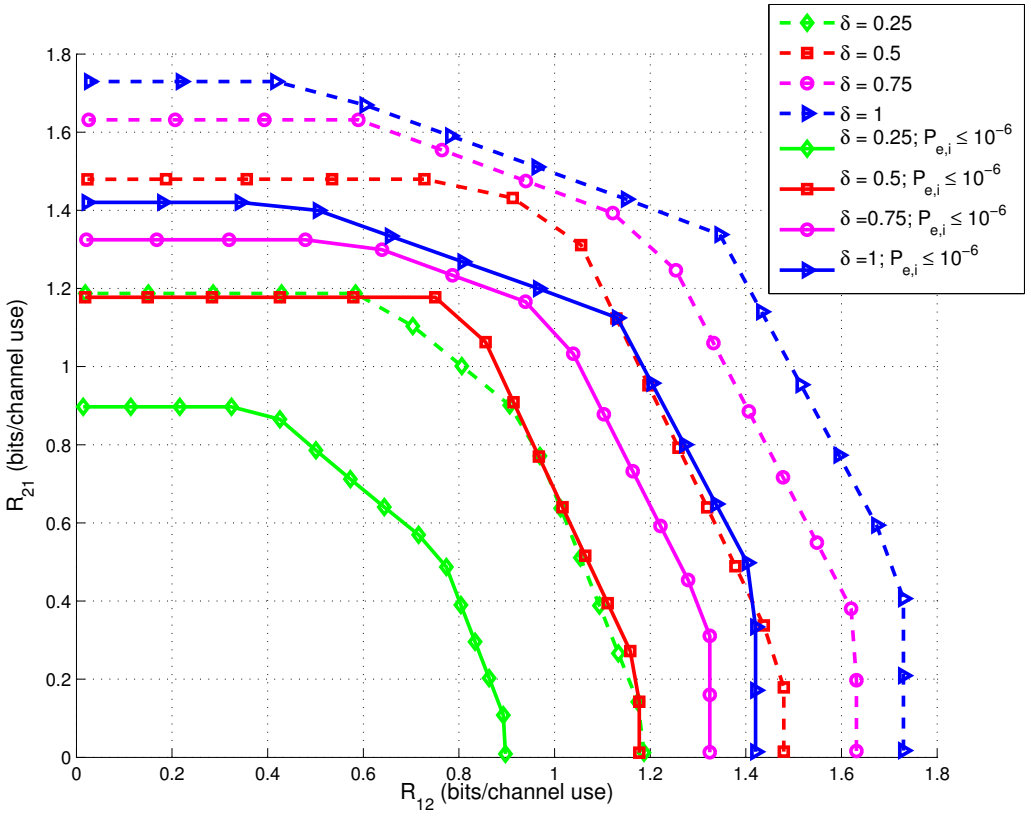

FIGURE 3.4: Maximum achievable rate regions for $P_{e,1}, P_{e,2} \leq 10^{-6}$, n = 500, $\mathrm{SNR}_1 = 10\mathrm{dB}$, $\mathrm{SNR}_2 = \delta\ \mathrm{SNR}_1$.

3.5 Conclusion

In this chapter, we investigated decode-and-forward strategy for two-way relay channel. With this strategy, the relay decodes jointly the transmitted signals from both communicating devices. We calculated end-to-end average error probabilities based on random coding error exponents. Then, we derived a DF rate region taking into account finite-length codewords and average error probability constraints. For this derivation, we optimized the time division between multiple access and broadcast phases. We also analyzed the dependence of the optimal time division as a function of the channel conditions of both communicating terminals and the rate requirement of both directions. Then, we considered optimal power allocation in the system. This has permitted the improvement of the rate region by more than 30 % over the fixed power allocation.

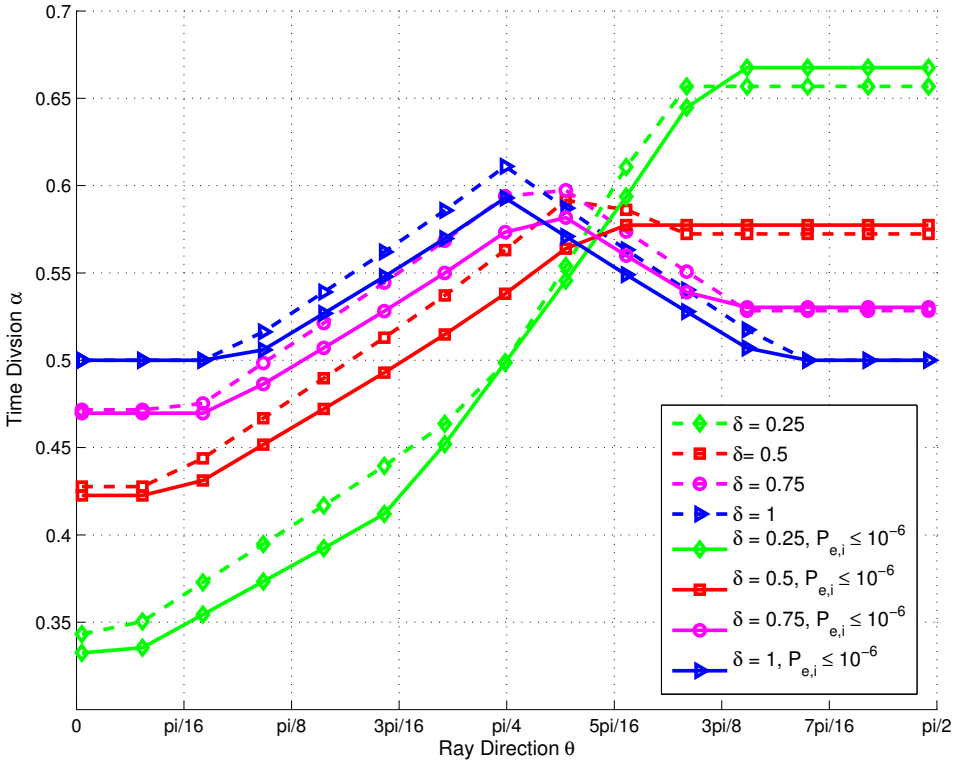

FIGURE 3.5: Optimal α for $P_{e,1}, P_{e,2} \leq 10^{-6}$, n = 500, SNR_1 =10dB, $\text{SNR}_2 = \delta\ \text{SNR}_1$.

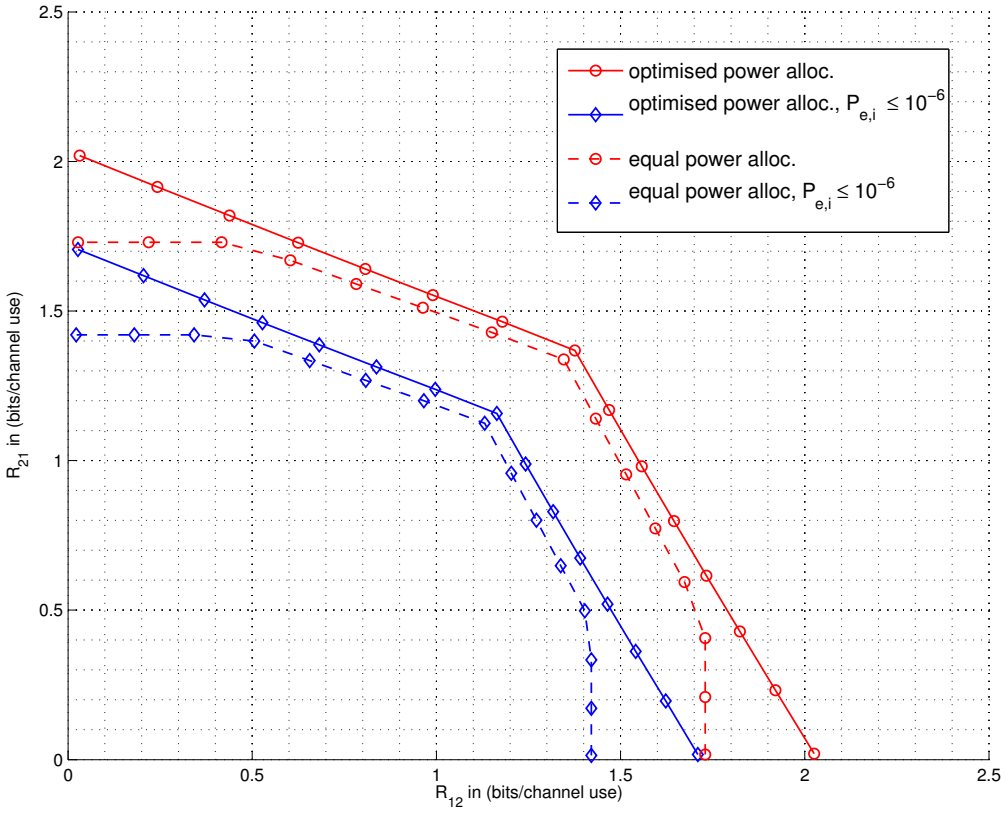

FIGURE 3.6: Achievable rate regions under fixed and optimized power allocations, SNR = 15dB, n= 500

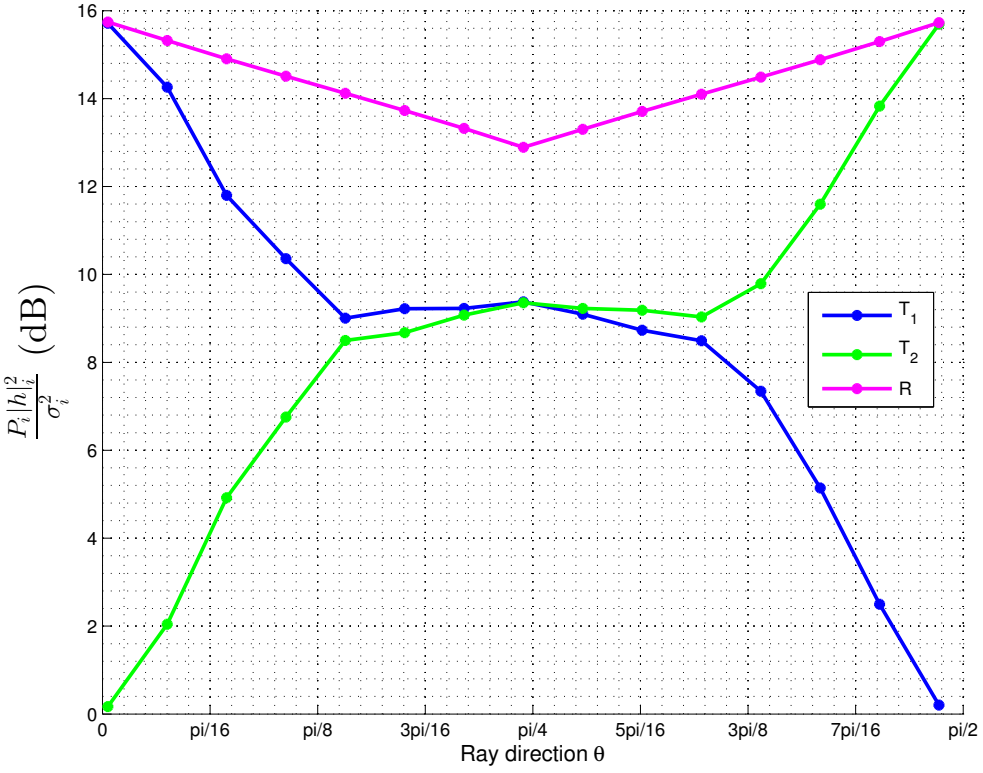

FIGURE 3.7: Power allocation for symmetric static channels, SNR = 15dB, n= 500

Chapter 4

Compress-and-Forward Schemes for Two-Way Relay Channel

In the previous chapters, achievable rate region of two-way relay channel have been presented for various relaying strategies based on random coding tools, which are impractical for real systems. Interestingly, structured codes have been found to be more advantageous in practical settings thanks to their reduced complexity [5]. Lattice codes represent an important class of structured codes that can be used in many wireless systems. They have the nice property to ensure that any integer-valued linear combination of codewords is a codeword. In this chapter, a scheme based on compress-and-forward lattice coding is first proposed. Then, this scheme is improved by performing a layered coding : a common layer is decoded by both receivers and a refinement layer is recovered only by the receiver which experiences the best channel conditions and the best side information. The achievable rates of the new scheme are characterized and are shown to be higher than those provided by the decode-and-forward strategy in some regions.

The content of this chapter has been partially published in [72].

4.1 Introduction

It has been shown in [14] that for an Additive White Gaussian Noise AWGN channel, lattice codes can achieve the Shannon capacity for Gaussian point-to-point communication. Based on this result, nested lattice codes are used in [81],[54] to implement pDF for Gaussian channels. In [77], the lattice based-scheme proposed in [81] has been extended for TWRC with more than one relay. However, the problem of pDF schemes is to guarantee phase coherence at the relay during the MAC phase [40].
With CF scheme, the relay does not decode any message, but rather compresses the received signal and sends a new message that includes some useful information about the original messages. This technique does not impose decoding rates at the relay as in DF-based schemes. The compression can be performed using Wyner-Ziv binning. This strategy has attracted particular attention since it offers a good trade-off between processing complexity at the relay and noise amplification. In this chapter, we propose a CF scheme that is based on nested lattice coding. In the MAC phase of this scheme, the communicating nodes simultaneously send their messages and the relay receives a mixture of the transmitted signals. The relay considers this mixture as a source which will be compressed and transmitted during the BC phase. Taking into account that each terminal has a partial knowledge of this source (namely, its own signal that has been transmitted during the MAC phase, which can then be considered as receiver side information), the BC phase is equivalent to a Wyner-Ziv compression setting with two decoders, each one having its own side information. Each user employs lattice decoding technique to retrieve its data based on the available side information. The proposed scheme can be seen as an extension of lattice quantization introduced in [91] to the TWRC model.

In the simplest situation, when a single "layer" of compression is performed, the relay broadcasts a common compressed message to both terminals. Therefore, it is easily understood that the achievable rates in both directions are constrained by the capacity of the worst channel. In this case, the user experiencing better channel and side information conditions is strongly constrained by this restriction on its

transmission rate. To overcome this limitation, the relay also sends an individual description of its output that serves as an enhancement compression layer to be recovered only by the best receiver. Therefore, the new scheme employs three nested lattices. The common message is encoded using two nested lattices while the refinement message is encoded with a finer lattice that contains the other two lattices. The channel codewords corresponding to the two layers are superimposed and sent during the BC phase. Through numerical analysis, we show that this layered scheme outperforms AF and CF strategies in all SNR regimes and DF strategy for specific SNR regions.

Layered coding for Wyner-Ziv problem has been addressed in [53] for lossy transmission over broadcast channel with degraded side information. In [26], the authors derive the achievable rate region of layered CF coding for TWRC, based on random coding approach. The authors in [52] and [78] proposed schemes for TWRC based on doubly nested lattice coding where different power constraints at all nodes are assumed. In these schemes, each of the two end terminals employs a different code (with carefully chosen rate) constructed from the lattice partition chain. The relay decodes a modulo-lattice sum of the transmitted codewords from the received signal. However, in [52] full-duplex nodes are considered and in [78], the direct link between both terminals is exploited and the transmission is performed in three phases. In these schemes, the relay follows a pDF strategy since it decodes a function of the transmitted lattice codewords. On the other hand, in our proposed enhancement scheme, doubly nested lattice coding is only employed at the relay for CF strategy and half-duplex terminals are considered with no direct link between the two end terminals. Furthermore, the relay does not need to know the other terminals' codebooks neither the total knowledge of the channel. It merely reconstructs its encoder from the channel module and the variances of the transmitted signals. To our knowledge, our work is the first that proposes a doubly nested lattice coding for CF relaying in TWRC. In order to derive the achievable rate regions of our proposed schemes, we first outline some preliminaries on lattice codes in the next section.

4.2 Preliminaries on Lattice Coding

We review the lattice properties that are required in the rest of this thesis. More details can be found in [5, 14].

A real n_1-dimensional lattice Λ is a subgroup of the Euclidean space $(\mathbb{R}^{n_1}, +)$. $\forall \lambda_1, \lambda_2 \in \Lambda$, $\lambda_1 + \lambda_2 \in \Lambda$. The nearest neighbour lattice quantizer of Λ is defined as $Q_\Lambda(\mathbf{x}) = \arg\min_{\lambda \in \Lambda} ||\mathbf{x} - \lambda||$ where $\mathbf{x} \in \mathbb{R}^{n_1}$ and $\|.\|$ is the Euclidean norm. The basic Voronoi cell of Λ is the set of points in $\mathbb{R}^{n_1}$ closer to the zero vector than to any other point of Λ ,

$$\mathcal{V}(\Lambda) = \{\mathbf{x} \mid Q_\Lambda(\mathbf{x}) = \mathbf{0}\}$$

The volume of a lattice

$$V := \mathrm{Vol}(\mathcal{V}(\Lambda)) = \int_{\mathbf{x}} dx$$

The second moment per dimension of Λ is

$$\sigma^2(\Lambda) := \frac{1}{n_1}.\frac{1}{V}\int_{\mathcal{V}(\Lambda)} ||\mathbf{x}||^2 d\mathbf{x}$$

The dimensionless normalized second moment is defined as

$$G(\Lambda) := \frac{\sigma^2(\Lambda)}{V^{2/n_1}}$$

The mod-Λ operation is defined as $\mathbf{x} \bmod \Lambda = \mathbf{x} - Q_\Lambda(\mathbf{x})$. It satisfies the distributive law:

(P1) $(\mathbf{x} \mod \Lambda + \mathbf{y}) \mod \Lambda = (\mathbf{x} + \mathbf{y}) \mod \Lambda$

A sequence of n_1-dimensional lattices $\Lambda^{(n_1)}$ is said to be good for quantization [90] if

$$G(\Lambda^{(n_1)}) \underset{n_1 \to \infty}{\longrightarrow} \frac{1}{2\pi e}$$

A sequence of n_1-dimensional lattices $\Lambda^{(n_1)}$ is said to be good for AWGN channel coding if for n_1-dimensional vector $\mathbf{Z} \sim \mathcal{N}(\mathbf{0}, \sigma^2 \mathbf{I}_{n_1})$, $P\{\mathbf{Z} \notin \mathcal{V}(\Lambda^{(n_1)})\}$ vanishes

when n_1 goes to ∞. In this case,

$$\mathrm{Vol}(\Lambda^{(n_1)}) \underset{n_1 \to \infty}{\longrightarrow} 2^{n_1 h(Z)}$$

where $h(\mathbf{Z}) = \frac{1}{2}\log(2\pi e\sigma^2)$ is the differential entropy of $\mathbf{Z}$ [58]. There exist lattices which are simultaneously good for quantization and channel coding in [12].

Lemma 4.1. *Crypto Lemma [14]. For a dither vector $\boldsymbol{T}$ independent of $\boldsymbol{X}$ and uniformly distributed over $\mathcal{V}(\Lambda)$, then $\boldsymbol{Y} = (\boldsymbol{X}+\boldsymbol{T}) \mod \Lambda$ is uniformly distributed over $\mathcal{V}(\Lambda)$ and is independent of $\boldsymbol{X}$*

We consider a pair of n_1-dimensional nested lattices (Λ_1, Λ_2) such as $\Lambda_2 \subset \Lambda_1$. The fine lattice is Λ_1 with basic Voronoi region $\mathcal{V}_1$ of volume V_1 and second moment per dimension $\sigma^2(\Lambda_1)$. The coarse lattice is Λ_2 with basic Voronoi region $\mathcal{V}_2$ of volume V_2 and second moment $\sigma^2(\Lambda_2)$. We remind the following property of nested lattices:

(P2) For $\Lambda_2 \subset \Lambda_1$, $Q_{\Lambda_2}(Q_{\Lambda_1}(x)) = Q_{\Lambda_1}(Q_{\Lambda_2}(x)) = Q_{\Lambda_2}(x)$

The points of the set $\Lambda_1 \cap \mathcal{V}_2 = \Lambda_1 \mod \Lambda_2$ represent the coset leaders of Λ_2 relative to Λ_1, where for each $\lambda \in \{\Lambda_1 \mod \Lambda_2\}$, the shifted lattice $\Lambda_{2,\lambda} = \Lambda_2 + \lambda$ is called a coset of Λ_2 relative to Λ_1. There are $\dfrac{V_2}{V_1}$ distinct cosets. It follows that the coding rate when using nested lattices is

$$R = \frac{1}{n_1}\log_2|\Lambda_1 \cap \mathcal{V}_2| = \frac{1}{n_1}\log_2\frac{V_2}{V_1} \quad \text{(bits per dimension)} \tag{4.1}$$

4.3 Achievable Rate Region for TWRC

Theorem 4.1. *For a Gaussian TWRC, under the assumptions a.1 to a.8, the convex hull of the following end-to-end rate-pairs (R_{12}, R_{21}) is achievable:*

$$R_{12} \leq \frac{\alpha}{2}\log_2\left(1+\frac{|h_1|^2P_1}{\sigma_R^2+\frac{\max\limits_{i\in\{1,2\}}|h_i|^2P_i+\sigma_R^2}{\left(1+\min\limits_{i\in\{1,2\}}\frac{|h_i|^2P_R}{\sigma_i^2}\right)^{\frac{1-\alpha}{\alpha}}-1}}\right) \tag{4.2}$$

$$R_{21} \leq \frac{\alpha}{2}\log_2\left(1+\frac{|h_2|^2P_2}{\sigma_R^2+\frac{\max\limits_{i\in\{1,2\}}|h_i|^2P_i+\sigma_R^2}{\left(1+\min\limits_{i\in\{1,2\}}\frac{|h_i|^2P_R}{\sigma_i^2}\right)^{\frac{1-\alpha}{\alpha}}-1}}\right) \tag{4.3}$$

for $\alpha \in [0,1]$.

The main idea of the proposed achievable scheme is the following: during the BC phase, the relay sends a quantized version of the signal that was received during the MAC phase. It uses nested lattices to generate a source index that will be sent using a rate achieving channel code. This index is decoded by both users and, based on their own information (sent during the MAC phase), each source node retrieves its destined message. The proof of Theorem4.1 is detailed in the next paragraphs: In Section 4.3.1, the lattice coding scheme for the source coding is presented. The end-to-end achievable rates are derived in Section 4.3.2 and finally in Section 4.3.3 the achievable rate region is obtained by appropriate optimization of lattice parameters.

4.3.1 Lattice-based Source Coding

We suppose that the elements of $\mathbf{X}_i$, $i = 1, 2$, are drawn from an independent identically distributed (i.i.d) Gaussian distribution with zero mean and variance P_i. Let $\mathbf{S}_i = h_i\mathbf{X}_i$ be the side information available at terminal T_i, $i = 1, 2$. The signal sent by the relay $\mathbf{Y}_R$ can be written in two ways as the sum of two independent Gaussian r.v.: the side information $\mathbf{S}_i$ and the unknown part $\mathbf{U}_i = \mathbf{Y}_R|\mathbf{S}_i = h_{\bar{i}}\mathbf{X}_{\bar{i}} + \mathbf{Z}_R$, $i \in \{1, 2\}$. From their received signals, each terminal T_i , $i \in \{1, 2\}$ decodes $\hat{\mathbf{U}}_i$ using $\mathbf{S}_i$. The variance per dimension of $\mathbf{U}_i$ is $\sigma^2_{U_i} = VAR(Y_R|S_i) = |h_{\bar{i}}|^2 P_{\bar{i}} + \sigma^2_R$.

In the following, we detail the proposed lattice source coding scheme.

4.3.1.1 Encoding

The lattice source encoding (LSE) operation is performed with four successive operations: first, the input signal $\mathbf{y}_R$ is scaled with a factor β. Then, a random dither $\mathbf{t}$ which is uniformly distributed over $\mathcal{V}_1$ is added. This dither, even random, is known by all nodes. The dithered scaled version of $\mathbf{y}_R$, $\beta\mathbf{y}_R + \mathbf{t}$ is quantized to the nearest point in Λ_1. The outcome of this operation is processed with a modulo-lattice operation in order to generate a vector $\mathbf{v}_R$ of size n_1 as shown in Fig.4.1.

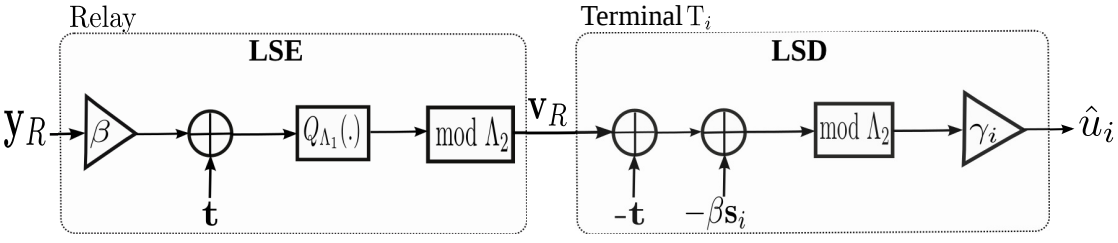

FIGURE 4.1: Lattice encoding at the relay and decoding at terminals T_i, $i = 1, 2$

$$\mathbf{v}_R = Q_{\Lambda_1}(\beta\mathbf{y}_R + \mathbf{t}) \mod \Lambda_2 \tag{4.4}$$

The relay sends the index of $\mathbf{v}_R$ that identifies a coset of Λ_2 relative to Λ_1 that contains $Q_{\Lambda_1}(\beta\mathbf{y}_R + \mathbf{t})$. By construction, the coset leader $\mathbf{v}_R$ is represented with $\log_2\left(\frac{V_2}{V_1}\right)$ bits. Thus, the rate of the source encoding scheme employed by the

relay is R given by equation (4.1). We assume further that Λ_1 is good for quantization and Λ_2 is good for channel coding [91]. For high dimension n_1 and according to the properties of good lattices, we have $\frac{1}{n_1}\log_2(V_i) \approx \frac{1}{2}\log_2(2\pi e\sigma^2(\Lambda_i))$, $i \in \{1,2\}$. Thus R reads

$$R = \frac{1}{2}\log_2\left(\frac{\sigma^2(\Lambda_2)}{\sigma^2(\Lambda_1)}\right) \tag{4.5}$$

4.3.1.2 Decoding

For both users, $\mathbf{v}_R$ is decoded first. Then $\hat{\mathbf{u}}_i$ is reconstructed with a lattice source decoder (LSD) using the side information $\mathbf{s}_i$ as

$$\hat{\mathbf{u}}_i = \gamma_i((\mathbf{v}_R - \mathbf{t} - \beta\mathbf{s}_i) \mod \Lambda_2),\ i = 1,2 \tag{4.6}$$

where γ_i, $i \in \{1,2\}$ are the scaling factors at each decoder.

4.3.2 Rate Analysis

At the relay, the message m_R corresponding to the index of $\mathbf{v}_R$ is mapped to a codeword $\mathbf{x}_R$ of size n_2. We suppose that the elements of the r.v. $\mathbf{X}_R$ are drawn from an i.i.d Gaussian distribution with zero mean and variance P_R. The broadcast rate from the relay to both terminals is bounded by the capacity of the worst individual relay-terminal channel capacity $\min(I(X_R;Y_1), I(X_R;Y_2))$. From the Shannon's source-channel separation theorem [6], we have

$$n_1 R \leq n_2 \min(I(X_R;Y_1), I(X_R;Y_2)) \tag{4.7}$$

Since real Gaussian codebooks are used for all transmissions, we have: $I(X_R;Y_i) = \frac{1}{2}\log_2\left(1 + \frac{|h_i|^2 P_R}{\sigma_i^2}\right)$, $i = 1,2$. Finally, by combining equations (4.5) and (4.7), we obtain the following constraint on the achievable rates

$$n_1 \log_2\left(\frac{\sigma^2(\Lambda_2)}{\sigma^2(\Lambda_1)}\right) \leq n_2 \log_2\left(1 + \min_{i\in\{1,2\}} \frac{|h_i|^2 P_R}{\sigma_i^2}\right) \tag{4.8}$$

This constraint ensures that index m_R is transmitted reliably to both terminals and $\mathbf{v}_R$ is available at the input of the LSD of both receivers. At terminal T_i, using the distributive property (P1), $\hat{\mathbf{u}}_i$ in (4.6) can be written as:

$$\hat{\mathbf{u}}_i = \gamma_i((\beta\mathbf{u}_i + \mathbf{e}_q) \bmod \Lambda_2) \tag{4.9}$$

$$\equiv \gamma_i(\beta\mathbf{u}_i + \mathbf{e}_q) \tag{4.10}$$

where $\mathbf{e}_q = Q_{\Lambda_1}(\beta\mathbf{y}_R + \mathbf{t}) - (\beta\mathbf{y}_R + \mathbf{t}) = -(\beta\mathbf{y}_R + \mathbf{t}) \mod \Lambda_1$, is the quantization error. By *Lemma 4.1*, $\mathbf{E}_q$ is independent from $\mathbf{Y}_R$, thus from $\mathbf{U}_i$, and it is uniformly distributed over $\mathcal{V}_1$ thus the variance of $\mathbf{E}_q$ per dimension is $\sigma^2(\Lambda_1)$. The equivalence between (4.9) and (4.10) is valid only if $\beta\mathbf{u}_i + \mathbf{e}_q \in \mathcal{V}_2$. According to [91], with good channel coding lattices, the probability $\Pr(\beta\mathbf{U}_i + \mathbf{E}_q \notin \mathcal{V}_2)$ vanishes asymptotically provided that:

$$\frac{1}{n_1}\mathbb{E}\|\beta\mathbf{U}_i + \mathbf{E}_q\|^2 = \beta^2\sigma^2_{U_i} + \sigma^2(\Lambda_1) \leq \sigma^2(\Lambda_2) \tag{4.11}$$

By replacing $\mathbf{U}_i$ by its value we conclude that:

$$\hat{\mathbf{U}}_i = \gamma_i(\beta(h_1\mathbf{X}_1 + \mathbf{Z}_R) + \mathbf{E}_q) \tag{4.12}$$

Let $\mathbf{Z}_{eq,i} = \gamma_i(\beta\mathbf{Z}_R + \mathbf{E}_q)$ be the effective additive noise at terminal T_i. For high dimension assumption, $n_1 \to \infty$, we can approximate the uniform variable $\mathbf{E}_q$ over $\mathcal{V}_1$ by a Gaussian variable $\mathbf{Z}_q$ with the same variance [90]. Therefore, the communication between T_1 and T_2 (resp. T_2 and T_1) is equivalent to a virtual additive Gaussian channel where the Gaussian noise is given by $\mathbf{Z}_{eq,i}$. The achievable rates of both links satisfy in this case:

$$nR_{12} \leq \frac{n_1}{2}\log_2\left(1 + \frac{\beta^2|h_1|^2P_1}{\beta^2\sigma_R^2 + \sigma^2(\Lambda_1)}\right) \tag{4.13}$$

$$nR_{21} \leq \frac{n_1}{2}\log_2\left(1 + \frac{\beta^2|h_2|^2P_2}{\beta^2\sigma_R^2 + \sigma^2(\Lambda_1)}\right) \tag{4.14}$$

4.3.3 Achievable Rate Region

The rate region that is achieved by the proposed scheme is characterized by the constraints (4.13), (4.14), (4.8) and (4.11). Without loss of generality, we assume that $|h_2|^2 P_2 \leq |h_1|^2 P_1$. With this setting, T_2 is the terminal who experiences the weakest side information. Denoting $\alpha = \dfrac{n_1}{n}$, from (4.8) and (4.11), the lower bound of $\sigma^2(\Lambda_1)$ is given by

$$\sigma^2(\Lambda_1) \geq \frac{\beta^2 \sigma_{U_2}^2}{\left(1 + \min\limits_{i \in \{1,2\}} \dfrac{|h_i|^2 P_R}{\sigma_i^2}\right)^{\frac{1-\alpha}{\alpha}} - 1} \tag{4.15}$$

The constraints on the achievable rates in (4.13) and (4.14) can be written as

$$R_{12} \leq \frac{\alpha}{2} \log_2 \left(1 + \mathrm{SNR}_{1\to 2}\right) \tag{4.16}$$

$$R_{21} \leq \frac{\alpha}{2} \log_2 \left(1 + \mathrm{SNR}_{2\to 1}\right) \tag{4.17}$$

where $\mathrm{SNR}_{1\to 2}$ and $\mathrm{SNR}_{2\to 1}$ are the virtual end-to-end SNRs, defined as follows:

$$\mathrm{SNR}_{1\to 2} = \frac{\beta^2 |h_1|^2 P_1}{\beta^2 \sigma_R^2 + \sigma^2(\Lambda_1)} \tag{4.18}$$

$$\mathrm{SNR}_{2\to 1} = \frac{\beta^2 |h_2|^2 P_2}{\beta^2 \sigma_R^2 + \sigma^2(\Lambda_1)} \tag{4.19}$$

We notice that $\mathrm{SNR}_{1\to 2}$ and $\mathrm{SNR}_{2\to 1}$ are maximized when $\sigma^2(\Lambda_1)$ is minimal. Thus the optimal choice on the second moment of Λ_1 is

$$\sigma^2(\Lambda_1)_{\min} = \frac{\beta^2 \sigma_{U_2}^2}{\left(1 + \min\limits_{i \in \{1,2\}} \dfrac{|h_i|^2 P_R}{\sigma_i^2}\right)^{\frac{1-\alpha}{\alpha}} - 1} \tag{4.20}$$

If $|h_1|^2 P_1 \leq |h_2|^2 P_2$, $\sigma_{U_2}^2$ is replaced with $\sigma_{U_1}^2$ in (4.20). Finally, replacing $\sigma^2(\Lambda_1)_{\min}$ in (4.18) and (4.19), Eq. (4.2) and (4.3) are verified and the proof is concluded.

Remark 4.1. For the transmission problem of the TWRC, the achievable rate region is independent from the choice of the decoders scaling factors γ_i. It is also independent of the encoder scaling factor β provided that $\sigma^2(\Lambda_1)$ is set to its

smallest value $\sigma^2(\Lambda_1)_{\min}$ in (4.20). As will be shown in the next section, these parameters are involved in the source coding problem addressed in [73].

4.3.4 Analog Signal Transmission

When using the relay to transmit analog signals; the distortion that affects the reconstructed signals becomes the main performance metric. The second moment of this distortion is given by

$$\frac{1}{n_1}\mathbb{E}\|\mathbf{Y}_R - \hat{\mathbf{Y}}_{Ri}\|^2 = D_i \ ; \ i \in \{1,2\} \tag{4.21}$$

where $\mathbf{Y}_R = \mathbf{U}_i + \mathbf{S}_i$ and $\hat{\mathbf{Y}}_{Ri} = \hat{\mathbf{U}}_i + \mathbf{S}_i$. By replacing $\hat{\mathbf{U}}_i$ by its value in (4.10), (4.21) becomes

$$D_i = (1-\gamma_i\beta)^2\sigma^2_{U_i} + \gamma_i^2\sigma^2(\Lambda_1) \ ; \ i \in \{1,2\} \tag{4.22}$$

For the analog signal transmission, this distortion has to be minimized to obtain the optimal source coding scheme. For fixed β, the distortion at T_i depends only on two parameters namely γ_i and $\sigma^2(\Lambda_1)$. The optimal distortion can be obtained by calculating the following derivatives:

$$\frac{\partial D_i}{\partial \gamma_i} = 0 \Rightarrow \gamma_i^* = \frac{\beta\sigma^2_{U_i}}{\beta^2\sigma^2_{U_i} + \sigma^2_{\Lambda_1}} \tag{4.23a}$$

$$\frac{\partial D_i}{\partial \sigma^2(\Lambda_1)} = 0 \Rightarrow \gamma_i^* = 0 \tag{4.23b}$$

where γ_i^*, $i \in \{1,2\}$ are the optimal decoder scaling factors.
Since $\gamma_i > 0$, $\frac{\partial D_i}{\partial \sigma^2(\Lambda_1)} > 0$. Thus, the function D_i is increasing with $\sigma^2(\Lambda_1)$ and $\sigma^2(\Lambda_1)_{\min}$ in (4.20) is the optimal choice that minimizes the distortion at each terminal. Therefore,

$$\gamma_i^* = \frac{\beta\sigma^2_{U_i}}{\beta^2\sigma^2_{U_i} + \sigma^2(\Lambda_1)_{\min}} \ , \ i \in \{1,2\} \tag{4.24}$$

By replacing $\sigma^2(\Lambda_1)$ and γ_i by their optimal values, we obtain the minimal value of $D_i^{\min}$ given by

$$D_i^{\min} = \frac{\sigma^2(\Lambda_1)_{\min}\sigma_{U_i}^2}{\beta^2\sigma_{U_i}^2 + \sigma^2(\Lambda_1)_{\min}} \tag{4.25}$$

$$= \frac{\sigma_{U_2}^2\sigma_{U_i}^2}{\left(\left(1 + \min\limits_{i\in\{1,2\}} \frac{|h_i|^2 P_R}{\sigma_i^2}\right)^{\frac{1-\alpha}{\alpha}} - 1\right)\sigma_{U_i}^2 + \sigma_{U_2}^2} \quad , \; i \in \{1,2\} \tag{4.26}$$

$D_i^{\min}$, $i \in \{1,2\}$, just like the achievable rates, are independent of β. However, for an arbitrary fixed β, the lattice parameters and receivers scaling factors depend on that choice.

Comments on the Distortions

At terminal T_2, the distortion writes:

$$\begin{aligned} D_2^{\min} &= \frac{\sigma_{U_2}^2\sigma_{U_2}^2}{(A-1)\sigma_{U_2}^2 + \sigma_{U_2}^2} \\ &= \frac{\sigma_{U_2}^2}{A} \end{aligned}$$

where $A = \left(1 + \min\limits_{i\in\{1,2\}} \frac{|h_i|^2 P_R}{\sigma_i^2}\right)^{\frac{1-\alpha}{\alpha}}$ that can be written as

$$\frac{\sigma_{U_2}^2}{D_2^{\min}} = \left(1 + \min_{i\in\{1,2\}} \frac{|h_i|^2 P_R}{\sigma_i^2}\right)^{\frac{1-\alpha}{\alpha}}$$

or equivalently,

$$\alpha \log_2\left(\frac{\sigma_{U_2}^2}{D_2^{\min}}\right) = (1-\alpha)\log_2\left(1 + \min_{i\in\{1,2\}} \frac{|h_i|^2 P_R}{\sigma_i^2}\right) \tag{4.27}$$

We find, in the left hand side of the equation, the Wyner-Ziv rate distortion function [85] of the Gaussian source $\mathbf{Y}_R$ with side information $\mathbf{S}_2$ at the decoder.

It is defined as the minimum rate needed to achieve $D_2^{\min}$ and is given by:

$$R_{WZ}(D_2^{\min}) = \frac{1}{2}\log_2\left(\frac{\sigma_{U_2}^2}{D_2^{\min}}\right) \tag{4.28}$$

Equation (4.27) represents the separate source-channel coding constraint at the optimality. On the other hand, the optimal value of γ_2 is

$$\gamma_2^* = \frac{\beta\sigma_{U_2}^2}{\beta^2\sigma_{U_2}^2 + \sigma^2(\Lambda_1)_{\min}} \tag{4.29}$$

$$= \frac{1}{\beta}\frac{A-1}{A} \tag{4.30}$$

We can verify that if $\beta = \gamma_2^*$ then $\beta = \sqrt{1 - \frac{D_2^{\min}}{\sigma_{U_2}^2}}$. The expression matches with the optimal scaling factor reported in [85, 73] for the optimum Gaussian forward test channel. In this case, $\sigma^2(\Lambda_1)_{\min} = D_2^{\min}$ which is consistent with the source coding parameters choices in [73]. By replacing the values of β and $D_2^{\min}$, one can verify that, in this case, the derived rate region coincides with random coding rate region given by equations (2.28), (2.29), (2.30) in Section 2.3.3 in Chapter 2.

At terminal T_1, the reconstruction distortion is lower than $D_2^{\min}$ of terminal T_2. This is compatible with the fact that T_1 has the best side information quality and the proposed achievable scheme is optimal for the worst user.

4.4 Improved Achievable Rate Region for TWRC

In the previous section, we presented a PNC scheme where a common information is sent from the relay to both users. The achievable rates by this scheme depend only on the ratio $\frac{\sigma^2(\Lambda_1)_{\min}}{\beta^2}$. This ratio is defined in equation (4.20) by the variance $\sigma_{U_i}^2$ of the unknown part of the source at the terminal T_i and the lowest channel coefficient amplitude $\min\limits_{i\in\{1,2\}} \frac{|h_i|^2}{\sigma_i^2}$. Thus, the achievable rates are limited by the user which has the weakest side information and also the worst channel conditions. In this case, the best user suffers from this limitation on its achievable rates. In order to improve its rate, an additional refinement information can be sent from

the relay, that can be only decoded by this user.

We have supposed previously that T_2 is the worst user, then T_1 is the best user which has better channel and side information i.e $|h_1| \geq |h_2|$ and $|h_1|^2 P_1 \geq |h_2|^2 P_2$. For the refinement scheme, an achievable rate region for TWRC is given in *Theorem 4.2*

Theorem 4.2. *For a Gaussian TWRC, under the assumptions a.1 to a.9, the convex hull of the following end-to-end rate pairs* (R_{12}, R_{21}) *is achievable:*

$$R_{12} \leq \frac{\alpha}{2} \log_2 \left(1 + \frac{|h_1|^2 P_1}{\sigma_R^2 + \frac{|h_1|^2 P_1 + \sigma_R^2}{\left(1 + \frac{\nu |h_2|^2 P_R}{(1-\nu)|h_2|^2 P_R + \sigma_2^2}\right)^{\frac{1-\alpha}{\alpha}} - 1}} \right) \tag{4.31}$$

$$R_{21} \leq \frac{\alpha}{2} \log_2 \left(1 + \frac{|h_2|^2 P_2}{\sigma_R^2 + \frac{|h_1|^2 P_1 + \sigma_R^2}{\left(1 + \frac{(1-\nu)|h_1|^2 P_R}{\sigma_1^2}\right)^{\frac{1-\alpha}{\alpha}} \left[\left(1 + \frac{\nu |h_2|^2 P_R}{(1-\nu)|h_2|^2 P_R + \sigma_2^2}\right)^{\frac{1-\alpha}{\alpha}} - 1 \right]}} \right) \tag{4.32}$$

for $\alpha, \nu \in [0, 1]$

The main idea of the rate achieving scheme is to broadcast a common message decodable by both users and a superimposed refinement message decodable only by the best user.

The proof of Theorem 4.2 is detailed in the following subsections.

4.4.1 Doubly Nested Lattices for Source Coding

We use a doubly nested lattice chain $(\Lambda_0, \Lambda_1, \Lambda_2)$ such as $\Lambda_2 \subset \Lambda_1 \subset \Lambda_0$. We require that Λ_2 is good for channel coding, Λ_1 is simultaneously good for channel and source coding and Λ_0 is good for source coding.

From these lattices, we form three codebooks

$$\mathcal{C}_c = \Lambda_1 \cap \mathcal{V}_2$$

$$\mathcal{C}_r = \Lambda_0 \cap \mathcal{V}_1$$

$$\mathcal{C}_1 = \Lambda_0 \cap \mathcal{V}_2$$

with the following coding rates:

$$R_c = \frac{1}{n_1}\log_2\left(\frac{V_2}{V_1}\right) \underset{n_1\to\infty}{\longrightarrow} \frac{1}{2}\log_2\left(\frac{\sigma^2(\Lambda_2)}{\sigma^2(\Lambda_1)}\right) \tag{4.33}$$

$$R_r = \frac{1}{n_1}\log_2\left(\frac{V_1}{V_0}\right) \underset{n_1\to\infty}{\longrightarrow} \frac{1}{2}\log_2\left(\frac{\sigma^2(\Lambda_1)}{\sigma^2(\Lambda_0)}\right) \tag{4.34}$$

$$R_1 = R_c + R_r = \frac{1}{n_1}\log_2\left(\frac{V_2}{V_0}\right) \underset{n_1\to\infty}{\longrightarrow} \frac{1}{2}\log_2\left(\frac{\sigma^2(\Lambda_2)}{\sigma^2(\Lambda_0)}\right) \tag{4.35}$$

where R_c is the common source rate, R_r is the refinement source rate and R_1 is the total source rate at terminal T_1.

4.4.1.1 Encoding

The input signal $\mathbf{y}_R$ is scaled with a factor β. Then, a random dither $\mathbf{t}$ which is uniformly distributed over $\mathcal{V}_1$ is added. This dither is known by all nodes. The dithered scaled version of $\mathbf{y}_R$, $\beta\mathbf{y}_R + \mathbf{t}$, is quantized to the nearest point in Λ_0. The outcome of this operation is processed two times to generate two messages: First, the coset leader of Λ_1 relative to Λ_0, $\mathbf{v}_{Rr}$, is generated by a modulo-lattice operation. The index of $\mathbf{v}_{Rr}$ identifies the refinement message. Second, another quantization to the nearest point in Λ_1 is performed and processed with another modulo-lattice operation to generate the coset leader of Λ_2 relative to Λ_1, $\mathbf{v}_{Rc}$. The index of $\mathbf{v}_{Rc}$ identifies the common message. Fig.4.2 shows the LSE operation.

$$\mathbf{v}_{Rr} = Q_{\Lambda_0}(\beta\mathbf{y}_R + \mathbf{t}) \mod \Lambda_1 \tag{4.36}$$

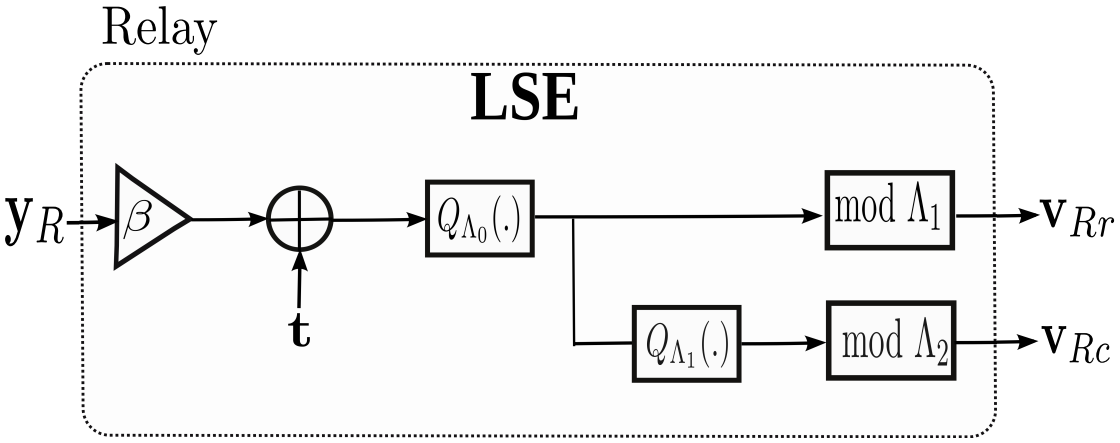

Figure 4.2: Layered Lattice encoding at the relay

We verify that $\mathbf{v}_{Rr} \in \mathcal{C}_r$

$$\mathbf{v}_{Rc} = Q_{\Lambda_1}(Q_{\Lambda_0}(\beta \mathbf{y}_R + \mathbf{t})) \mod \Lambda_2 \tag{4.37}$$

$$= Q_{\Lambda_1}(\beta \mathbf{y}_R + \mathbf{t}) \mod \Lambda_2 \tag{4.38}$$

We also verify that $\mathbf{v}_{Rc} \in \mathcal{C}_c$ and we find the same common message generated in (4.4). In addition, the total message sent to T_1, $\mathbf{v}_{R1} \in \mathcal{C}_1$ is given by

$$\mathbf{v}_{R1} = \mathbf{v}_{Rc} + \mathbf{v}_{Rr} \tag{4.39a}$$

$$= Q_{\Lambda_0}(\beta \mathbf{y}_R + \mathbf{t}) \mod \Lambda_1 + Q_{\Lambda_1}(\beta \mathbf{y}_R + \mathbf{t}) \mod \Lambda_2 \tag{4.39b}$$

$$= Q_{\Lambda_0}(\beta \mathbf{y}_R + \mathbf{t}) - Q_{\Lambda_1}(Q_{\Lambda_0}(\beta \mathbf{y}_R + \mathbf{t})) + Q_{\Lambda_1}(\beta \mathbf{y}_R + \mathbf{t}) - Q_{\Lambda_2}(Q_{\Lambda_1}(\beta \mathbf{y}_R + \mathbf{t})) \tag{4.39c}$$

$$= Q_{\Lambda_0}(\beta \mathbf{y}_R + \mathbf{t}) - Q_{\Lambda_2}(\beta \mathbf{y}_R + \mathbf{t}) \tag{4.39d}$$

$$= Q_{\Lambda_0}(\beta \mathbf{y}_R + \mathbf{t}) - Q_{\Lambda_2}(Q_{\Lambda_0}(\beta \mathbf{y}_R + \mathbf{t})) \tag{4.39e}$$

$$= Q_{\Lambda_0}(\beta \mathbf{y}_R + \mathbf{t}) \mod \Lambda_2 \tag{4.39f}$$

The equalities follow from the definition of modulo-Λ operation and the nested lattice property (P2) presented in Section 4.2.

4.4.1.2 Decoding

At terminal T_2, $\mathbf{v}_{Rc}$ is decoded. Then $\hat{\mathbf{u}}_2$ is reconstructed with an LSD using the side information $\mathbf{s}_2$ as

$$\hat{\mathbf{u}}_2 = \gamma_2((\mathbf{v}_{Rc} - \mathbf{t} - \beta\mathbf{s}_2) \mod \Lambda_2) \tag{4.40}$$

At terminal T_1, $\mathbf{v}_{Rc}$ and $\mathbf{v}_{Rr}$ are both decoded correctly. These messages are used to recalculate the total message $\mathbf{v}_{R1}$ from (4.39a). Finally the decoder reconstructs $\hat{\mathbf{u}}_1$ defined by (4.41) and shown in Fig. 4.3.

$$\hat{\mathbf{u}}_1 = \gamma_1((\mathbf{v}_{R1} - \mathbf{t} - \beta\mathbf{s}_1) \mod \Lambda_2) \tag{4.41}$$

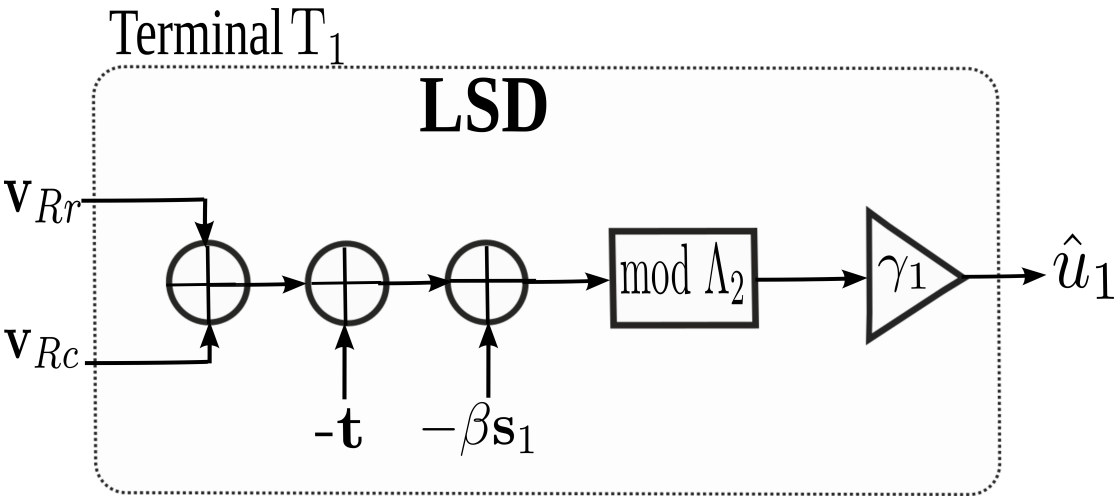

FIGURE 4.3: Lattice source decoding at the Terminal T_1

4.4.2 Rate Analysis

At the relay, the indices of $\mathbf{v}_{Rc}$ and $\mathbf{v}_{Rr}$ are generated. Then they are mapped to the channel codewords $\mathbf{x}_{Rc}$ and $\mathbf{x}_{Rr}$. The relay sends $\mathbf{x}_R(m_R)$ which is the superposition of $\mathbf{x}_{Rc}$ and $\mathbf{x}_{Rr}$ with transmit power νP_R and $(1-\nu)P_R$, $\nu \in \{0, 1\}$, respectively. The refinement codeword $\mathbf{x}_{Rr}$ is encoded on top of the common

codeword $\mathbf{x}_{Rc}$ and it is treated as an interference while decoding the common message. Thus, $\mathbf{X}_{Rc} \rightarrow \mathbf{X}_r \rightarrow (\mathbf{Y}_1, \mathbf{Y}_2)$ form a Markov chain. As described in previous one layer PNC scheme, the transmission rate at the relay is bounded by the worst relay-terminal channel capacity for the common message, and by the relay-T_1 channel for the refinement message. In addition, the source-channel separation ensures that the codewords $\mathbf{x}_{Rc}$ and $\mathbf{x}_{Rr}$ are transmitted reliably to the terminals and that $\mathbf{v}_{Rc}$ and $\mathbf{v}_{Rr}$ are available at the LSD input of corresponding receivers. Therefore, the rates verify the following conditions

$$n_1 R_c \leq n_2 \min\{I(X_{Rc}; Y_1), I(X_{Rc}; Y_2)\} \tag{4.42}$$

$$n_1 R_r \leq n_2 I(X_{Rr}; Y_1 | X_{Rc}) \tag{4.43}$$

For real Gaussian codebooks, we have

$$I(X_{Rc}; Y_1) = \frac{1}{2} \log_2 \left(1 + \frac{\nu |h_1|^2 P_R}{(1-\nu)|h_1|^2 P_R + \sigma_1^2}\right)$$

$$I(X_{Rc}; Y_2) = \frac{1}{2} \log_2 \left(1 + \frac{\nu |h_2|^2 P_R}{(1-\nu)|h_2|^2 P_R + \sigma_2^2}\right)$$

$$I(X_{Rr}; Y_1 | X_{Rc}) = \frac{1}{2} \log_2 \left(1 + \frac{(1-\nu)|h_1|^2 P_R}{\sigma_1^2}\right)$$

Since $|h_2| \leq |h_1|$, $\min\{I(X_{Rc}; Y_1), I(X_{Rc}; Y_2)\} = I(X_{Rc}; Y_2)$. Using equations (4.33), (4.34), (4.42) and (4.43), the rates' conditions become

$$n_1 \log_2 \left(\frac{\sigma^2(\Lambda_2)}{\sigma^2(\Lambda_1)}\right) \leq n_2 \log_2 \left(1 + \frac{\nu |h_2|^2 P_R}{(1-\nu)|h_2|^2 P_R + \sigma_2^2}\right) \tag{4.44}$$

$$n_1 \log_2 \left(\frac{\sigma^2(\Lambda_1)}{\sigma^2(\Lambda_0)}\right) \leq n_2 \log_2 \left(1 + \frac{(1-\nu)|h_1|^2 P_R}{\sigma_1^2}\right) \tag{4.45}$$

Now, $\hat{\mathbf{u}}_1$ and $\hat{\mathbf{u}}_2$ can be calculated from (4.41) and (4.40).

At terminal T_2, $\hat{\mathbf{u}}_2$ can be written as:

$$\hat{\mathbf{u}}_2 = \gamma_2((\beta \mathbf{u}_2 + \mathbf{e}_{q,1}) \mod \Lambda_2) \tag{4.46}$$

$$\equiv \gamma_2(\beta \mathbf{u}_2 + \mathbf{e}_{q,1}) \tag{4.47}$$

Where $\mathbf{e}_{q,1}$ is the quantization error at lattice Λ_1 given by

$$\mathbf{e}_{q,1} = Q_{\Lambda_1}(\beta\mathbf{y}_R + \mathbf{t})) - (\beta\mathbf{y}_R + \mathbf{t}) = -(\beta\mathbf{y}_R + \mathbf{t}) \mod \Lambda_1$$

Following the same analysis of Section 4.3.2, the equivalence between (4.46) and (4.47) is verified and $\Pr(\beta\mathbf{U}_2 + \mathbf{E}_{q,1} \notin \mathcal{V}_2)$ vanishes asymptotically provided that:

$$\frac{1}{n_1}\mathbb{E}\|\beta\mathbf{U}_2 + \mathbf{E}_{q,1}\|^2 = \beta^2\sigma_{U_2}^2 + \sigma^2(\Lambda_1) \leq \sigma^2(\Lambda_2) \tag{4.48}$$

In this case, the achievable rate at T_2 is

$$nR_{12} \leq \frac{n_1}{2}\log_2\left(1 + \frac{\beta^2|h_1|^2P_1}{\beta^2\sigma_R^2 + \sigma^2(\Lambda_1)}\right) \tag{4.49}$$

At terminal T_1, $\hat{\mathbf{u}}_1$ can be written as:

$$\hat{\mathbf{u}}_1 = \gamma_1((\beta\mathbf{u}_1 + \mathbf{e}_{q,0}) \mod \Lambda_2) \tag{4.50}$$

$$\equiv \gamma_1(\beta\mathbf{u}_1 + \mathbf{e}_{q,0}) \tag{4.51}$$

Where $\mathbf{e}_{q,0}$ is the quantization error at lattice Λ_0 given by

$$\mathbf{e}_{q,0} = Q_{\Lambda_0}(\beta\mathbf{y}_R + \mathbf{t}) - (\beta\mathbf{y}_R + \mathbf{t}) = -(\beta\mathbf{y}_R + \mathbf{t}) \mod \Lambda_0$$

We can prove by using *Lemma 1* that $\mathbf{E}_{q,0}$ is independent from $\mathbf{Y}_R$, thus from $\mathbf{U}_1$, and it is uniformly distributed over $\mathcal{V}_0$. Therefore, $\mathrm{VAR}(E_{q,0}) = \sigma^2(\Lambda_0)$. The equivalence between (4.50) and (4.51) is valid only if $\beta\mathbf{u}_1 + \mathbf{e}_{q,0} \in \mathcal{V}_2$. Choosing again good channel coding lattices, the probability $\Pr(\beta\mathbf{U}_1 + \mathbf{E}_{q,0} \notin \mathcal{V}_2)$ vanishes asymptotically provided that:

$$\frac{1}{n_1}\mathbb{E}\|\beta\mathbf{U}_1 + \mathbf{E}_{q,0}\|^2 = \beta^2\sigma_{U_1}^2 + \sigma^2(\Lambda_0) \leq \sigma^2(\Lambda_2) \tag{4.52}$$

Thus,

$$\hat{\mathbf{U}}_1 = \gamma_1(\beta h_1\mathbf{X}_2 + \beta\mathbf{Z}_R + \mathbf{E}_{q,0})$$

Equivalently, the communication between T_2 and T_1 is equivalent to a virtual additive Gaussian channel where the noise is given by $\gamma_1(\beta\mathbf{Z}_R+\mathbf{E}_{q,0})$. The achievable rate of this link satisfies:

$$nR_{21} \leq \frac{n_1}{2}\log_2\left(1+\frac{\beta^2|h_2|^2P_2}{\beta^2\sigma_R^2+\sigma^2(\Lambda_0)}\right) \tag{4.53}$$

4.4.3 Achievable Rate Region

The maximum achievable rate region can be calculated from the inequalities (4.44),(4.45), (4.48) and (4.52) that define the constraints on $\sigma^2(\Lambda_0)$, $\sigma^2(\Lambda_1)$ and $\sigma^2(\Lambda_2)$. Using $\frac{n_1}{n}=\alpha$, we get the following system

$$\begin{cases} \dfrac{\sigma^2(\Lambda_2)}{\sigma^2(\Lambda_1)} \leq \left(1+\dfrac{\nu|h_2|^2P_R}{(1-\nu)|h_2|^2P_R+\sigma_2^2}\right)^{\frac{1-\alpha}{\alpha}} \\ \dfrac{\sigma^2(\Lambda_1)}{\sigma^2(\Lambda_0)} \leq \left(1+\dfrac{(1-\nu)|h_1|^2P_R}{\sigma_1^2}\right)^{\frac{1-\alpha}{\alpha}} \\ \sigma^2(\Lambda_1) \leq \sigma^2(\Lambda_2)-\beta^2\sigma_{U_2}^2 \\ \sigma^2(\Lambda_0) \leq \sigma^2(\Lambda_2)-\beta^2\sigma_{U_1}^2 \end{cases}$$

Since $\sigma^2(\Lambda_2) \geq \sigma^2(\Lambda_1) \geq \sigma^2(\Lambda_0)$, the last constraint in the system is not active. Thus we obtain the following bounds on the second moment of the lattices:

$$\sigma^2(\Lambda_1) \geq \frac{\beta^2\sigma_{U_2}^2}{\left(1+\dfrac{\nu|h_2|^2P_R}{(1-\nu)|h_2|^2P_R+\sigma_2^2}\right)^{\frac{1-\alpha}{\alpha}}-1} \tag{4.54}$$

$$\sigma^2(\Lambda_0) \geq \frac{\sigma_{\Lambda_1}^2}{\left(1+\dfrac{(1-\nu)|h_1|^2P_R}{\sigma_1^2}\right)^{\frac{1-\alpha}{\alpha}}} \tag{4.55}$$

The achievable rate region (R_{12}, R_{21}) in (4.49) and (4.53) are limited by these constraints and can be written as

$$R_{12} \leq \frac{\alpha}{2}\log_2\left(1+\mathrm{SNR}_{1\to2}\right) \tag{4.56}$$

$$R_{21} \leq \frac{\alpha}{2}\log_2\left(1+\mathrm{SNR}_{2\to1}\right) \tag{4.57}$$

where the virtual end-to-end SNRs are redefined as follows:

$$\mathrm{SNR}_{1\to 2} = \frac{\beta^2|h_1|^2P_1}{\beta^2\sigma_R^2+\sigma^2(\Lambda_1)} \tag{4.58}$$

$$\mathrm{SNR}_{2\to 1} = \frac{\beta^2|h_2|^2P_2}{\beta^2\sigma_R^2+\sigma^2(\Lambda_0)} \tag{4.59}$$

Once again the achievable rate region of the refinement scheme is obtained by maximizing the virtual SNR for $\alpha \in [0,1]$. This is equivalent to minimizing $\sigma^2(\Lambda_1)$ and $\sigma^2(\Lambda_0)$. Since they are bounded respectively by (4.54) and (4.55), the optimal choice on the second moment of Λ_1 is

$$\sigma^2(\Lambda_1)_{\min} = \frac{\beta^2\sigma_{U_2}^2}{\left(1+\dfrac{\nu|h_2|^2P_R}{(1-\nu)|h_2|^2P_R+\sigma_2^2}\right)^{\frac{1-\alpha}{\alpha}}-1} \tag{4.60}$$

and the optimal choice on the second moment of Λ_0 is

$$\sigma^2(\Lambda_0)_{\min} = \frac{\beta^2\sigma_{U_2}^2}{\left(1+\frac{(1-\nu)|h_1|^2P_R}{\sigma_1^2}\right)^{\frac{1-\alpha}{\alpha}}\left[\left(1+\frac{\nu|h_2|^2P_R}{(1-\nu)|h_2|^2P_R+\sigma_2^2}\right)^{\frac{1-\alpha}{\alpha}}-1\right]} \tag{4.61}$$

Finally by replacing $\sigma^2(\Lambda_1)_{\min}$ and $\sigma^2(\Lambda_0)_{\min}$ in (4.58) and (4.59), equations (4.31) and (4.32) are verified and the proof of the theorem is concluded.

Remark 4.2. The obtained achievable rates are independent from the choice of the scaling factors β and γ_i. The optimal choice of these parameters is explained when considering the source coding problem as explained in the next section.

4.4.4 Analog Signal Transmission

Following the same analysis of Section 4.3.4, the optimal scaling factors γ_i that minimize the distortion at each terminal are given by:

$$\gamma_1^* = \frac{\beta\sigma^2(\Lambda_1)}{\beta^2\sigma_{U_2}^2+\sigma^2(\Lambda_1)} \tag{4.62}$$

$$\gamma_2^* = \frac{\beta\sigma^2(\Lambda_0)}{\beta^2\sigma_{U_1}^2+\sigma^2(\Lambda_0)} \tag{4.63}$$

then, the minimal distortion at terminal T_2 is

$$D_2^{\min} = \frac{\sigma_{U_2}^2}{\left(1 + \frac{\nu|h_2|^2 P_R}{(1-\nu)|h_2|^2 P_R + \sigma_2^2}\right)^{\frac{1-\alpha}{\alpha}}} \tag{4.64}$$

and the minimal distortion at terminal T_1 is

$$D_1^{\min} = \frac{\sigma_{U_1}^2 \sigma^2(\Lambda_0)_{\min}}{\beta^2 \sigma_{U_1}^2 + \sigma^2(\Lambda_0)_{\min}} \tag{4.65}$$

$$= \frac{\sigma_{U_2}^2 \sigma_{U_1}^2}{\left(1 + \frac{(1-\nu)|h_1|^2 P_R}{\sigma_1^2}\right)^{\frac{1-\alpha}{\alpha}} \left(\left(1 + \frac{\nu|h_2|^2 P_R}{(1-\nu)|h_2|^2 P_R + \sigma_2^2}\right)^{\frac{1-\alpha}{\alpha}} - 1\right) \sigma_{U_1}^2 + \sigma_{U_2}^2} \tag{4.66}$$

The new distortion $D_1^{\min}$ allowed by the layered coding scheme is less than the first one presented in (4.25). Thus the layered scheme enhances the achievable rates and minimizes the distortion for this user.

As a conclusion, if we are interested in the distortion problem in addition to the transmission problem addressed in this paper, the choice of β can be left to the designer. The optimal lattice parameters and the receivers' scaling factors that depend on this choice are given by equations (4.20) and (4.24) for the first scheme and (4.60), (4.61), (4.62) and (4.63) for the second scheme. However, this choice does not affect the optimal achievable rates and distortions that depend only on the system parameters.

4.5 Numerical Results

This section presents numerical results of the achievable rates of our proposed schemes compared to AF and DF protocols and the outer-bound capacity given in [40, 36]. We characterize the whole achievable rate regions by optimizing the time division $\alpha \in [0, 1]$ between MAC and BC phases. The bounds are determined by maximizing the weighted sum of the rates R_{12} and R_{21} for each protocol. For

example, for the proposed scheme in Section 4.4, we solve the following problem for all values of $\eta \in [0, 1]$

$$\begin{aligned} \max \quad & \eta R_{12} + (1-\eta) R_{21} && \text{(4.67a)} \\ \text{s.t.} \quad & (R_{12}, R_{21}) \text{ satisfy (4.31) and (4.32)} && \text{(4.67b)} \\ & \text{for } \alpha \text{ and } \nu \in [0, 1] && \text{(4.67c)} \end{aligned}$$

It is worth noting that the time division α with AF relaying scheme is always equal to $\frac{1}{2}$. This ensures that there is no data loss between MAC and BC transmission phases.

We consider equal noise variances $\sigma_1^2 = \sigma_2^2 = \sigma_R^2 = 1$, different transmit powers and asymmetric channels where $|h_1|^2 P_1 \geq |h_2|^2 P_2$. We refer to the coding schemes of Theorems *4.1* and *4.2* by LCF1 and LCF2 respectively.

Fig.4.4 draws the achievable rate regions of DF, AF and LCF1 with two settings respectively: T_1 has the best transmit power P_1 and the worst channel module $|h_1|$ and vice-versa. LCF1 scheme is a CF relaying strategy based on lattice coding. we have proved in [73] that the lattice based CF scheme achieves rates equal to those achievable by random coding derived in 2.3.3. Thus, the performance of our scheme is the same as CF for TWRC in [36, 26]. It has been shown in [36], that CF strategy achieves rates greater than AF for symmetric channels. However, this result is not verified for asymmetric channels. This is shown in Fig.4.4 where the difference between the rate regions of AF and LCF1 is negligible for middle SNR regime and asymmetric channels.

Fig. 4.5 illustrates the performance of all schemes in the symmetric case. End-to-end equal rates $R_{12} = R_{21}$ as a function of the transmit SNR are drawn for equal channel and power conditions for all nodes. Define $\text{SNR}_{ij} = \frac{|h_{ij}|^2 P_i}{\sigma_j^2}$. It can be clearly seen that LCF1 outperforms DF for SNRs ≥ 12 dB. This result can be justified analytically. In fact, one can verify that for low SNR regime, DF rate approaches

$$R_{DF} \to \max_{\alpha} \min\{\alpha SNR, (1-\alpha) SNR\} = \frac{1}{4} SNR$$

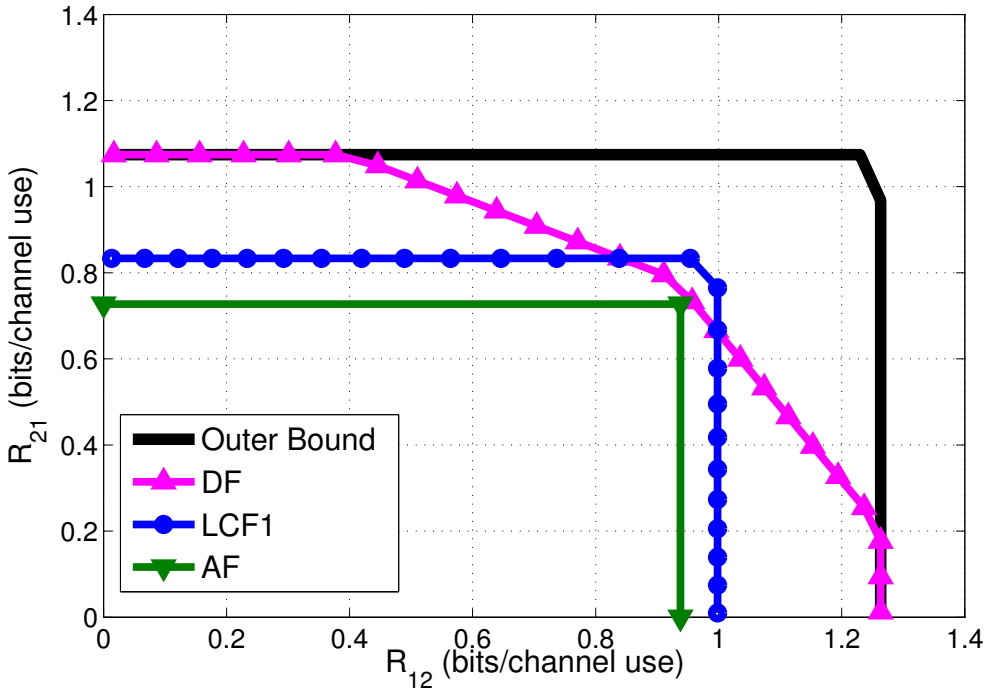

(A) $P_1 = 15$ dB, $P_2 = 10$ dB, $P_R = 20$ dB, $|h_1|^2 = 0.5$, $|h_2|^2 = 1$

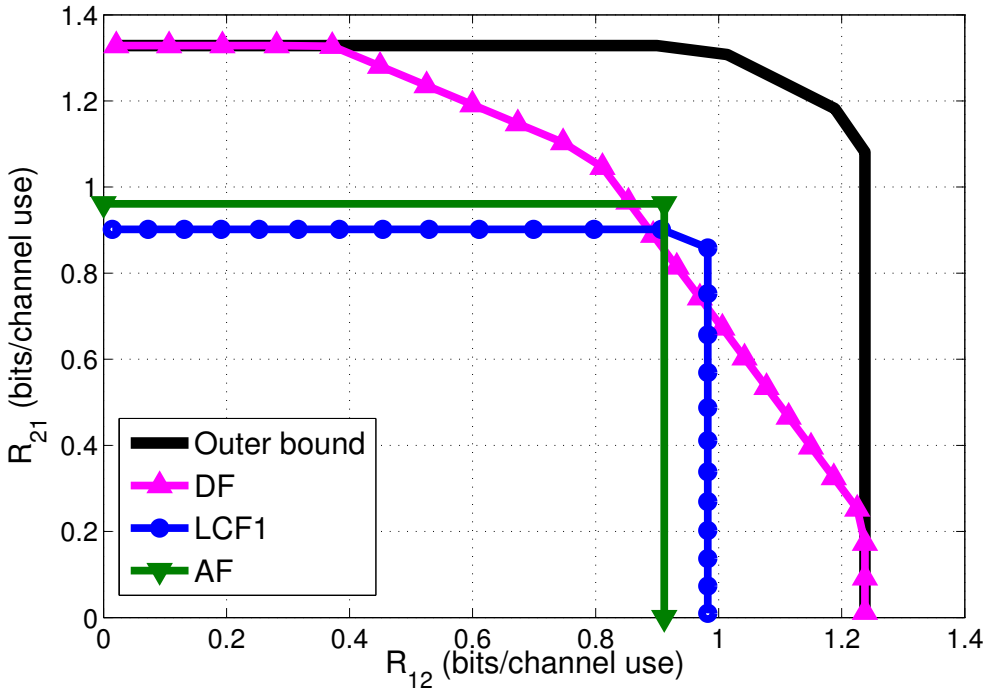

(B) $P_1 = 10$ dB, $P_2 = 15$ dB, $P_R = 20$ dB, $|h_1|^2 = 2$, $|h_2|^2 = 0.5$

Figure 4.4: Achievable rate regions and the outer bound capacity of the Gaussian TWRC. In the left, T_1 has the best transmit power and the worst channel, in the right, T_2 has the best transmit power and the worst channel.

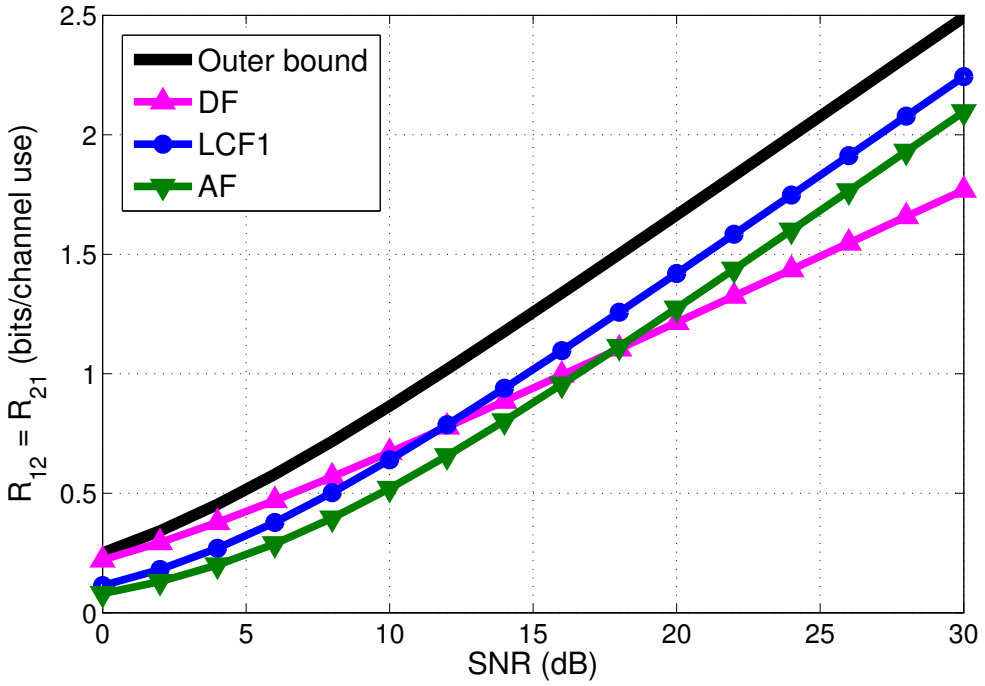

FIGURE 4.5: Equal rates $R_{12} = R_{21}$ for symmetric channels: SNR = SNR_{1R} = SNR_{R1} = SNR_{2R} =SNR_{R2}. LCF1 outperforms AF and DF for SNR > 11 dB

While LCF1 rate approaches

$$R_{LCF1} \to \frac{((\sqrt{SNR+1}-1)+(SNR-2\sqrt{SNR}+2)\sqrt{SNR})SNR^2}{2(\sqrt{SNR+1}-1)+\sqrt{SNR}}$$

In this case, $R_{LCF1} \leq R_{DF}$. On the other hand, for high SNR, DF rate can be approximated by

$$R_{DF} \to \frac{1}{6}\log_2(SNR)$$

and LCF1 rate by

$$R_{LCF1} \to \frac{1}{4}(\log_2(SNR)-1)$$

One can verify also that, for SNR sufficiently large ($SNR \geq 10$ dB), $R_{LCF1} \geq R_{DF}$ which is consistent with the result in Fig. 4.5.

Consider in the sequel the case when $h_1|^2P_1 \geq |h_2|^2P_2$ and $|h_1|^2 \geq |h_2|^2$. Fig.4.6 draws the achievable rate regions of LCF1 and LCF2. One can see that the two-layer based scheme (LCF2) enlarges the rate region compared to the basic scheme since the relay sends additional information to the best terminal T_1. For the

setting presented in Fig. 4.6a, the achievable rate R_{21} increases by 60% with the refinement while it increases by more than 100% in the second setting in Fig. 4.6b.

Finally, when compared to DF and AF relaying schemes, simulations show that LCF2 scheme outperforms AF in all SNR regimes for symmetric and asymmetric channels.

Fig.4.7 illustrates the achievable rate regions of DF, AF and both lattice-based schemes, LCF1 and LCF2, for various SNR settings. In low SNR regime, although LCF2 scheme improves the rate region compared to the basic LCF1 rate region, both relaying schemes along with AF scheme remain far from DF scheme. In fact, in this SNR region, DF approaches the outer bound capacity and coincides with it in sufficiently large area as can be seen in Fig. 4.7d. This result is consistent with the results in [36, 37] that showed that DF scheme is better than the other relaying schemes for low SNR region.

In very high SNR regime, LCF1 and LCF2 achieve better sum-rates than DF as shown in Fig. 4.7a. In middle to high SNR, LCF2 scheme enlarges the region of rates compared to DF. These results are represented in Figs. 4.7b and 4.7c.

Remark 4.3. Comments on the channel knowledge at nodes
We have assumed in our system model perfect CSI. However, in the proposed two lattice-based coding schemes (LCF1 and LCF2), this perfect knowledge of the channel state can be relaxed. In fact, in order to compress its received system, the relay needs only the module of the channel gains to reconstruct the LSE scheme. For each terminal, the decoder uses the available side information $\mathbf{S}_i = h_i\mathbf{X}_i$ that depends on its terminal-relay channel. Appropriate training sequences can be employed to estimate the channel of the relay. Furthermore, the decoder output is an estimate of only the unknown part of the relay received signals which is equivalent to the output of a virtual Gaussian channel as shown in Sections 4.3.2 and 4.4.2 for both proposed schemes. Thus, a training sequence can also be used in order to estimate the other link channel.

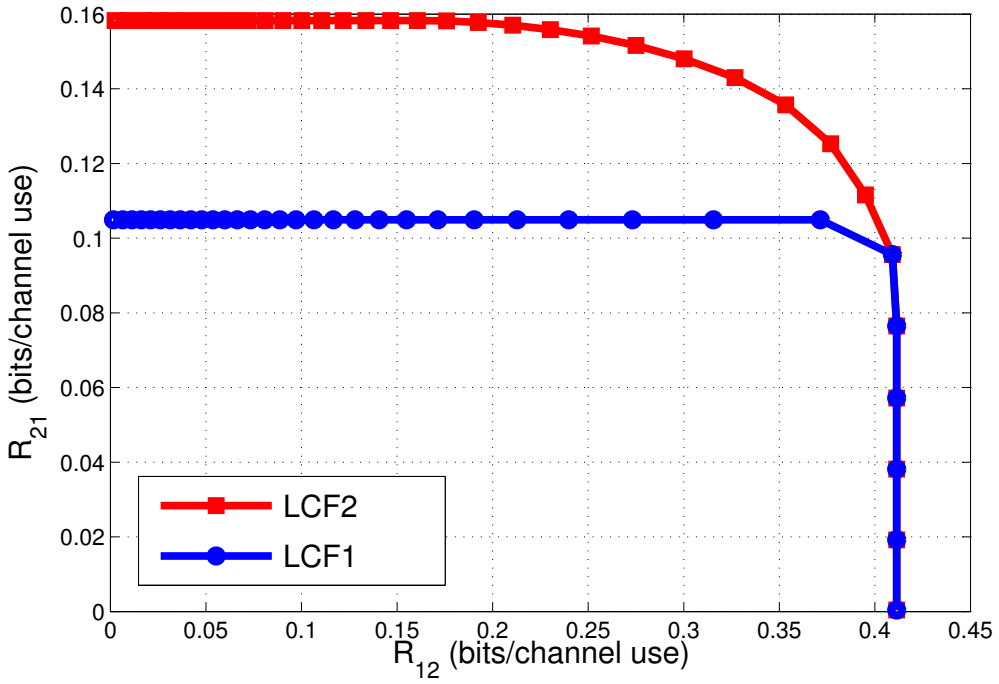

(A) $P_1 = 10$ dB, $P_2 = P_R = 5$ dB, $|h_1|^2 = 2$, $|h_2|^2 = 0.5$

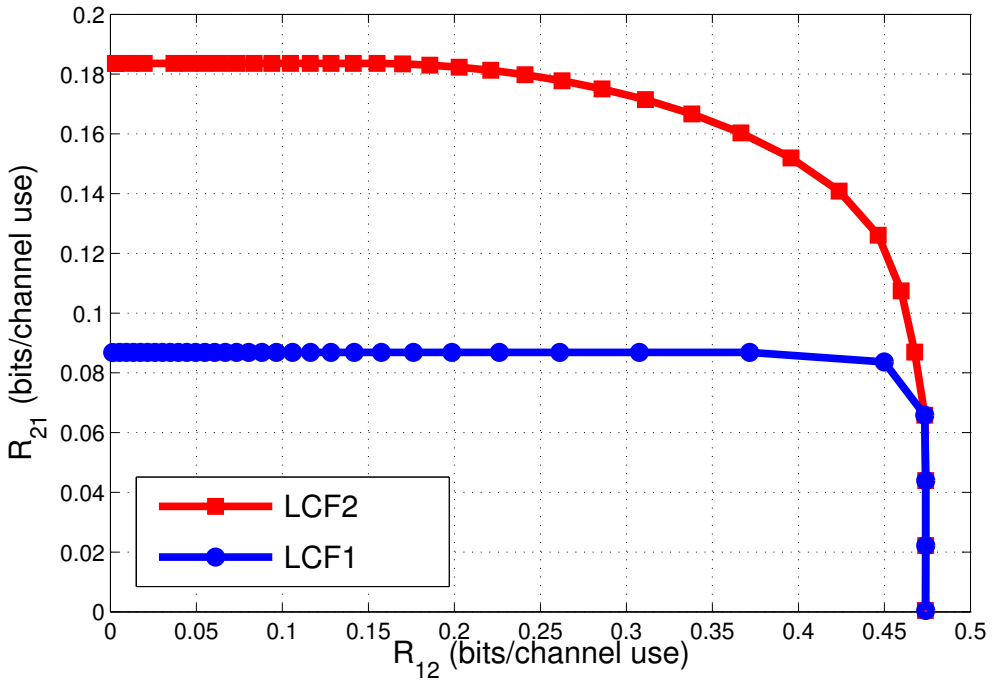

(B) $P_1 = 10$ dB, $P_2 = P_R = 5$ dB, $|h_1|^2 = 6$, $|h_2|^2 = 0.5$

FIGURE 4.6: Achievable rate regions of LCF1 and LCF2. LCF2 achieves greater end-to-end rates at T_1

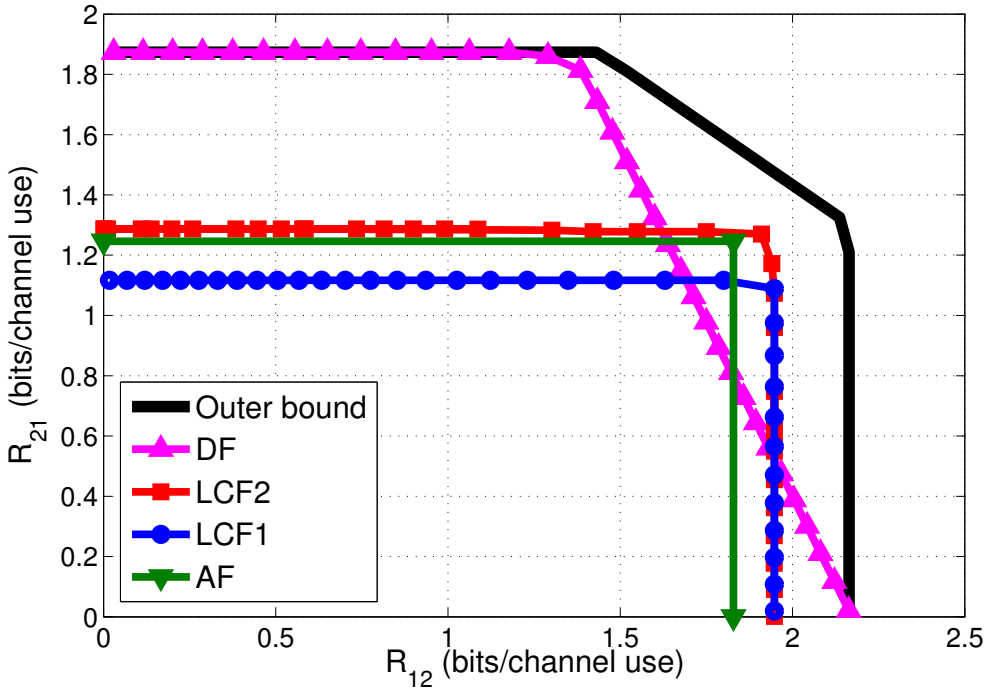

(A) $P_1 = 30$ dB, $P_2 = 25$ dB, $P_R = 30$ dB, $|h_1|^2 = 1$, $|h_2|^2 = 0.2$

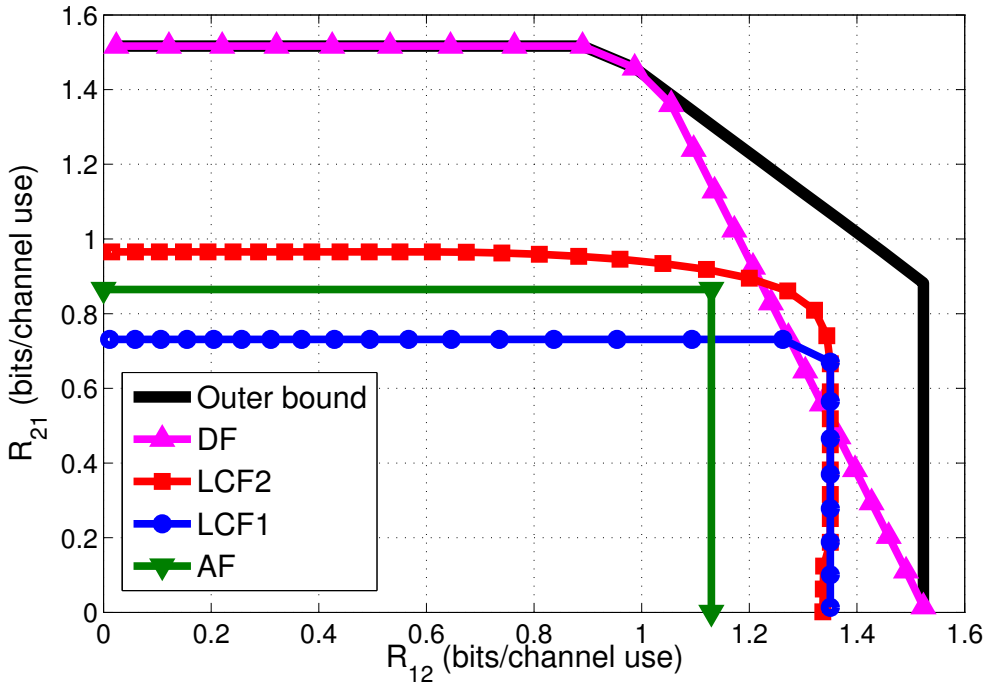

(B) $P_1 = 20$ dB, $P_2 = 18$ dB, $P_R = 17$ dB, $|h_1|^2 = 4$, $|h_2|^2 = 0.5$

Figure 4.7: Achievable rate regions of DF, AF, LCF1 and LCF2 in different channel and power settings

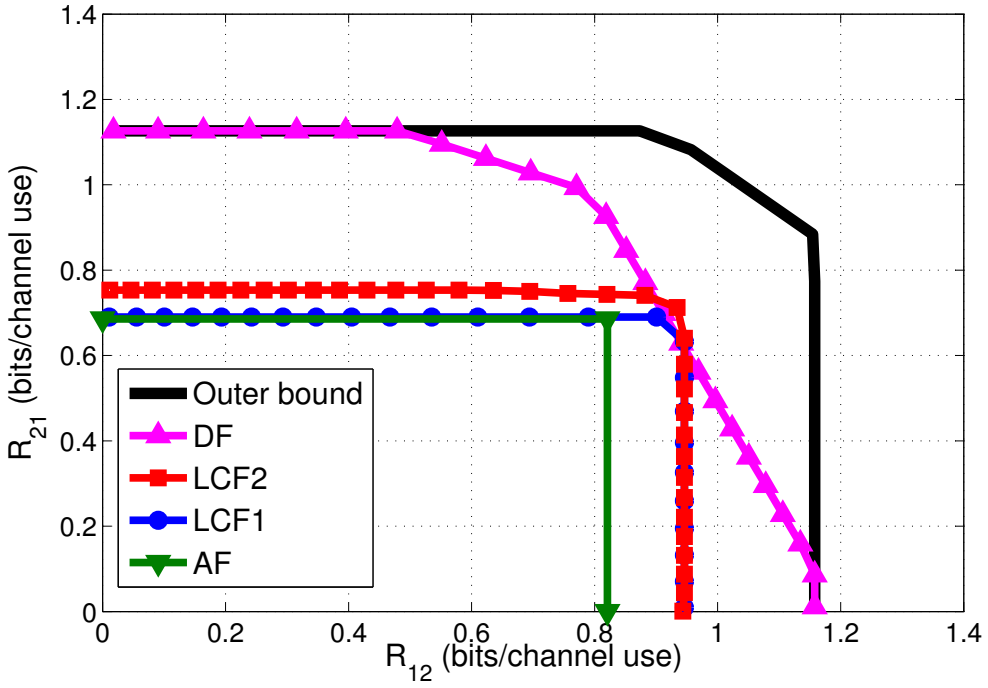

(c) $P_1 = 10$ dB, $P_2 = 9$ dB, $P_R = 9$ dB, $|h_1|^2 = 4$ and $|h_2|^2 = 2$

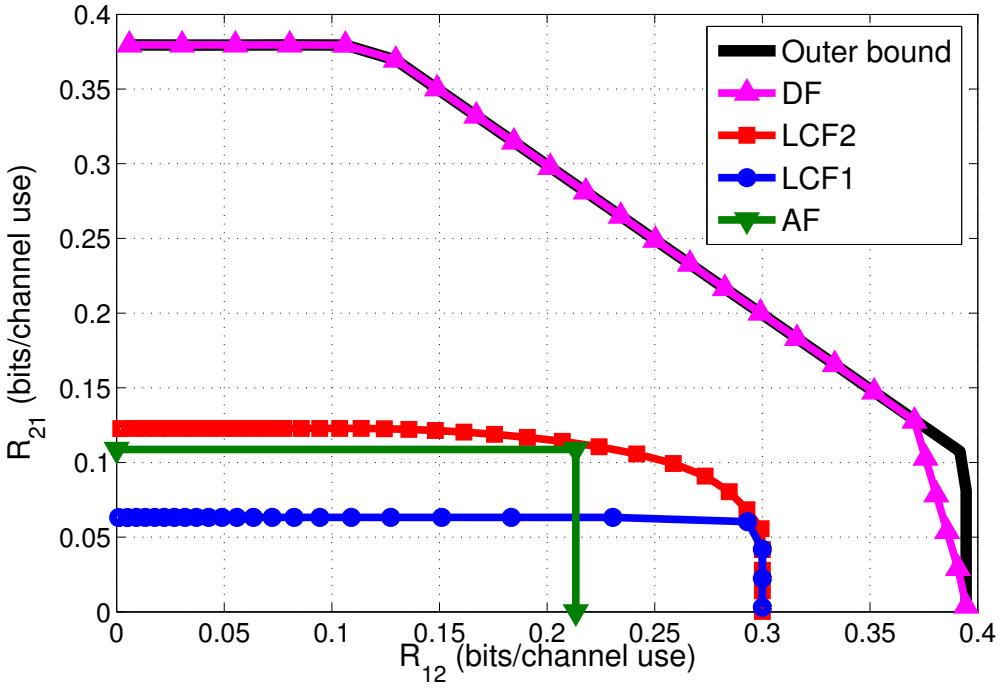

(d) $P_1 = 5$ dB, $P_2 = 3$ dB, $P_R = 3$ dB, $|h_1|^2 = 4$ and $|h_2|^2 = 0.5$

FIGURE 4.7: Achievable rate regions of DF, AF, LCF1 and LCF2 in different channel and power settings (cont.)

4.6 Conclusion

In this chapter, we derived two achievable rate regions based on compress-and-forward lattice coding. In the proposed schemes, the relay uses a lattice based Wyner-Ziv encoding by taking into account the presence of the side information at each node i.e. the signal broadcasted by the relay includes also the signal that has been transmitted by each user to the relay during the first MAC transmission phase.

First, we developed a coding scheme in which the relay broadcasts the same signal to both terminals. We show that this scheme offers the same performance as random coding based compress-and-forward protocol [73]. Then, we proposed, and analyzed the performance of, an improved coding scheme in which the relay sends not only a common description of its output, but also an individual description that is destined to be recovered by only the user who experiences better channel conditions and better side information. We showed that this results in substantial gains in rates. Numerical results demonstrated an enhancement of the achievable rate region over the basic scheme up to 100% for moderate SNR regime and asymmetric channel conditions. Also, the improved scheme outperforms classic amplify-and-forward at all SNR values, and classic decode-and-forward for certain SNR regimes.

Chapter 5

Finite Dimension Compress-and-Forward Scheme for Two-Way Relay Channel

5.1 Introduction

For the TWRC channel (cf. Fig.2.5), we consider PNC schemes where the overall communication takes two phases namely MAC and BC. For this channel we have proposed in the previous chapter two compress-and-forward lattice coding schemes where high dimension lattices have been used to guarantee an error free decoding. We derived achievable rate regions of these schemes. We have shown that the first scheme based on single-layer lattice coding achieves, at the limit of arbitrarily large dimension, the same rate as that offered by the random coding-based conventional compress-and-forward. For this scheme, we noticed that with carefully chosen source coding factors, the results match with the optimum forward test channel.

With finite dimension lattices, the decoding error probability cannot be arbitrarily small. Based on this observation, we investigate, in this chapter, the single-layer scheme with finite dimension lattices. We characterize the rate regions allowed by our coding scheme by considering non vanishing yet constrained decoding error

probabilities. We investigate also the analog transmission problem where the distortion is optimized. Then, we discuss the design criteria of our coding scheme, and illustrate our results with numerical examples. In this chapter, for simplicity, we will employ the term "achievable rate region" to designate the region of rates where the error probability at the decoder does not exceed a predefined threshold.

The content of this chapter has been partially published in [74].

5.2 Achievable Rate Region for TWRC

Theorem 5.1. *Let (Λ_1, Λ_2), a pair of two nested lattices of dimension n_1, with $\Lambda_2 \subset \Lambda_1$. For a Gaussian TWRC, under the assumptions a.1 to a.9 detailed in Section 2.2, the convex hull of all end-to-end rate pairs (R_{12}, R_{21}) satisfying the following inequalities is achievable:*

$$R_{12} \leq \frac{\alpha}{2}\log_2\left(1+\frac{|h_1|^2P_1}{\sigma_R^2+\frac{|h_1|^2P_1+\sigma_R^2}{\left(1+\min\limits_{i\in\{1,2\}}\frac{|h_i|^2P_R}{\sigma_i^2}\right)^{\frac{1-\alpha}{\alpha}}-G(\Lambda_1)\mu(\Lambda_2)}}\right) \tag{5.1}$$

$$R_{21} \leq \frac{\alpha}{2}\log_2\left(1+\frac{|h_2|^2P_2}{\sigma_R^2+\frac{|h_1|^2P_1+\sigma_R^2}{\left(1+\min\limits_{i\in\{1,2\}}\frac{|h_i|^2P_R}{\sigma_i^2}\right)^{\frac{1-\alpha}{\alpha}}-G(\Lambda_1)\mu(\Lambda_2)}}\right) \tag{5.2}$$

with $G(\Lambda_1)$ is the normalized second moment of Λ_1, $\mu(\Lambda_2)$ is the volume to noise ratio of Λ_2 [88], and $\alpha \in [0,1]$.

Remark 5.1. For $n_1 \to \infty$, the term $G(\Lambda_1)\mu(\Lambda_2)$ reduces to 1. This term corresponds to the penalty of using finite dimension, that vanishes asymptotically as will be discussed in the next paragraphs. Thus the achievable rate region coincides with the achievable rate region derived in Theorem 4.1 for sufficiently large n.

5.3 Proof of Theorem 5.1

In this section, we present a detailed proof of Theorem 5.1 following the same analysis of section 4.3 in Chapter 4. We investigate also the analog transmission problem where the distortion is the main metric to be optimized. The main idea of the proposed scheme is the following: during the BC phase, the relay station sends a compressed version of the signal received during the MAC phase. The relay employs a lossy compression Wyner-Ziv scheme using nested lattices that is tuned to the side information of the user with the weakest side information. The proof is detailed in the next paragraphs: in Section 5.3.1, the lattice coding scheme is introduced and the transmission rates are derived in Section 5.3.2.

5.3.1 Lattice-based Source Coding

We suppose that the elements of $\mathbf{X}_i$, $i = 1, 2$, are drawn from an independent identically distributed (i.i.d) Gaussian distribution with zero mean and variance P_i. Let $\mathbf{S}_i = h_i\mathbf{X}_i$ be the side information available at terminal T_i, $i = 1, 2$. Without loss of generality, we assume that $|h_2|^2P_2 \leq |h_1|^2P_1$. With this setting, T_2 is the terminal who experiences the weakest side information. The quantization performed by the relay is tuned so that T_2 reconstructs a local version $\hat{\mathbf{Y}}_{r,2}$ of $\mathbf{Y}_r$ with a distortion D_2:

$$\frac{1}{n_1}\mathbb{E}\|\mathbf{Y}_r - \hat{\mathbf{Y}}_{r,2}\|^2 \leq D_2 \tag{5.3}$$

.

The signal sent by the relay $\mathbf{Y}_R$ can be written in two ways as the sum of two independent Gaussian r.v.: the side information $\mathbf{S}_i$ and the unknown part $\mathbf{U}_i = \mathbf{Y}_R|\mathbf{S}_i = h_{\bar{i}}\mathbf{X}_{\bar{i}} + \mathbf{Z}_R$, $i \in \{1, 2\}$. From their received signals, each terminal T_i, $i \in \{1, 2\}$, decodes $\hat{\mathbf{U}}_i$ using $\mathbf{S}_i$. The variance per dimension of $\mathbf{U}_i$ is $\sigma^2_{U_i} = VAR(Y_R|S_i) = |h_{\bar{i}}|^2P_{\bar{i}} + \sigma^2_R$.

In the following, we detail the proposed lattice source coding scheme.

5.3.1.1 Encoding

Consider two n_1-dimensional nested lattices (Λ_1, Λ_2) such as $\Lambda_2 \subset \Lambda_1$. Λ_1 is good for quantization with basic Voronoi region $\mathcal{V}_1$ of volume V_1 and second moment per dimension $\sigma^2(\Lambda_1) = D_2$. This choice of $\sigma^2(\Lambda_1)$ is motivated by the results in 4.3.4. It permits to obtain the minimal possible distortion at terminal T_2.
The coarse lattice Λ_2 is good for channel coding with basic Voronoi region $\mathcal{V}_2$ of volume V_2 and second moment $\sigma^2(\Lambda_1) = \sigma^2_{U_2}$. This specific choice of the lattices parameters permits to reconstruct the optimum Gaussian forward test channel [85]. This result has been discussed in Section 4.3.4.

The lattice source encoding (LSE) operation is performed with four successive operations: first, the input signal $\mathbf{y}_R$ is scaled with a factor β. Then, a random dither $\mathbf{t}$ which is uniformly distributed over $\mathcal{V}_1$ is added. This dither is known by all nodes. The dithered scaled version of $\mathbf{y}_R$, $\beta\mathbf{y}_R + \mathbf{t}$ is quantized to the nearest point in Λ_1. The outcome of this operation is processed with a modulo-lattice operation in order to generate a vector $\mathbf{v}_R$ of size n_1.

$$\mathbf{v}_R = Q_{\Lambda_1}(\beta\mathbf{y}_R + \mathbf{t}) \mod \Lambda_2 \tag{5.4}$$

The relay sends the index of $\mathbf{v}_R$ that identifies a coset of Λ_2 relative to Λ_1 that contains $Q_{\Lambda_1}(\beta\mathbf{y}_R + \mathbf{t})$. By construction, the coset leader $\mathbf{v}_R$ is represented with $\log_2\left(\frac{V_2}{V_1}\right)$ bits. Thus, the rate of the source encoding scheme employed by the relay is R given by equation (4.1):

$$R = \frac{1}{n_1}\log_2\frac{V_2}{V_1} \quad \text{(bits per dimension)}$$

Given that $V_1 = \left(\frac{\sigma^2(\Lambda_1)}{G(\Lambda_1)}\right)^{n_1/2}$ where $G(\Lambda_1)$ is the normalized second moment (NSM) of Λ_1, the coding rate in (4.1) reads:

$$\begin{aligned} R &= \frac{1}{2}\log_2\left(\frac{\sigma^2(\Lambda_2)}{\sigma^2(\Lambda_1)}\right) + \frac{1}{2}\log_2\left(G(\Lambda_1)\mu(\Lambda_2)\right) \\ &= \frac{1}{2}\log_2\left(\frac{\sigma^2_{U_2}}{D_2}\right) + \frac{1}{2}\log_2\left(G(\Lambda_1)\mu(\Lambda_2)\right) \end{aligned} \tag{5.5}$$

The coding rate presents an additional term $L = \frac{1}{2}\log_2\left(G(\Lambda_1)\mu(\Lambda_2)\right)$ comparing to WZ rate distortion function given in (4.28) and the coding rate in equation (5.5) corresponding to high dimension lattices.

For a probability P_e and a lattice Λ with volume V, $\mu(\Lambda) = V^{\frac{2}{n_1}}/\sigma^2$, σ^2 is the variance of a Gaussian noise $\mathbf{Z}$ which verifies $\Pr(\mathbf{Z} \notin \mathcal{V}) \leq P_e$. This term has been introduced by Poltyrev in [58] for lattice codes in AWGN setting. By analogy to our problem, taking into account the constraints expressed in (5.11) and (5.12), the Λ_2 volume to noise ratio (VNR) associated to probability of error P_e is given by (5.6).

$$\mu(\Lambda_2) = \frac{V_2^{\frac{2}{n_1}}}{\sigma^2_{U_2}} \tag{5.6}$$

5.3.1.2 Decoding

For both users, $\mathbf{v}_R$ is decoded first. Then $\hat{\mathbf{u}}_i$ is reconstructed with a lattice source decoder (LSD) using the side information $\mathbf{s}_i$ as

$$\hat{\mathbf{u}}_i = \beta((\mathbf{v}_R - \mathbf{t} - \beta\mathbf{s}_i) \mod \Lambda_2),\ i = 1, 2 \tag{5.7}$$

Note that, in this scheme, β is also the decoders scaling factor while in equation (4.6) γ_i, $i \in \{1, 2\}$ are the scaling factors at each decoder. This choice permits to reconstruct the optimum Gaussian forward channel as mentioned in (4.3.4).

5.3.2 Rate Analysis

At the relay, message m_R corresponding to the index of $\mathbf{v}_R$ is mapped to a codeword $\mathbf{x}_R$ of size n_2. We suppose that the elements of the r.v. $\mathbf{X}_R$ are drawn from an i.i.d Gaussian distribution with zero mean and variance P_R. The broadcast rate from the relay to both terminals is bounded by the capacity of the worst individual relay-terminal channel. We assume that the penalty between AWGN capacity

with infinite and finite block-length can be neglected with carefully chosen block-lengths. Thus the following upper-bound can be valid for Gaussian codebooks:

$$n_1 R \leq n_2 \min_{i\in\{1,2\}} \frac{1}{2}\log_2\left(1+\frac{|h_i|^2 P_r}{\sigma_i^2}\right) \tag{5.8}$$

This constraint ensures that index m_R is transmitted reliably to both terminals and $\mathbf{v}_R$ is available at the input of the LSD of both receivers. At terminal T_i, $\hat{\mathbf{u}}_i$ in (5.7) can be written as:

$$\hat{\mathbf{u}}_i = \beta((\beta\mathbf{u}_i + \mathbf{e}_q) \bmod \Lambda_2) \tag{5.9}$$

$$\equiv \beta(\beta\mathbf{u}_i + \mathbf{e}_q) \tag{5.10}$$

where $\mathbf{e}_q = Q_1(\beta\mathbf{y}_r + \mathbf{t}) - (\beta\mathbf{y}_r + \mathbf{t}) = -(\beta\mathbf{y}_r + \mathbf{t}) \mod \Lambda_1$, is the quantization error. By the Crypto Lemma, $\mathbf{E}_q$ is independent from $\mathbf{Y}_r$, thus from $\mathbf{U}_2$, and it is uniformly distributed over $\mathcal{V}_1$ i.e $\mathrm{VAR}(E_q) = \sigma^2(\Lambda_1) = D_2$. The equivalence between (5.9) and (5.10) is valid only if $\beta\mathbf{u}_i + \mathbf{e}_q \in \mathcal{V}_2$. With finite dimension lattices, the volume of $\mathcal{V}_2$ should be large enough to enclose this signal. In this case, provided that

$$\frac{1}{n_1}\mathbb{E}\|\mathbf{E}_q + \beta\mathbf{U}_i\|^2 = D_2 + \beta^2\sigma_{U_i}^2 \leq \sigma^2(\Lambda_2), \tag{5.11}$$

the rates are calculated by ensuring that the probability $\Pr(\beta\mathbf{U}_i + \mathbf{E}_q \notin \mathcal{V}_2)$ does not exceed a fixed threshold.

$$\Pr(\beta\mathbf{U}_i + \mathbf{E}_q \notin \mathcal{V}_2) \leq P_e \tag{5.12}$$

As mentioned above we are interested in the analog transmission problem. For this problem, the parameter β has to be chosen so that to verify (5.11) and (5.3).

We have,

$$\begin{aligned}\mathbf{Y}_r - \hat{\mathbf{Y}}_{r,2} &= \mathbf{U}_2 + \mathbf{S}_2 - \hat{\mathbf{U}}_2 + \mathbf{S}_2 \\ &= \mathbf{U}_2 - \hat{\mathbf{U}}_2 \\ &= (1-\beta^2)\mathbf{U}_2 - \beta\mathbf{E}_q\end{aligned} \tag{5.13}$$

Thus (5.3) reads:

$$\begin{aligned}\frac{1}{n_1}\mathbb{E}\|\mathbf{Y}_r - \hat{\mathbf{Y}}_{r,2}\|^2 &= \frac{1}{n_1}\mathbb{E}\|(1-\beta^2)\mathbf{U}_2 - \beta\mathbf{E}_q\|^2 \\ &= \frac{1}{n_1}\mathbb{E}||(1-\beta^2)\mathbf{U}_2||^2 + \frac{1}{n_1}\mathbb{E}||\beta\mathbf{E}_q||^2 \\ &= (1-\beta^2)^2\sigma_{U_2}^2 + \beta^2 D_2 \\ &\leq D_2\end{aligned}$$

Thus, the optimal scaling factor β is equal to $\sqrt{1-\frac{D_2}{\sigma_{U_2}^2}}$ which matches with the optimal scaling factor reported in [85, 91].

By replacing $\mathbf{U}_2$ by its value we conclude that:

$$\hat{\mathbf{U}}_2 = \beta^2 h_1 \mathbf{X}_1 + \beta^2 \mathbf{Z}_r + \beta\mathbf{E}_q \tag{5.14}$$

Let $\mathbf{Z}_{eq} = \beta^2\mathbf{Z}_r + \beta\mathbf{E}_q$ be the effective additive noise. The communication between T_1 and T_2 is equivalent to a virtual additive Gaussian channel where the noise is given by $\mathbf{Z}_{eq}$. Let $\mathbf{Z}_q$ be a Gaussian variable with same variance as $\mathbf{E}_q$. Based on the results in [89], we have

$$\mathcal{D}(\beta^2 U_2 + \beta E_q, \beta^2 U_2 + \beta Z_q) = h(\beta^2 U_2 + \beta Z_q) - h(\beta^2 U_2 + \beta E_q) \tag{5.15}$$

where $\mathcal{D}(.,.)$ is the Kullback-Leibler divergence or the relative entropy. For a random variable (r.v.) X and a Gaussian r.v. X^* having the same mean and variance, $\mathcal{D}(X, X^*)$ is the divergence of X from Gaussianity defined as:

$$\mathcal{D}(X, X^*) = \int f_X(x)\log(\frac{f_X(x)}{f_X^*(x)})dx = h(X^*) - h(X)$$

where $f_X(.)$ and $f_X^*(.)$ are the probability density functions of X and X^* respectively, h(.) is the entropy and $h(X^*) = \frac{1}{2}\log_2(2\pi e\sigma_X^2)$.

On the other hand, let $\lambda = \dfrac{D_2}{\sigma_{U_2}^2}$, $M = \dfrac{E_q}{\sqrt{\lambda}}$ and $M^* = \dfrac{Z_q}{\sqrt{\lambda}}$, one can verify that

$$h(\beta^2 U_2 + \beta E_q) = h(\sqrt{\lambda}M + \sqrt{1-\lambda}M^*).$$

Since U_2 is Gaussian, this entropy decreases to zero monotonically as D_2 goes from zero to $\sigma_{U_2}^2$ as shown in [89]. Thus for high resolution assumption as $D_2 \to 0$,

$$\begin{aligned} h(\beta^2 U_2 + \beta E_q) \quad \to h(M*) \quad &= h(Z_q) - \log_2(\sqrt{\lambda}) \\ &= \frac{1}{2}\log_2(2\pi e D_2) - \frac{1}{2}\log_2\left(\frac{D_2}{\sigma_{U_2}^2}\right) \end{aligned}$$

Besides $h(\beta^2 U_2 + \beta Z_q) = \frac{1}{2}\log_2(2\pi e\sigma_{U_2}^2)$. Thus equation (5.15) is written as

$$\begin{aligned} D(\hat{U}_2, \beta^2 U_2 + \beta Z_q) \quad &\to -\frac{1}{2}\log_2\left(\frac{D_2}{\sigma_{U_2}^2}\right) + \frac{1}{2}\log_2\left(\frac{D_2}{\sigma_{U_2}^2}\right) \\ &= 0. \end{aligned}$$

We conclude that, in the divergence sense, for high resolution assumption as $D_2 \to 0$, we can approximate the decoded signal with a Gaussian one. Thus the transmission rate of this link satisfies:

$$nR_{12} \leq \frac{n_1}{2}\log_2\left(1 + \frac{\beta^2|h_1|^2 P_1}{\beta^2\sigma_r^2 + D_2}\right). \tag{5.16}$$

At terminal T_1, the decoder is tailored to the side information $\mathbf{S}_1$. Thus, at the decoder we subtract $\beta\mathbf{s}_1$ and $\hat{\mathbf{u}}_1$ is reconstructed similarly to $\hat{\mathbf{u}}_2$ in (5.9). Since $\sigma_{S_1}^2 \geq \sigma_{S_2}^2$, we have

$$\begin{aligned} \sigma_{U_1}^2 &\leq \sigma_{U_2}^2, \\ \Pr(\beta\mathbf{U}_1 + \mathbf{E}_q \notin \mathcal{V}_2) &\leq \Pr(\beta\mathbf{U}_2 + \mathbf{E}_q \notin \mathcal{V}_2), \\ D_1 = \frac{1}{n_1}\mathbb{E}\|\mathbf{Y}_r - \hat{\mathbf{Y}}_{r,1}\|^2 &\leq D_2 \end{aligned}$$

The communication between T_2 and T_1 is equivalent to a virtual Gaussian channel with an additive noise $\mathbf{Z}_{eq}$ and a rate:

$$nR_{21} \leq \frac{n_1}{2}\log_2\left(1+\frac{\beta^2|h_2|^2P_2}{\beta^2\sigma_r^2+D_2}\right) \tag{5.17}$$

The transmission rates R_{12} and R_{21} are maximized when D_2 is minimized for fixed β. Denoting $\frac{n_1}{n}=\alpha$, from (5.5) and (5.8), the lower bound on D_2 is given by

$$D_2^{min}=\frac{\beta^2\sigma_{U_2}^2}{\left(1+\min\limits_{i\in\{1,2\}}\frac{|h_i|^2P_R}{\sigma_i^2}\right)^{\frac{1-\alpha}{\alpha}}-G(\Lambda_1)\mu(\Lambda_2)}.$$

By replacing D_2 with D_2^{min} in (5.16) and (5.17), this verifies (5.1) and (5.2) and concludes the proof. The whole coding scheme is summarized in Fig.5.1.

5.4 Numerical Implementation

In this section, we present the rate region for practical finite dimension lattices. In this case, a rate loss is incurred in the coding rate comparing to the WZ rate distortion function as described in previous sections (5.2 and 5.3). Since T_2 is the user with the weakest side information, we have $\sigma_{U_2}^2 \geq \sigma_{U_1}^2$. The rate region is calculated by ensuring that the error probability verifies (5.18).

$$Pr(\beta\mathbf{U}_2+\mathbf{E}_q \notin \mathcal{V}_2) \leq P_e. \tag{5.18}$$

The analytical derivation of the error probability for practical lattice pairs is difficult in the general case since it requires the integration over the Voronoi region of the coarse lattice. Though it can be computed numerically using Monte Carlo integration or approximated by an upper bound.

Furthermore, given that the error probability of the scheme is defined by the goodness of the coarse lattice, the performance of the end-to-end scheme depends more on this lattice rather than the choice of the fine lattice. Therefore, the

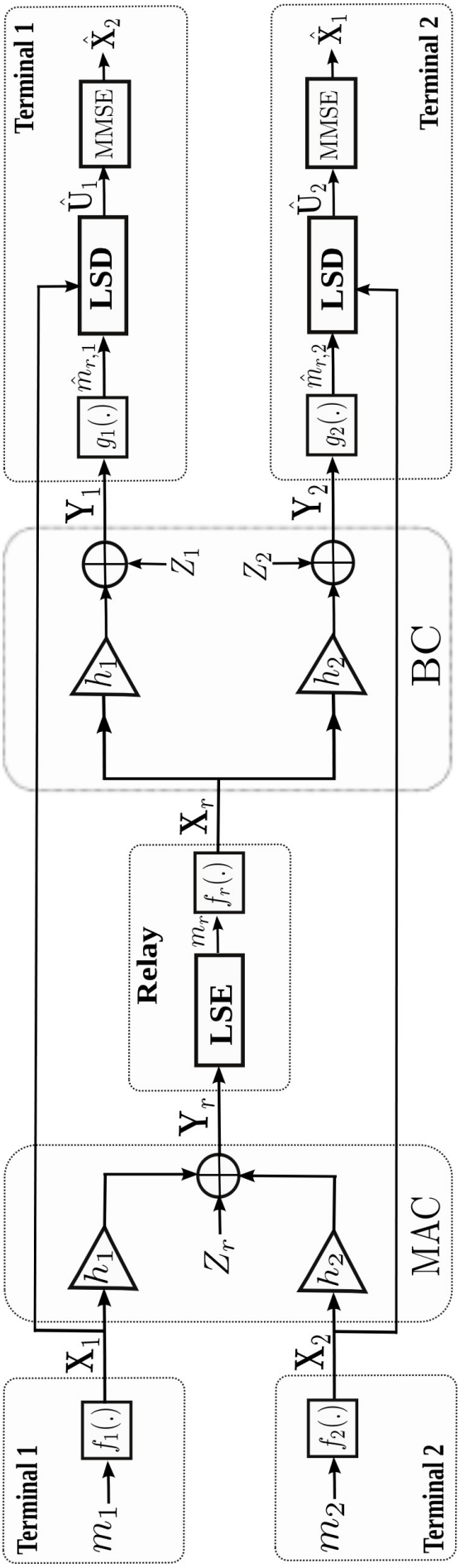

Figure 5.1: Lattice coding scheme for TWRC

simple cubic lattice $\mathbb{Z}^{n_1}$ with NSM $G(\Lambda_1) = \frac{1}{12}$ will be the preferred choice for the fine lattice. In this case, for a good coarse lattice with NSM $G(\Lambda_2) = \frac{1}{2\pi e}$, the rate loss with respect to the ideal WZ scheme is only $\frac{1}{2}\log_2(2\pi e/12) = 0.2546$ bit per sample. Moreover, in the quantization problem, the choice of the fine (resp. coarse) lattice is equivalent to the choice of the coarse (resp. fine) lattice for the dual channel coding problem. It has been shown in [33] that practically $\mathbb{Z}^{n_1}$ suffices as a shaping lattice that verifies arbitrary small error probability. Thus, a sublattice of $\mathbb{Z}^{n_1}$ can be a simple engineering choice for the fine lattice. In the sequel, Λ_1 is a scaled version of $\mathbb{Z}_1^n$ i.e. $\Lambda_1 = \eta\mathbb{Z}^{n_1}$. In this case, equation (5.19) gives an approximation of the error probability by using union bound and Chernoff bound (see section 5.6 for the proof).

Proposition 5.2.

$$Pr(\beta\,\boldsymbol{U}_2 + \boldsymbol{E}_q \notin \mathcal{V}_2) \approx K(\Lambda_2)\exp\left(-\frac{1}{8}\gamma_c(\Lambda_2)\mu(\Lambda_2, P_e)\right) \tag{5.19}$$

for sufficiently large $\mu(\Lambda_2, P_e)$. $\gamma_c(\Lambda_2) = \dfrac{d_{min}^2(\Lambda_2)}{V(\Lambda_2)^{2/n_1}}$ *is the coding gain of* Λ_2 *with* $d_{min}(\Lambda_2)$ *is the minimum distance between two points in* Λ_2. $K(\Lambda_2)$ *is the kissing number of* Λ_2 *which is defined as the number of the nearest neighbors to any lattice points in* Λ_2.

From (5.19), we choose the VNR $\mu(\Lambda_2)$ in (5.5) as follows

$$\mu(\Lambda_2, P_e) \approx \frac{8}{\gamma_c(\Lambda_2)}\log_2\left(\frac{K(\Lambda_2)}{P_e}\right). \tag{5.20}$$

Note that $\mu(\Lambda_2, P_e) \gg \dfrac{1}{\gamma_c(\Lambda_2)}$ for small error probability. This guarantees that the union bound approximation is valid and the error probability is upper bounded by P_e.

We characterize the whole achievable rate region of the proposed scheme by optimizing the time division $\alpha \in [0, 1]$ between MAC and BC phases and the distortion choice at the relay. The boundary points are determined by maximizing the weighted sum of both rates R_{12} and R_{21}. We solve the following problem for all

Table 5.1: Some important binary lattices and their useful properties

Lattice Λ	dimension n_1	$G(\Lambda)$	$\gamma_c(\Lambda)$	$K(\Lambda)$
$\mathbb{Z}^k$	k	0.0833	1	$2k$
D_4	4	0.07660	$\sqrt{2}$	24
E_8	8	0.071682	2	240
Λ_{16}	16	0.06829	$2^{3/2}$	4320
Λ_{24}	24	0.00657	4	196560

values of $\eta \in [0, 1]$:

$$\max \quad \eta R_{12} + (1-\eta) R_{21} \tag{5.21a}$$

$$\text{s.t.} \quad (R_{12}, R_{21}) \text{ satisfy (5.1) and (5.2)} \tag{5.21b}$$

$$\mu(\Lambda_2) \text{is given by(5.20)} \tag{5.21c}$$

$$\text{for } \alpha \in [0, 1]. \tag{5.21d}$$

Table 5.1 gives the kissing number and the coding gain for a set of commonly used finite lattices, that can be used to calculate $\mu(\Lambda_2, P_e)$ for fixed P_e using (5.20). Comparison between lattice pairs can be found in Fig. 5.2 for symmetric static channels, equal SNRs and $P_e = 10^{-5}$. We notice that the difference between the infinite scheme and the pair $(\mathbb{Z}^4, \Lambda_{24})$ is about 0.15 bit/channel use. In Fig. 5.3, we present the achievable rates for asymmetric channels and different power constraints at all nodes. For the asymptotic regime, the maximal rate pair that can be achieved under the considered constraints is $(R_{12} = 0.8, R_{21} = 0.29)$. The maximal gap between the considered finite dimension lattices and the high dimension lattices is about 0.2 bit/dimension for R_{12} and 0.06 bit/dimension for R_{21}. This represents a loss of 25% and 20% for R_{12} and R_{21} respectively with finite dimension lattices relative to to the high dimensional regime.

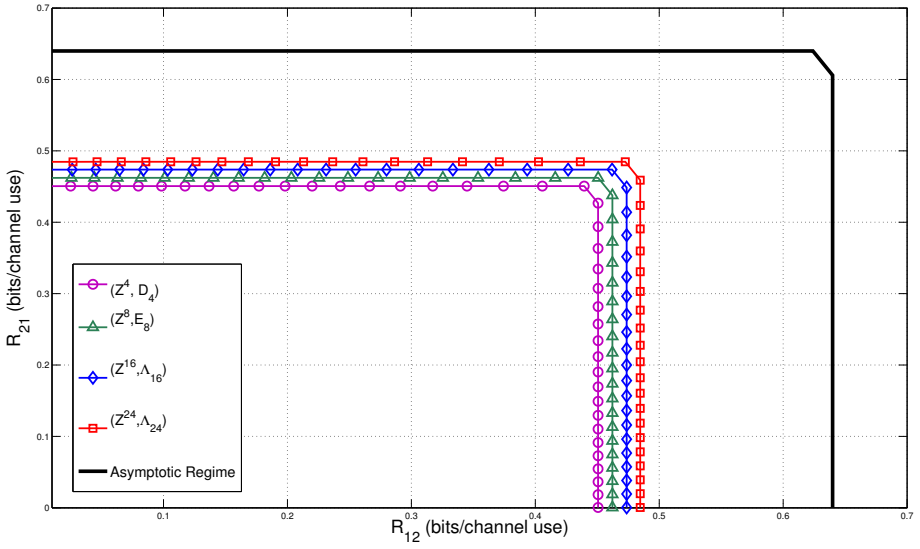

FIGURE 5.2: Achievable rate region of different finite dimension lattice pairs compared to the high dimension achievable region for $\mathrm{SNR}_1 = \mathrm{SNR}_2 = \mathrm{SNR}_r =$ 10 dB. A difference of 0.15 bit/dimension between infinite and finite dimension lattices

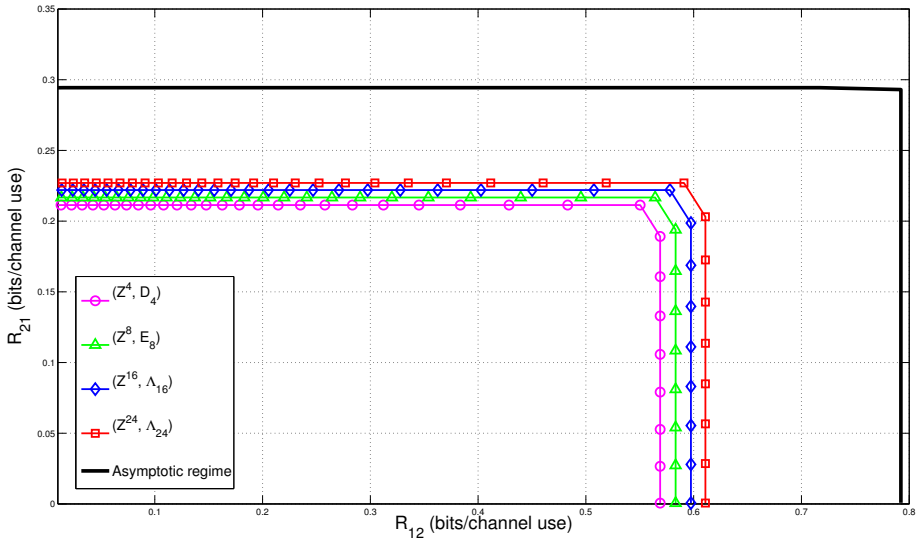

FIGURE 5.3: Achievable rate region of different finite dimension lattice pairs compared to the high dimension achievable region for $\mathrm{P}_1 = 8$ dB, $\mathrm{P}_2 = 5$ dB, $\mathrm{P}_r = 10$ dB, $|h_1| = 2$ and $|h_2| = 1$

5.5 Conclusion

In this chapter, we first derived an achievable rate region for finite dimension lattice based compress-and-forward strategy in TWRC scenario. The proposed scheme follows the same analysis as in Section 4.3 where single-layer compress-and-forward scheme was proposed for an asymptotic regime. However, we considered here analog signal problem in which the distortion at the decoders is optimized. This permits to reconstruct the optimal Gaussian forward test channel at the decoder with the worst side information. The derived scheme is based on Wyner-Ziv source coding strategy and nested lattice codes. We also provided a numerical assessment of the transmission rates with practical finite dimension lattices with good channel/source coding properties. For this purpose, we approximated the error probability at the decoder using union bound and Chernoff bound. The derived probability has been integrated in the transmission rates to characterize a new rate region for TWRC.

5.6 Appendix : Proof of Proposition 5.2

Proof. By definition, the basic Voronoi region of Λ_2 is

$$\mathcal{V}_2 = \{\mathbf{x} \in \mathbb{R}^{n_1} : \|\mathbf{x} - \mathbf{0}\| \leq \|\mathbf{x} - \boldsymbol{\lambda}\|,\ \forall \boldsymbol{\lambda} \in \Lambda_2\}.$$

Let $\mathrm{Nbr}(\Lambda_2) \subset \Lambda_2$, the set of neighbors of $\mathbf{0}$ in Λ_2 i.e. the smallest subset of Λ_2 such that

$$\mathcal{V}_2 = \{\mathbf{x} \in \mathbb{R}^{n_1} : \|\mathbf{x} - \mathbf{0}\| \leq \|\mathbf{x} - \boldsymbol{\lambda}\|,\ \forall \boldsymbol{\lambda} \in \mathrm{Nbr}(\Lambda_2)\}.$$

For a random vector $\mathbf{Z}$ taking values in $\mathbb{R}^{n_1}$, we have

$$\Pr(\mathbf{Z} \in \mathcal{V}_\mathbf{2}) = \Pr\left(\|\mathbf{Z}\|^\mathbf{2} \leq \|\mathbf{Z} - \boldsymbol{\lambda}\|^\mathbf{2}, \forall \boldsymbol{\lambda} \in \mathrm{Nbr}(\boldsymbol{\Lambda}_\mathbf{2})\right).$$

Note that for $\mathbf{z} \in \mathbb{Z}^{\mathbf{n_1}}$ if $\|\mathbf{z}\| = \|\mathbf{z} - \boldsymbol{\lambda}\|$, then $\mathbf{z}$ lays in the border point of $\mathcal{V}_2$. Thus,

$$\begin{aligned}
\Pr(\mathbf{Z} \notin \mathcal{V}_\mathbf{2}) &= \Pr[\exists \boldsymbol{\lambda} \in \mathrm{Nbr}(\Lambda_2),\ \|\mathbf{Z}\|^\mathbf{2} \geq \|\mathbf{Z} - \boldsymbol{\lambda}\|^\mathbf{2}] && (5.22)\\
&\leq \sum_{\boldsymbol{\lambda} \in \mathrm{Nbr}(\Lambda_2)} \Pr[\boldsymbol{\lambda}^\intercal \mathbf{Z} \geq \|\boldsymbol{\lambda}\|^\mathbf{2}/\mathbf{2}] && (5.23)\\
&\leq \sum_{\boldsymbol{\lambda} \in \mathrm{Nbr}(\Lambda_2)} \exp\left(\frac{-t\|\boldsymbol{\lambda}\|^2}{2}\right) \mathbf{E}[\mathbf{e}^{\mathbf{t}\boldsymbol{\lambda}^\intercal \mathbf{Z}}] && (5.24)
\end{aligned}$$

where (5.23) follows from the union bound and (5.24) follows from the Chernoff bound. In our case, $\mathbf{Z} = \beta \mathbf{U}_2 + \mathbf{E}_q$, where $U_2 \sim \mathcal{N}(0, \sigma^2_{U_2})$ and $E_q \sim \mathcal{U}nif(\mathcal{V}_1)$ and U_2 is independent from E_q, thus

$$\mathbf{E}[\mathbf{e}^{\mathbf{t}\boldsymbol{\lambda}^\intercal \mathbf{Z}}] \ = \mathbf{E}[\mathbf{e}^{\mathbf{t}\beta\boldsymbol{\lambda}^\intercal \mathbf{U_2}}]\mathbf{E}[\mathbf{e}^{\mathbf{t}\boldsymbol{\lambda}^\intercal \mathbf{E_q}}]. \quad (5.25)$$

From the moment generating functions of Gaussian and uniform random variables respectively, and by using Taylor expansion, we have

$$E[e^{t\beta\boldsymbol{\lambda}^\intercal \mathbf{U}_2}] = \exp\left(\frac{t^2\beta^2\|\boldsymbol{\lambda}\|^2\sigma^2_{U_2}}{2}\right)$$

and

$$E[e^{t\boldsymbol{\lambda}^{\intercal}\mathbf{E}_q}] \;= \exp(t^2\|\boldsymbol{\lambda}\|^2\eta^2/24) \tag{5.26}$$

Since in one hand $\frac{1}{n_1}E\|\mathbf{E}_q\|^2 = \sigma^2(\Lambda_1) = D_2$ and on the other hand $\sigma^2(\Lambda_1) = \sigma^2(\eta\mathbb{Z}^{n_1}) = \dfrac{\eta^2}{12}$, and by replacing β^2 by its value, we have

$$\begin{aligned}\mathbf{E}[\mathbf{e}^{\mathbf{t}\boldsymbol{\lambda}^{\intercal}\mathbf{Z}}] &= \exp\left(\frac{t^2\beta^2\|\boldsymbol{\lambda}\|^2\sigma_{U_2}^2}{2}\right)\exp\left(\frac{t^2\|\boldsymbol{\lambda}\|^2 D_2}{2}\right)\\ &= \exp\left(\frac{t^2\|\boldsymbol{\lambda}\|^2\sigma_{U_2}^2}{2}\right).\end{aligned} \tag{5.27}$$

Choosing t that minimizes the upper bound thus $t = \frac{1}{2\sigma_{U_2}^2}$, hence

$$P(\beta\mathbf{U}_2 + \mathbf{E}_q \notin \mathcal{V}_2) \leqslant \sum_{\boldsymbol{\lambda}\in \mathrm{Nbr}(\Lambda_2)} \exp\left(\frac{-\|\boldsymbol{\lambda}\|^2}{8\sigma_{U_2}^2}\right). \tag{5.28}$$

Furthermore, let $K(\Lambda_2)$ the kissing number of Λ_2 (the average number of the nearest neighbors to any point in Λ_2) and $d_{min}(\Lambda_2)$ the minimum distance between two elements of Λ_2. The right-hand side in (5.28) is dominated by its first term for small $\frac{\sigma_{U_2}^2}{d_{min}^2}$. Given that the coding gain ofΛ_2 is written as $\gamma_c(\Lambda_2) = \dfrac{d_{min}^2(\Lambda_2)}{V(\Lambda_2)^{2/n_1}}$, and μ is the VNR defined in (5.6)

$$\begin{aligned}P(\beta\mathbf{U}_2 + \mathbf{E}_q \notin \mathcal{V}_2) &\approx K(\Lambda_2)\exp\left(-\tfrac{d_{min}^2(\Lambda_2)}{8\sigma_{U_2}^2}\right)\\ &= K(\Lambda_2)\exp\left(-\tfrac{1}{8}\gamma_c(\Lambda_2)\mu(\Lambda_2, P_e)\right).\end{aligned} \tag{5.29}$$

This union bound estimate is tight for $\mu(\Lambda_2, P_e) \gg \frac{1}{\gamma_c(\Lambda_2)}$, thus equation (5.19) is verified. □

Chapter 6

Application: Compress-and-Forward Scheme for Parallel Gaussian Two-Way Relay Channel

Parallel two-way relay channel models a cooperative communication scenario where a relay helps two terminals to exchange their messages over a set of independent Gaussian channels. For the single channel case, we have shown in Chapter 4 that lattice-based physical layer network coding achieves the same rate as compress-and-forward scheme with a random coding strategy. A direct extension of this lattice-based scheme to parallel Gaussian channel is to repeat the same strategy for each sub-channel. However, this approach is not scalable with the number of sub-channels since the complexity of the PNC scheme becomes prohibitive when a large number of sub-channels is employed. In this chapter, we investigate a lattice-based PNC scheme where the relay jointly processes all the sub-channels together. We characterize the rate region allowed by this coding scheme. We assess then the performance penalty compared to the separate channel processing approach.

The content of this chapter has been partially published in [75].

6.1 Introduction

A significant number of modern communication scenarios are modeled by a parallel Gaussian channel: multi-carrier systems (OFDM [1], OFDMA[2] and SC-FDMA [3]), multi-stream transmission with multiple antennas, spread spectrum with multiple sequences to name a few. For these systems, two-way relaying offers a competitive solution for range extension. Two-way relaying over parallel Gaussian channel have been addressed in [28] and [32] for AF scheme, in [25] and [27] for DF scheme and in [29] and [30] for XOR emulation approach by duplicating the single channel strategy for all sub-channels. However, CF strategy has been only extended to parallel Gaussian channel for one-way relaying in [45]. To the best of our knowledge, it was not extended to TWRC.

In this chapter, we design a new relaying scheme for parallel TWRC based on the single-layer CF strategy that we have proposed in Chapter 4. We consider a joint lattice-based coding scheme at the relay, where the signals received over all the channels are compressed together. The proposed scheme offers a reduced complexity compared to the separate processing of each sub-channel. We derive the achievable rate region for both, joint and separate source compression. Then, we assess the gap between both strategies.

6.2 System Model

Consider a two-way relaying scenario where K parallel Gaussian channels are employed. Two nodes T_1 and T_2 exchange two individual messages m_1 and m_2, with the help of a relay R. The relay operates in half-duplex mode. The communication takes n channel uses that are split into two phases: a MAC phase during which each node sends its message to the relay (cf. Fig. 6.1) and a BC phase where the relay sends a signal which helps each node to decode its destined message (cf.

[1] Orthogonal Frequency-Division Multiplexing
[2] Orthogonal Frequency-Division Multiple Access
[3] Single-Carrier FDMA

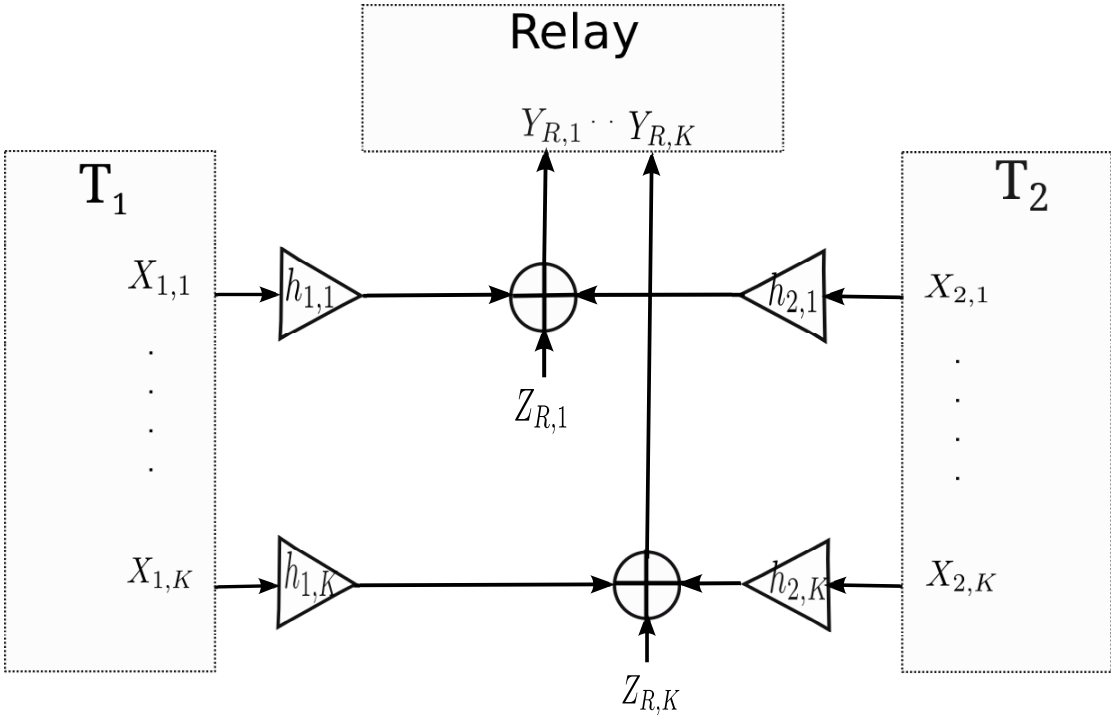

FIGURE 6.1: Multiple access phase of parallel Gaussian TWRC

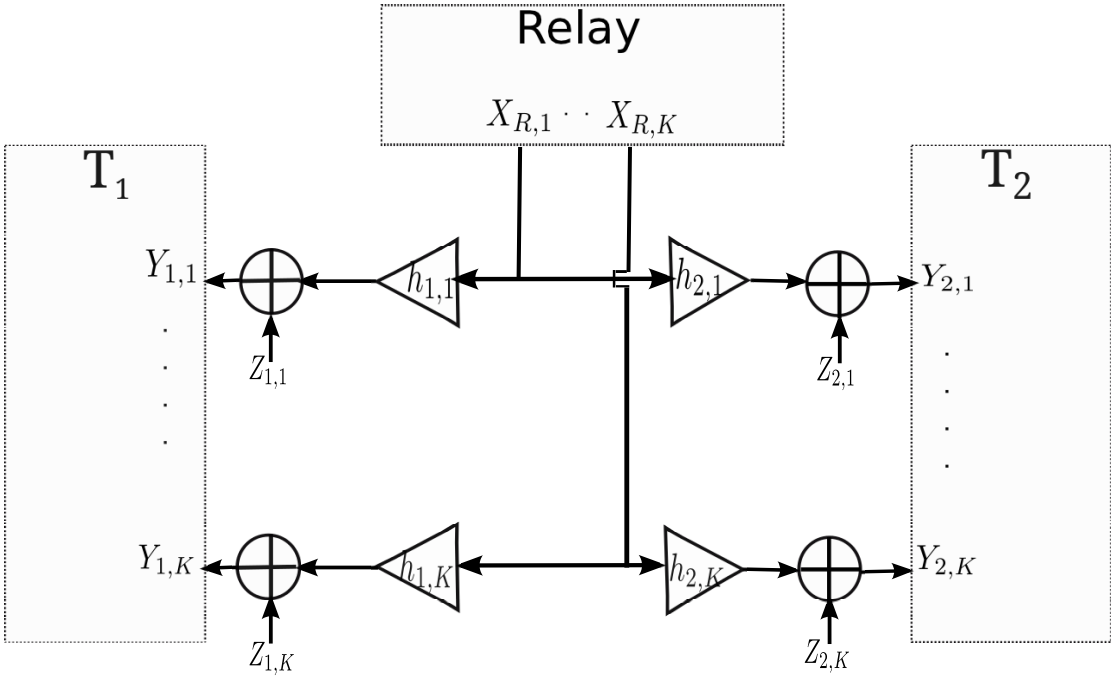

FIGURE 6.2: Broadcast phase of parallel Gaussian TWRC

Fig. 6.2). The MAC and BC phases are of lengths $n_1 = \alpha n$ and $n_2 = (1-\alpha)n$, $\alpha \in [0,1]$ respectively. The channel coefficient between node T_i and the relay in sub-channel k (respectively the relay and node T_i) is denoted $h_{i\to R,k}$ (respectively $h_{R\to i,k}$). Without loss of generality, channel reciprocity is assumed for each sub-channel, i.e. $h_{i\to R,k} = h_{R\to i,k} = h_{i,k}$.

During the MAC phase, node T_i, $i \in \{1,2\}$ draws a message m_i from a set $\mathcal{M}_i = \{1, 2, \cdots, 2^{nR_{i\bar{i}}}\}$ according to a uniform distribution, where $R_{i\bar{i}}$ denotes the message rate of node T_i destined to $\mathrm{T}_{\bar{i}}$. Each message m_i, $i \in \{1,2\}$ is encoded to a codeword $\mathbf{x}_i(m_i) = [\mathbf{x}_{i,1}(m_i) \cdots \mathbf{x}_{i,K}(m_i)]$ which is spread over K sub-channels and n_1 channel uses. $\mathbf{x}_{i,k}(m_i)$ is a n_1-sized row vector codeword which is sent by node T_i in the sub-channel k. Transmission at node T_i is subject to an individual power constraint P_i such as:

$$\sum_{k=1}^{K} P_{i,k} \leq P_i \tag{6.1}$$

with $P_{i,k}$ is the allocated power in sub-channel k.

The messages are transmitted simultaneously through memoryless Gaussian sub-channels and the relay R receives in each sub-channel k a signal $\mathbf{Y}_{R,k}$ given by

$$\mathbf{Y}_{R,k} = h_{1,k}\mathbf{X}_{1,k} + h_{2,k}\mathbf{X}_{2,k} + \mathbf{Z}_{R,k} \tag{6.2}$$

where $Z_{R,k} \sim \mathcal{N}(0, \sigma^2_{R,k})$ is an i.i.d additive white Gaussian noise, AWGN.

Let $\mathbf{Y}_R = [\mathbf{Y}_{R,1} \cdots \mathbf{Y}_{R,K}]$ be the row-wise concatenation of all signals received by the relay during the MAC phase.

During the BC phase, the relay generates a codeword $\mathbf{x}_R(m_R) = [\mathbf{x}_{R,1}(m_R) \cdots \mathbf{x}_{R,K}(m_R)]$ which is spread over n_2 channel uses and K sub-channels. The signals $\mathbf{X}_{R,k}$ are transmitted through broadcast memoryless channels and the received signals at node T_i are $\mathbf{Y}_{i,k}$, $i = 1,2$ for $k \in \{1, 2, \cdots, K\}$

$$\mathbf{Y}_{i,k} = h_{i,k}\mathbf{X}_{R,k} + \mathbf{Z}_{i,k}, \tag{6.3}$$

$Z_{i,k} \sim \mathcal{N}(0, \sigma_{i,k}^2)$ is an i.i.d AWGN. We assume that perfect CSI is available for all nodes and that noise components are independent of each other and from the channel inputs. In the sequel, we investigate achievable rate regions of our system model and we detail our coding schemes.

6.3 Achievable rate region for Joint Lattice Coding Scheme

Theorem 6.1. *For parallel Gaussian TWRC, the convex hull of the following end-to-end rates* (R_{12}, R_{21}) *is achievable:*

$$R_{12} \leq \frac{\alpha}{2} \sum_{k=1}^{K} \log_2 \left(1 + \frac{|h_{1,k}|^2 P_{1,k}}{\sigma_{R,k}^2 + \frac{\max\limits_{i\in\{1,2\}} \sum\limits_{k=1}^{K} |h_{i,k}|^2 P_{i,k} + \sigma_{R,k}^2}{\min\limits_{i\in\{1,2\}} \prod\limits_{k=1}^{K} \left(1 + \frac{|h_{i,k}|^2 P_{R,k}}{\sigma_{i,k}^2} \right)^{\frac{1-\alpha}{\alpha}} - 1}} \right) \tag{6.4}$$

$$R_{21} \leq \frac{\alpha}{2} \sum_{k=1}^{K} \log_2 \left(1 + \frac{|h_{2,k}|^2 P_{2,k}}{\sigma_{R,k}^2 + \frac{\max\limits_{i\in\{1,2\}} \sum\limits_{k=1}^{K} |h_{i,k}|^2 P_{i,k} + \sigma_{R,k}^2}{\min\limits_{i\in\{1,2\}} \prod\limits_{k=1}^{K} \left(1 + \frac{|h_{i,k}|^2 P_{R,k}}{\sigma_{i,k}^2} \right)^{\frac{1-\alpha}{\alpha}} - 1}} \right) \tag{6.5}$$

with $\alpha \in [0, 1]$.

In this next paragraphs, we present a detailed proof of Theorem 6.1. The main idea of the proposed scheme is the following: during the BC phase, the relay station

sends a compressed version of the collection of signals received during the MAC phase. The relay employs nested lattice coding that is tuned to the user with the global weakest side information. The proof is divided into three paragraphs: Section 6.3.1 introduces the lattice coding scheme. Section 6.3.2 analyses the end-to end rates of the proposed scheme and finally Section 6.3.3 derives the achievable rate region.

6.3.1 Lattice-based source coding

We assume that the elements of $\mathbf{X}_{i,k}$, $i = 1, 2$, are drawn from an independent identically distributed (i.i.d) Gaussian distribution with zero mean and variance $P_{i,k}$ for all $k \in [1, K]$. Let $\mathbf{S}_i = [h_{i,1}\mathbf{X}_{i,1}, h_{i,2}\mathbf{X}_{i,2}, \cdots, h_{i,K}\mathbf{X}_{i,K}]$, be the collection of side information available at terminal T_i, $i = 1, 2$.

The source $\mathbf{Y}_R$, of dimension $n_1 K$, can be written, in two ways, as the sum of two independent Gaussian random vectors: the side information $\mathbf{S}_i$ and the unknown part $\mathbf{U}_i = \mathbf{Y}_R|\mathbf{S}_i$ for $i \in 1, 2$.

6.3.1.1 Encoding

We use a pair of $(n_1 K)$-dimensional nested lattices (Λ_1, Λ_2). The fine lattice Λ_1 is good for quantization with basic Voronoi region $\mathcal{V}_1$ of volume V_1 and second moment per dimension $\sigma^2(\Lambda_1)$. The coarse lattice Λ_2 is good for channel coding with basic Voronoi region $\mathcal{V}_2$ of volume V_2 and second moment $\sigma^2(\Lambda_2)$. The lattice source encoder (LSE) operation is performed with four successive operations: first, the input signal $\mathbf{Y}_R$ is scaled with a factor β. Then, a random dither which is uniformly distributed over $\mathcal{V}_1$ is added. This dither is known by all nodes. The dithered scaled version of $\mathbf{Y}_R$, $\beta\mathbf{y}_R + \mathbf{t}$ is quantized to the nearest point in Λ_1. The outcome of this operation is processed with a modulo-lattice operation in order to generate a vector $\mathbf{v}_R$ of size $n_1 K$.

$$\mathbf{v}_R = Q_1(\beta\mathbf{y}_R + \mathbf{t}) \mod \Lambda_2 \tag{6.6}$$

The relay recovers the index of $\mathbf{v}_R$ that identifies a coset of Λ_2 relative to Λ_1 that contains $Q_1(\beta \mathbf{y}_R + \mathbf{t})$. The coset leader $\mathbf{v}_R$ is represented with $\frac{V_2}{V_1}$ bits. Thus, the global source coding rate of the scheme is

$$R = \frac{1}{n_1 K} \log_2 |\Lambda_1 \cap \mathcal{V}_2| = \frac{1}{n_1 K} \log_2 \frac{V_2}{V_1} \quad \text{(bits/dim.)} \tag{6.7}$$

According to the properties of good lattices, we have

$$\frac{1}{n_1 K} \log_2(V_i) \approx \frac{1}{2} \log_2(2\pi e \sigma^2(\Lambda_i)) \ , \ i \in \{1, 2\}.$$

Thus the coding rate in (6.7) reads:

$$R = \frac{1}{2} \log_2 \left(\frac{\sigma^2(\Lambda_2)}{\sigma^2(\Lambda_1)} \right) \tag{6.8}$$

The relay sends Kn_2-sized codewords to represent $\mathbf{v}_R$.

6.3.1.2 Decoding

At both users, $\mathbf{v}_R$ is generated from the sub-channels' received codewords concatenation. $\hat{\mathbf{Y}}_{R,i} | \hat{\mathbf{S}}_i = \hat{\mathbf{U}}_i$ is reconstructed with a lattice source decoder LSD using the side information $\mathbf{S}_i$ as

$$\hat{\mathbf{u}}_i = \gamma_i((\mathbf{v}_R - \mathbf{t} - \beta \mathbf{s}_i) \mod \Lambda_2), \ i = 1, 2 \tag{6.9}$$

with γ_i ,$i = 1, 2$ is the decoder scaling factor.

6.3.2 Rate analysis

At the relay, the coset leader $\mathbf{v}_R$ is represented with a message m_R which is mapped to Kn_2-sized codewords $\mathbf{X}_R$. We suppose that the elements of the r.v. $\mathbf{X}_{R,k}$ are drawn from an i.i.d Gaussian distribution with zero mean and variance $P_{R,k}$ for

all $k \in [1, K]$. The broadcast rate at the relay is bounded by

$$n_1 R \leq n_2 \min \left\{ \sum_{k=1}^{K} I\left(X_{R,k}; Y_{1,k}\right), \sum_{k=1}^{K} I\left(X_{R,k}; Y_{2,k}\right) \right\} \tag{6.10}$$

Since real Gaussian codebooks are used for all transmissions, we have:

$$I(X_{R,k}; Y_{i,k}) = \frac{1}{2} \log_2 \left(1 + \frac{|h_{i,k}|^2 P_{R,k}}{\sigma_{i,k}^2} \right) \ , \ i = 1, 2.$$

The constraint (6.10) ensures that the index m_R is transmitted reliably to both terminals over all sub-channels and $\mathbf{v}_R$ is available at the input of LSD at both receivers. At terminal T_i, $\hat{\mathbf{u}}_i$ in (6.9) can be written as:

$$\hat{\mathbf{u}}_i = \gamma_i((\beta \mathbf{u}_i + \mathbf{e}_q) \bmod \Lambda_2) \tag{6.11}$$

$$\equiv \gamma_i(\beta \mathbf{u}_i + \mathbf{e}_q) \tag{6.12}$$

where $\mathbf{e}_q = Q_1(\beta \mathbf{y}_R + \mathbf{t}) - (\beta \mathbf{y}_R + \mathbf{t}) = -(\beta \mathbf{y}_R + \mathbf{t}) \mod \Lambda_1$, is the quantization error. By the Crypto Lemma 4.1, $\mathbf{E}_q$ is independent from $\mathbf{Y}_R$, thus from $\mathbf{U}_i$, and it is uniformly distributed over $\mathcal{V}_1$. The equivalence between (6.11) and (6.12) is valid only if $\beta \mathbf{u}_i + \mathbf{e}_q \in \mathcal{V}_2$. According to [91], with good channel coding lattices, the probability $\Pr(\beta \mathbf{U}_i + \mathbf{E}_q \notin \mathcal{V}_2)$ vanishes asymptotically provided that:

$$\frac{1}{n_1 K} \mathbb{E} \|\beta \mathbf{U}_i + \mathbf{E}_q\|^2 \leq \sigma^2(\Lambda_2) \tag{6.13}$$

Replacing $\mathbf{U}_i$ by its value in (6.12), we conclude that:

$$\hat{\mathbf{U}}_i = \gamma_i \left(\begin{bmatrix} \beta h_{i,1} \mathbf{X}_{i,1} + \beta \mathbf{Z}_{R,1} \\ \cdots \\ \beta h_{i,K} \mathbf{X}_{i,K} + \beta \mathbf{Z}_{R,K} \end{bmatrix}^{\mathrm{T}} + \mathbf{E}_q \right) \tag{6.14}$$

Let $\mathbf{Z}_{eq,i,k} = \gamma_i \left(\beta \mathbf{Z}_{R,k} + \mathbf{E}_q(n_1(k-1) : n_1 k) \right)$ be the effective global additive noise at terminal T_i. $\mathbf{E}_q(n_1(k-1) : n_1 k)$ stands for all the n_1-components of the quantization error on subchannel k.

The communication between T_1 and T_2 (resp. T_2 and T_1) is equivalent to virtual additive parallel Gaussian channels where the noise components are given by $\mathbf{Z}_{eq,i,k}$ for $k \in \{1, \cdots, K\}$. We approximate $\mathbf{E}_q$ by a Gaussian variable $\mathbf{Z}_q$ with the same variance. The equivalence is valid for asymptotic regime as $n_1 \to \infty$ [90]. Thus the achievable rate of both links satisfy:

$$nR_{12} \leq \frac{n_1}{2} \sum_{k=1}^{K} \log_2 \left(1 + \frac{\beta^2 |h_{1,k}|^2 P_{1,k}}{\beta^2 \sigma_{R,k}^2 + \sigma^2(\Lambda_1)} \right) \tag{6.15}$$

$$nR_{21} \leq \frac{n_1}{2} \sum_{k=1}^{K} \log_2 \left(1 + \frac{\beta^2 |h_{2,k}|^2 P_{2,k}}{\beta^2 \sigma_{R,k}^2 + \sigma^2(\Lambda_1)} \right) \tag{6.16}$$

We refer to the proposed coding scheme as joint-LCF with stands for joint-lattice compress and forward coding scheme.

6.3.3 Achievable rate region

The rate region that is achieved by the proposed scheme is characterized by the constraints (6.10), (6.13) (6.15) and (6.16). The equations (6.10) and (6.13) are rewritten as

$$\begin{cases} \dfrac{\sigma^2(\Lambda_2)}{\sigma^2(\Lambda_1)} \leq \min\limits_{i \in \{1,2\}} \displaystyle\prod_{k=1}^{K} \left(1 + \frac{|h_{i,k}|^2 P_{R,k}}{\sigma_{i,k}^2} \right)^{\frac{1-\alpha}{\alpha}} \\ \sigma^2(\Lambda_1) + \beta^2 \sigma_{U_i}^2 \leq \sigma^2(\Lambda_2) \ , \ \text{for } i \in \{1,2\} \end{cases} \tag{6.17}$$

Let T^* be the user that has the lowest global side information variance given by $\min\limits_{i \in \{1,2\}} \sum\limits_{k=1}^{K} |h_{i,k}|^2 P_{i,k}$. We will refer to its corresponding variables by $(.)^*$. Note that the variance per dimension of $\mathbf{U}^*$ is

$$\sigma_{U^*}^2 = VAR(Y_R | S^*) = \max_{i \in \{1,2\}} \sum_{k=1}^{K} |h_{i,k}|^2 P_{i,k} + \sigma_{R,k}^2 \tag{6.18}$$

Denoting $\alpha = \frac{n_1}{n}$, from the system (6.17), the minimal bound of $\sigma^2(\Lambda_1)$ is given by

$$\sigma^2(\Lambda_1) \geq \frac{\beta^2 \sigma^2_{U^*}}{\min\limits_{i\in\{1,2\}} \prod\limits_{k=1}^{K} \left(1 + \frac{|h_{i,k}|^2 P_{R,k}}{\sigma^2_{i,k}}\right)^{\frac{1-\alpha}{\alpha}} - 1} \tag{6.19}$$

The constraints on the achievable rates in (6.15) and (6.16) can be written as

$$R_{12} \leq \frac{\alpha}{2} \sum_{k=1}^{K} \log_2 \left(1 + \mathrm{SNR}_{1\to 2,k}\right) \tag{6.20}$$

$$R_{21} \leq \frac{\alpha}{2} \sum_{k=1}^{K} \log_2 \left(1 + \mathrm{SNR}_{2\to 1,k}\right) \tag{6.21}$$

where $\mathrm{SNR}_{1\to 2,k}$ and $\mathrm{SNR}_{2\to 1,k}$ are the virtual end-to-end SNRs at each subchannel k, defined as follows:

$$\mathrm{SNR}_{1\to 2,k} = \frac{\beta^2 |h_{1,k}|^2 P_{1,k}}{\beta^2 \sigma^2_{R,k} + \sigma^2(\Lambda_1)} \tag{6.22}$$

$$\mathrm{SNR}_{2\to 1,k} = \frac{\beta^2 |h_{2,k}|^2 P_{2,k}}{\beta^2 \sigma^2_{R,k} + \sigma^2(\Lambda_1)} \tag{6.23}$$

Note that for $k \in [1, K]$, $\mathrm{SNR}_{1\to 2,k}$ and $\mathrm{SNR}_{2\to 1,k}$ are maximized when $\sigma^2(\Lambda_1)$ is minimal. Thus the optimal choice on the second moment of Λ_1 is $\sigma^2(\Lambda_1)_{\min}$ is equal to the lowest bound defined in (6.19). Finally by replacing $\sigma^2(\Lambda_1)_{\min}$ in (6.22) and (6.23), equations (6.4) and (6.5) are verified and the proof is concluded.

6.4 Achievable Rate Region for Separate Lattice Coding Scheme

The first proposed scheme is based on joint processing at the relay of the signals received from all sub-channels. For comparison purpose, we present in this section another achievable rate region for parallel TWRC based on separate processing scheme at the relay. The achievable rate region is given in Theorem 6.2.

Theorem 6.2. *For parallel Gaussian TWRC, the convex hull of the following end-to-end rates* (R_{12}, R_{21}) *is achievable:*

$$R_{12} \leq \frac{\alpha}{2}\sum_{k=1}^{K}\log_2\left(1+\frac{|h_{1,k}|^2P_{1,k}}{\sigma_{R,k}^2+\frac{\max\limits_{i\in\{1,2\}}|h_{i,k}|^2P_{i,k}+\sigma_{R,k}^2}{\min\limits_{i\in\{1,2\}}\left(1+\frac{|h_{i,k}|^2P_{R,k}}{\sigma_{i,k}^2}\right)^{\frac{1-\alpha}{\alpha}}-1}}\right) \tag{6.24}$$

$$R_{21} \leq \frac{\alpha}{2}\sum_{k=1}^{K}\log_2\left(1+\frac{|h_{2,k}|^2P_{2,k}}{\sigma_{R,k}^2+\frac{\max\limits_{i\in\{1,2\}}|h_{i,k}|^2P_{i,k}+\sigma_{R,k}^2}{\min\limits_{i\in\{1,2\}}\left(1+\frac{|h_{i,k}|^2P_{R,k}}{\sigma_{i,k}^2}\right)^{\frac{1-\alpha}{\alpha}}-1}}\right) \tag{6.25}$$

with $\alpha \in [0,1]$.

Sketch of the proof:

The proposed scheme is to repeat the single-layer lattice coding strategy presented in Section 4.3 in Chapter 4 for every sub-channel. In this case, K different n_1-dimensional nested lattices are used: $(\Lambda_{1,k}, \Lambda_{2,k})$ for $k \in [1, K]$. Thus, K different lattice parameters, i.e. the second moments of $\Lambda_{1,k}$, should be optimized to retrieve the presented achievable rate region.

Let T_k^* be the user that has the lowest side information variance at sub-channel k given by $\min_{1,2}|h_{i,k}|^2P_{i,k}$. In this case, $\sigma^2_{U_k^*}$, is the variance per dimension of the unknown part of $Y_{R,k}$ at user T_k^* is $\mathbf{U}_\mathbf{k}^*$.

$$\sigma^2_{U_k^*} = \max_{i\in\{1,2\}}|h_{i,k}|^2P_{i,k}+\sigma^2_{R,k}$$

The end-to-end achievable rates of the scheme are the sum of the rates at all subchannels:

$$R_{12} \leq \frac{\alpha}{2} \sum_{k=1}^{K} \log_2 \left(1 + \mathrm{SNR}_{1\to 2,k}\right) \tag{6.26}$$

$$R_{21} \leq \frac{\alpha}{2} \sum_{k=1}^{K} \log_2 \left(1 + \mathrm{SNR}_{2\to 1,k}\right) \tag{6.27}$$

For each sub-channel, the end-to-end SNRs are given by

$$\mathrm{SNR}_{1\to 2,k} = \frac{\beta^2 |h_{1,k}|^2 P_{1,k}}{\beta^2 \sigma_{R,k}^2 + \sigma^2(\Lambda_{1,k})} \tag{6.28}$$

$$\mathrm{SNR}_{2\to 1,k} = \frac{\beta^2 |h_{2,k}|^2 P_{2,k}}{\beta^2 \sigma_{R,k}^2 + \sigma^2(\Lambda_{1,k})} \tag{6.29}$$

where the optimal choice of $\sigma^2(\Lambda_{1,k})$, $k \in [1, K]$ is

$$\sigma^2(\Lambda_{1,k}) = \frac{\beta^2 \sigma_{U_k^*}^2}{\left(1 + \min\limits_{i\in\{1,2\}} \frac{|h_{i,k}|^2 P_{R,k}}{\sigma_{i,k}^2}\right)^{\frac{1-\alpha}{\alpha}} - 1} \tag{6.30}$$

Replacing (6.28) and (6.28) in (6.26) (6.27) concludes the proof.
We refer to this scheme as Separate-LCF. This approach is not scalable with the number of sub-channels since the complexity of the PNC scheme becomes prohibitive when a large number of sub-channels is employed.

6.5 Numerical Results

In this section, we present the optimization problem that represents the optimal power allocation for our Joint-LCF and Separate-LCF schemes. Then, we compare them through some simulation results.

6.5.1 Optimization problem

We characterize the whole region of achievable rates (R_{12}, R_{21}) of Joint-LCF scheme by considering all possible values for the time division coefficient $\alpha \in [0, 1]$, and by optimizing power allocation and distortions. The boundary points are determined by maximizing the weighted sum of both rates R_{12} and R_{21}. The rate maximization problem can be expressed as follows:

$$\max \qquad \eta R_{12} + (1-\eta) R_{21} \tag{6.31a}$$

$$\text{s.t.} \qquad 0 \leq \alpha \leq 1, \tag{6.31b}$$

$$\sum_{k=1}^{K} P_{i,k} \leq P_i \ , \ i = 1, 2, R \tag{6.31c}$$

$$P_{i,k} \geq 0, \tag{6.31d}$$

$$\text{for all values of} \eta \in [0, 1]. \tag{6.31e}$$

The optimization problem that corresponds to the separate-LCF achievable rates presented in Theorem 6.1 is different from joint-LCF scheme since it requires to optimize over each sub-channel k. A total of 3+K and 2+2K parameters are to optimize for Joint-LC and Separate-LCF, respectively.

The considered optimization problems are not convex in general. Thus, the joint power/time allocation policy for this problem cannot be expressed in a simple form. Hence, we provide in the sequel numerical results using interior-point method.

6.5.2 Simulations

We consider $K = 8$ sub-channels. The channel gains are generated using 4 i.i.d Rayleigh distributed time-domain taps. The noise variance is identical for all sub-channels. We present the results obtained through Monte Carlo for this setting where the optimization problems of Joint-LCF and Separate-LCF are solved.

In Fig. 6.3, we consider the same power at all receivers, i.e., $P_1 = P_2 = P_R = P$. We can observe that Separate-LCF is only 0.1 bit/channel use better than Joint-

LCF rate region.

In Fig. 6.4, we consider different power constraints at all nodes. We can notice

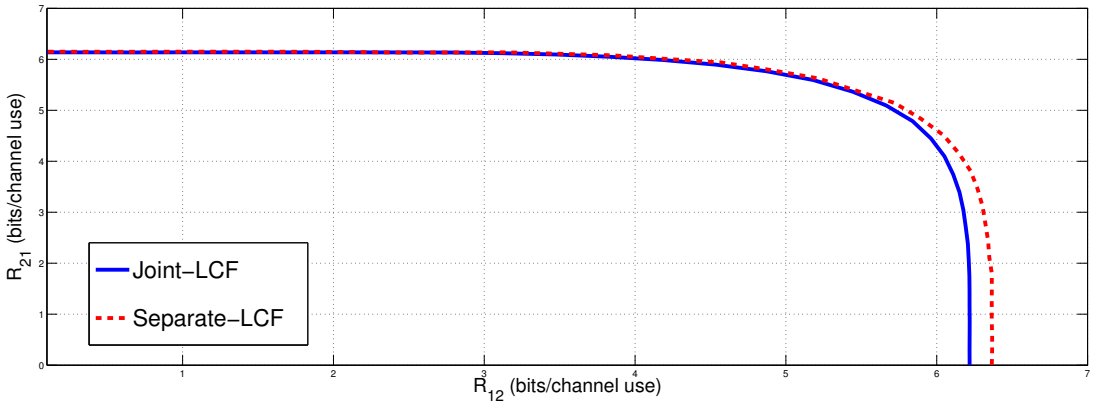

Figure 6.3: Achievable rate regions of Joint-LCF and Separate-LCF for equal powers, P = 10 dB

that Joint-LCF improves compared to Separate-LCF with achievable rates $R_{21} > R_{12}$ for $P_1 > P_2$.

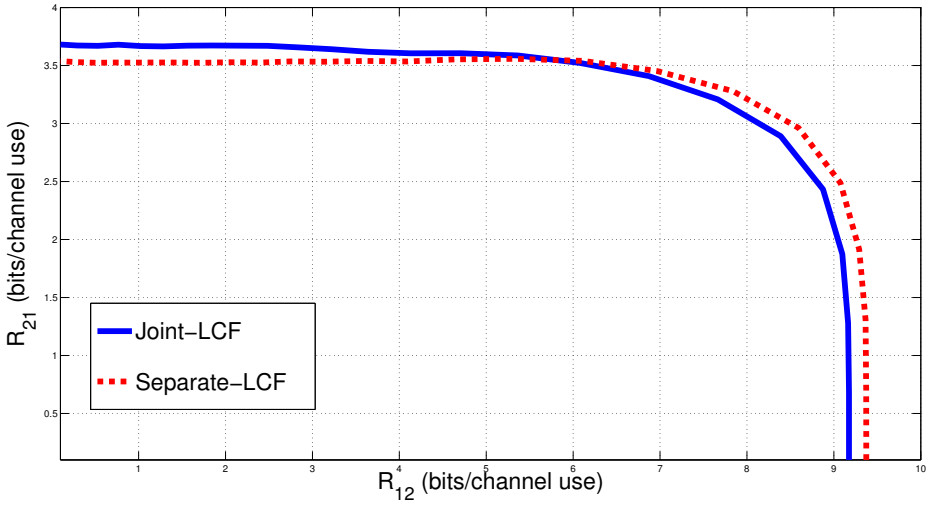

Figure 6.4: Achievable rate regions of Joint-LCF and Separate-LCF rates for $P_1 = 15$ dB, $P_2 = 5$ dB and $P_R = 10$ dB

In addition, it is worth noting that Joint-LCF scheme offers a significant complexity gain compared to Separate-LCF scheme. The relay performs four operations with Joint-LCF (one multiplication, one addition, one quantification and one modulation). With Separate-LCF, 4K operations are needed. In fact, every operation is repeated K times since K different lattices should be used in the coding process.

6.6 Conclusion

In this chapter, we derived two achievable rate regions for parallel Gaussian TWRC. For this purpose, we first proposed a practical lattice-based physical-layer network coding scheme. The scheme is based on nested lattice codes proposed in Chapter 4 where joint processing is performed at the relay for all sub-channels. Then, another separate processing scheme is proposed based on the direct extension of the single-layer scheme presented in Chapter 4 for each sub-channel. Numerical results show that the joint processing scheme permits to achieve rates close to separate processing at each sub-channel with reduced complexity.

Chapter 7

Conclusion

In this concluding chapter, we will first summarize the main investigations and corresponding outcomes that have been carried out during thesis. Then, we give perspectives for further research works.

7.1 Thesis Summary

Better spectral efficiency is the key performance enhancement that can be achieved through physical-layer network coding (PNC) in wireless cooperative networks. This thesis provides principally analysis and design of PNC schemes that can achieve new transmission rates for Two-Way relay channel (TWRC).

In Chapter 3, we have analyzed finite dimension PNC scheme with Decode-and-Forward (DF) strategy employed at the relay. We have derived the individual average error probabilities at both terminals' decoders based on the random error exponents metric. Then, we have analyzed the impact of finite-length codewords and constrained error probabilities on the end-to-end transmission rates. For this analysis, we have optimized the time division between multiple access and broadcast phases. We have also analyzed the dependence of the optimal time division as a function of the channel conditions of both communicating terminals and the rate requirement of both directions. Then, we have considered optimal power al-

location in the system. This has permitted the improvement of the rate region by more than 30 % over the fixed power allocation.

DF relaying is optimal in various SNR regimes for TWRC. It introduces significant complexity at the relay and is incompatible with implementations relying on low capabilities relaying nodes. Moreover, in practice, the relay node needs to know the modulation and coding schemes that are employed by the communicating nodes, which introduces additional signalling. That's why we have investigated in Chapter 4 the design of PNC schemes that have lower complexity than DF and achieve comparable performance. We have proposed two schemes based on compress-and-forward (CF) lattice coding. On one hand, with CF strategy, the relay does not need to decode its received signal but to only generate a compressed version of it. On the other hand, lattice codes, which are structured codes, can be adapted to real implementations contrary to random codes which can be used only as a theoretical tool. In the first proposed scheme, the relay broadcasts a common message to both decoders. Therefore, the achievable rates in both directions are constrained by the capacity of the worst channel. In this case, the user experiencing better channel conditions will suffer from this restriction on its transmission rate. To overcome this limitation, we have proposed and analyzed the performance of an improved coding scheme in which the relay sends not only a common description of its output, but also an individual description that is destined to be recovered only by the user who experiences better channel conditions. Simulations have shown that the second scheme outperforms classic amplify-and-forward at all SNR regimes, and classic decode-and-forward for certain SNR regimes.

Previous PNC schemes have been investigated for infinite lattice dimensions. The impact of finite dimension on the CF lattice coding scheme has been analyzed in Chapter 5. We have considered the analog transmission problem where the distortion is optimized. We have analyzed the end-to-end transmission rates when finite dimension lattices are used. Then, we have discussed the design criteria of our coding scheme. Finally, we have illustrated our results with some numerical examples were practical lattices are employed.

The last chapter of the thesis has presented an application of CF lattice coding scheme to parallel Gaussian TWRC. This channel can model multi-carrier systems such as OFDM technology which represents the modulation of choice for future wideband wireless systems. The multi-carrier technique along with PNC schemes can achieve higher data rates in cooperative networks with frequency selective channels. To this end, we have derived an achievable rate region by considering CF lattice coding at the relay. In the coding scheme, the relay processes all sub-channels together. This technique has been compared to the direct extension of the first proposed scheme in Chapter 4 where the relay applies the coding scheme at each sub-channel separately. Simulations have shown that the proposed joint-processing scheme achieves rates close to separate-processing at each sub-channel with reduced complexity.

7.2 Perspectives

Throughout this document, we have considered full Channel State Information (CSI) in our analyses. We investigated in Chapter 4 the channel knowledge requirements and their impact in practical implementation in terms of signalling. Further study can be achieved on the impact of imperfect CSI knowledge on the proposed schemes. Furthermore, only chapter 3 and 6 have addressed the power allocation. Adaptive power allocation can be investigated in the design of the proposed schemes.

We have also studied the analog transmission problem for finite dimension lattices only in the case of single-layer of compression where the relay broadcasts a common compressed message to both terminals. This study can be extended for the layered scheme where the relay generates with the common layer another refinement layer addressed to the best user.

It is worth mentioning that our schemes are based on structured codes that are closer to real implementations than random coding techniques. However, in these schemes, lattice codewords are used only at the relay while Gaussian codewords

are used at both transmitting terminals. Although Gaussian assumptions (channel and codebooks) are not realistic they allow to derive theoretical schemes that can be converted into practical strategies. An interesting perspective of the present work is to consider lattice codes for all the nodes which can be even more appropriate for practical systems.

Finally, in this work, we have considered the TWRC model. This setting can be applied to cellular, ad-hoc, or hybrid networks in order to enhance the wireless coverage and to increase the total throughput. It can also be integrated in a wireless mesh network architecture. Thus, a two-way communication via a relay in a network with more than two users can open up new opportunities for further studies. In this case, the signals transmitted from multiple nodes to the same relay interfere and thus they can weaken the bidirectional communication between two communicating nodes. This interference, however, can improve the system performance if it is considered as additional information. Careful study should be realized to go further in this perspective along with other problems such as synchronization between transmitting terminals.

For a practical implementation, one should deal with many problems. However, we are convinced that further studies on physical-layer network coding will pay off regarding its advantages in avoiding spectral loss and thus enhancing the system throughput in a cooperative network.

Bibliography

[1] R. Ahlswede. Multiway communication channels. In *Proc. of the 2nd International Symposium on Information Theory (ISIT)*, Tsahkadsor, Armenia, USSR, 1971.

[2] R. Ahlswede, N. Cai, S.-Y. R. Li, and R. W. Yeung. Network information flow. *IEEE Transactions on Information Theory*, 46(4):1204–1216, July 2000.

[3] W. K. M. Ahmed and P. J. McLane. Random coding error exponents for two-dimensional flat fading channels with complete channel state information. *IEEE Transactions on Information Theory*, 45(4):1338–1346, 1999.

[4] S. Chachulski, M. Jennings, S. Katti, and D. Katabi. Trading structure for randomness in wireless opportunistic routing. In *Proc. of ACM SIGCOMM'07*, volume 37, 2007.

[5] J. H. Conway and N. J. Sloane. *Sphere packings, lattices and groups*. Springe-Verlag, New York, USA, 3rd ed., 1998.

[6] T. Cover and J. Thomas. *Elements of Information Theory*. Wiley, New York, 1991.

[7] T. M. Cover. Broadcast channels. *IEEE Transactions on Information Theory*, 18(1):2–14, January 1972.

[8] T. M. Cover and A. El Gamal. Capacity theorems for the relay channel. *IEEE Transactions on Information Theory*, 25(5):572–584, 1979.

[9] M. Dankberg. Paired carrier multiple access (pcma) for satellite communications. In *Proc. of Pacific Telecommunications Conference*, January 1998.

[10] d.S. Lun, M. Médard, and R. Koetter. Efficient operation of wireless packet networks using network coding. In *Proc. of International Workshop on Convergent Technologies (IWCT)*, volume 33, 2005.

[11] AG. Dyachkov. Random constant composition codes for multiple access channels. *Probl. of Control and Information Theory*, 13:357–369, 1984.

[12] U. Erez, S. Litsyn, and R. Zamir. Lattices which are good for (almost) everything. *IEEE Transactions on Information Theory*, 51(10):3401–3416, October 2005.

[13] U. Erez, S. Shamai (Shitz), and R. Zamir. Capacity and lattice strategies for canceling known interference. *IEEE Transactions on Information Theory*, 51(11):3820–3833, November 2005.

[14] U. Erez and R. Zamir. Achieving $\frac{1}{2}\log(1+\mathrm{SNR})$ on the AWGN channel with lattice encoding and decoding. *IEEE Transactions on Information Theory*, 50(10):2293–2314, October 2004.

[15] S. Sandhu F. Xue. Phy-layer network coding for broadcast channel with side information. In *Proc. of IEEE Information Theory Workshop*, Lake Tahoe, California, September 2007.

[16] R. M. Fano. Transmission of information: A statistical theory of communications. *American Journal of Physics*, 29:793–794, 1961.

[17] A. Feinstein. Error bounds in noisy channels without memory. *IRE Transactions on Information Theory*, 1(2):13–14, 1955.

[18] C. Fragouli, J. L. Boudec, and J. Widmer. Network coding: an instant primer. In *Proc. of ACM SIGCOMM*, pages 63–68, January 2006.

[19] H. Gacanin and F. Adachi. Broadband analog network coding. *IEEE Transactions on Wireless Communications*, 9(5):1577–1583, 2010.

[20] R. Gallager. A simple derivation of the coding theorem and some applications. *IEEE Transactions on Information Theory*, 11(1):3–18, 1965.

[21] R. Gallager. The random coding bound is tight for the average code. *IEEE Transactions on Information Theory*, 19(2):244–246, 1973.

[22] R. G. Gallager. *Information Theory and Reliable Communication*. New York: Wiley, 1968.

[23] R. G. Gallager. A perspective on multiaccess channels. *IEEE Transactions on Information Theory*, 31(2):124 – 142, March 1985.

[24] T. Guess and M. K. Varanasi. Error exponents for maximum-likelihood and successive decoder for the gaussian cdma channel. *IEEE Transactions on Information Theory*, 46(4):1683 – 1691, July 2000.

[25] D. Gunduz and M. Payaró. Gaussian two-way relay channel with arbitrary outputs. In *Proc. of IEEE 21st International Symposium on Personal Indoor and Mobile Radio Communications (PIMRC)*, Istanbul, turkey, September 2010.

[26] D. Gunduz, E. Tuncel, and J. Nayak. Rate regions for the separated two-way relay channel. In *Proc. of the 46th Annual Allerton Conference on Communication, Control and Computing*, pages 1333–1340, Illinois, September 2008.

[27] F. He, Y. Sun, X. Chen, L. Xiao, and S. Zhou. Optimal power allocation for two way decode and forward OFDM relay networks. In *Proc. of IEEE International Conference on Communications (ICC)*, Ottawa, Canada, June 2012.

[28] C. K. Ho, R. Zhang, and Y.-C. Liang. Two-way relaying over OFDM: Optimized tone permutation and power allocation. In *Proc. of IEEE International Conference on Communications (ICC)*, Beijing, China, May 2008.

[29] Y.C. Huang, K.R. Narayanan, and T. Liu. Coding for parallel gaussian bidirectional relay channels: A deterministic approach. In *Proc of the 49th*

Annual Allerton Conference on Communication, Control, and Computing, IL, USA, September 2011.

[30] Y.C. Huang, N. E. Tunali, and K. R. Narayanan. On the exchange rate for bi-directional relaying over inter-symbol interference channels. In *Proc. of IEEE Global Communications Conference*, Houston, USA, December 2011.

[31] International Telecommunication Union. The world in 2013: ICT facts and figures, February 2013.

[32] Y.-U. Jang, E.-R. Jeong, and Y. H. Lee. A two-step approach to power allocation for OFDM signals over two-way amplify-and-forward relay. *IEEE Transactions on Signal Processing*, 58(4):2426–2430, April 2010.

[33] G. D. Forney Jr., M. D. Trott, and S. Y. Chung. Sphere-bound-achieving coset codes and multilevel coset codes. *IEEE Transactions on Information Theory*, 46(3):820–850, May 2000.

[34] S. Katti, S. Gollakota, and D. Katabi. Embracing wireless interference: Analog network coding. In *Proc. of ACM SIGCOMM'07*, Kyoto, Japan, August 2007.

[35] S. Katti, H. Rahul, W. Hu, D. Katabi, M. Médard, and J. Crowcroft. Xors in the air: practical wireless network coding. In *Proc. of ACM SIGCOMM*, volume 36, pages 243–254, 2006.

[36] S. J. Kim, N. Devroye, P. Mitran, and V. Tarokh. Comparison of bi-directional relaying protocols. In *Proc. of IEEE Sarnoff Symposium*, Princeton, NJ, April 2008.

[37] S. J. Kim, N. Devroye, P. Mitran, and V. Tarokh. Achievable rate regions and performance comparison of half duplex bi-directional relaying protocols. *IEEE Transactions on Information Theory*, 57(10):6405–6418, 2011.

[38] S. J. Kim, P. Mitran, and V. Tarokh. Performance bounds for bi-directional coded cooperation protocols. *IEEE Transactions on Information Theory*, 54(11):5235–5241, November 2008.

[39] R. Knopp. Two-way radio networks with a star topology. In *Proc. of International Zurich Seminar on Communications*, Zurich, February 2006.

[40] R. Knopp. Two-way wireless communication via a relay station. In *GDR-ISIS meeting*, Paris, France, March 2007.

[41] T. Koike-Akino, P. Popovski, and V. Tarokh. Denoising maps and constellations for wireless network coding in two-way relaying systems. In *Proc. of IEEE Global Communications Conference (GLOBECOM)*, pages 1–5, New Orleans, 2008.

[42] T. Koike-Akino, P. Popovski, and V. Tarokh. Optimized constellations for two-way wireless relaying with physical network coding. *IEEE Journal on Selected Areas in Communications*, 27(5):773–787, 2009.

[43] G. Kramer, M. Gastpar, and P. Gupta. Cooperative strategies and capacity theorems for relay networks. *IEEE Transactions on Information Theory*, 51:3037–3063, September 2005.

[44] G. Kramer and S. Shamai. Capacity for classes of broadcast channel with receiver side information. In *Proc. of IEEE Information Theory Workshop*, Lake Tahoe, Californi, September 2007.

[45] K. Lee and A. Yener. Iterative power allocation algorithms for amplify/estimate/compress-and-forward multiband relay channels. In *Proc. of Conference on Information Sciences and Systems (CISS)*, Princeton, NJ, USA, March 2006.

[46] H. Liao. A coding theorem for multiple-access communications. In *Proc. of International Symposium on Information Theory (ISIT)*, Asilomar, CA, 1972.

[47] S. H. Lim, Y-H. Kim, A. El Gamal, and S-Y. Chung. Noisy network coding. *IEEE Transactions on Information Theory*, 57(5):3132–3152, 2011.

[48] Y-S Liu and B. L Hughes. A new universal random coding bound for the multiple-access channel. *IEEE Transactions on Information Theory*, 42(2):376–386, 1996.

[49] D. S. Lun, M. Médard, T. Ho, and R. Koetter. Network coding with a cost criterion. In *Proc. of International Symposium on Information Theory and its Applications (ISITA)*, October 2004.

[50] I. Maric, A. Goldsmith, and M. Medard. Analog network coding in the high-snr regime. In *Proc. of IEEE Wireless Network Coding Conference (WiNC)*, pages 1–6, 2010.

[51] Mark J. Miller Mark D. Dankberg and Michael G. Mulligan. Self-interference cancellation for two-party relayed communication, jan 1997.

[52] W. Nam, S.-Y Chung, and Y. H. Lee. Capacity of the gaussian two-way relay channel to within $\frac{1}{2}$ bit. *IEEE Transactions on Information Theory*, 56(11):5488–5494, November 2010.

[53] J. Nayak, E. Tuncel, and D. Gunduz. Wyner-ziv coding over broadcast channels: Digital schemes. *IEEE Transactions on Information Theory*, 56(4):1782–1799, April 2010.

[54] B. Nazer and M. Gastpar. Compute-and-forward: Harnessing interference through structured codes. *IEEE Transactions on Information Theory*, 57(10):6463–6486, 2011.

[55] T. Oechtering, I. Bjelakovic, C. Schnurr, and H. Boche. Broadcast capacity region of two-phase bidirectional relaying. *IEEE Transactions on Information Theory*, 54(1):454–458, January 2008.

[56] T. J. Oechtering, C. Schnurr, I. Bjelakovic, and H. Boche. Achievable rate region of a two phase bidirectional relay channel. In *Proc. of Conference on Information Sciences and Systems (CISS)*, Baltimore, MD, mar 2007.

[57] J. Pokorny and H. Wallmeier. Random coding bound and codes produced by permutations for the multiple-access channel. *IEEE Transactions on Information Theory*, 31(6):741–750, 1985.

[58] G. Poltyrev. On coding without restrictions for the AWGN channel. *IEEE Transactions on Information Theory*, 40(52):409–417, March 1994.

[59] P. Popovski and H. Yomo. Physical network coding in two-way wireless relay channels. In *Proc. of IEEE International Conference on Communications (ICC)*, Glasgow, Scotland.

[60] P. Popovski and H. Yomo. The anti-packets can increase the achievable throughput of a wireless multi-hop network. In *Proc. of IEEE International Conference on Communications (ICC)*, pages 3885–3890, 2006.

[61] P. Popovski and H. Yomo. Wireless network coding by amplify-and-forward for bi-directional traffic flows. *IEEE Communications Letters*, 11(1):16–18, 2007.

[62] B. Rankov and A. Wittneben. Spectral efficient protocols for nonregenerative half-duplex relaying. In *Proc. of the 43rd Allerton Conference on Communication, Control and Computing*, October 2005.

[63] B. Rankov and A. Wittneben. Spectral efficient signaling for half-duplex relay channels. In *Proc. of Asilomar Conference on Signals, Systems and Computers (ACSSC)*, Asilomar, CA, November 2005.

[64] B. Rankov and A. Wittneben. Achievable rate regions for the two-way relay channel. In *Proc. of IEEE International Symposium on Information Theory*, Seattle, July 2006.

[65] C. Schnurr, T. J. Oechtering, and S. Stanczak. Achievable rates for the restricted half-duplex two-way relay channel. In *Proc. of the 41st Asilomar Conference on Signals, Systems and Computers (ACSSC)*, Asilomar, CA, November 2007.

[66] C. Schnurr, T. J. Oechtering, and S. Stanczak. On coding for the broadcast phase in the two-way relay channel. In *Proc. of Conference on Information Sciences and Systems (CISS)*, Baltimore, MD, March 2007.

[67] C. E. Shannon. Probability of error for optimal codes in a gaussian channel. *Bell System Technical Journal*, 38(3):611–656, 1959.

[68] C. E. Shannon. Two-way communication channel. In *Proc. of the 4th Berkeley Symposium on Math Stat. and Prob.*, volume 1, pages 611–644, 1961.

[69] C. E. Shannon, R. G. Gallager, and E. R. Berlekamp. Lower bounds to error probability for coding on discrete memoryless channels. *Information and Control*, 10(1):65–103, 1967.

[70] D. Slepian and J. K. Wolf. Noiseless coding of correlated information sources. *IEEE Transactions on Information Theory*, 19:471–480, July 1973.

[71] S. Smirani, M. Kamoun, and P. Duhamel. Physical network coding for TWR channel: Capacity region and error exponents. In *Proc. of IFIP Wireless Days (WD)*, Niagara Falls, Canada, October 2011.

[72] S. Smirani, M. Kamoun, M. Sarkiss, A. Zaidi, and P. Duhamel. Achievable rate regions for two-way relay channel using nested lattice coding. *IEEE Transactions on Wireless Communications*. Submitted for publication (2013).

[73] S. Smirani, M. Kamoun, M. Sarkiss, A. Zaidi, and P. Duhamel. Wyner-Ziv lattice coding for two-way relay channel. In *Proc. of International Conference on Advanced Technologies for Communications (ATC)*, Hanoi, Vietnam, October 2012.

[74] S. Smirani, M. Kamoun, M. Sarkiss, A. Zaidi, and P. Duhamel. Finite dimension nested lattices based wyner-ziv coding for two-way relay channel. In *Proc. of IEEE International Workshop on Signal Processing Advances for Wireless Communications (SPAWC)*, Darmstadt, Germany, 2013.

[75] S. Smirani, M. Kamoun, M. Sarkiss, A. Zaidi, and P. Duhamel. Lattice-based wyner-ziv coding for parallel gaussian two-way relay channels. In *Proc. of IEEE Wireless Communications and Networking Conf.(WCNC)*, pages 2405–2409, Shanghai, Japan, 2013.

[76] L. Song, G. Hong, B. Jiao, and M. Debbah. Joint relay selection and analog network coding using differential modulation in two-way relay channels. *IEEE Transactions on Vehicular Technology*, 59(6):2932–2939, 2010.

[77] Y. Song, N. Devroye, H-R Shao, and C. Ngo. Lattice coding for the two-way two-relay channel. In *IEEE Int. Symposium on Information Theory (ISIT)*, pages 1312–1316, 2013.

[78] Y. Tian, D. Wu, C. Yang, and An. F. Molisch. Asymmetric two-way relay with doubly nested lattice codes. *IEEE Transactions on Information Theory*, 11(2):694–702, February 2012.

[79] E. Tuncel. Slepian-wolf coding over broadcast channels. *IEEE Transactions on Information Theory*, 52(4):1469–1482, April 2006.

[80] H-M. Wang, X-G. Xia, and Q. Yin. A linear analog network coding for asynchronous two-way relay networks. *IEEE Transactions on Wireless Communications*, 9(12):3630–3637, 2010.

[81] M. P. Wilson, K. Narayanan, H. D. Pfister, and A. Sprintson. Joint physical layer coding and network coding for bidirectional relaying. *IEEE Transactions on Information Theory*, 56(11):5641–5654, November 2010.

[82] Y. Wu, P. A. Chou, and S.-Y. Kung. Information exchange in wireless networks with network coding and physical-layer broadcast. In *Proc. of Conference on Information Sciences and Systems (CISS)*, pages 16–18, March 2005.

[83] Y. Wu, P. A. Chou, and S.-Y. Kung. Minimum-energy multicast in mobile ad hoc networks using network coding. *IEEE Transactions on Communications*, 53(11):1906–1918, 2005.

[84] Y. Wu, P. A. Chou, Q. Zhang, K. Jain, W. Zhu, and S.-Y. Kung. Network planning in wireless ad hoc networks: a cross- layer approach. *IEEE Journal on Selected Areas in Communication*, January 2005.

[85] A. Wyner. The rate-distortion function for source coding with side information at the decoder-II: General sources. *Information and Control*, 38(1):60–80, July 1978.

[86] A. Wyner and J. Ziv. The rate-distortion function for source coding with side information at the decoder. *IEEE Transactions on Information Theory*, 22(1):1–10, January 1976.

[87] L. Xiao, T. E. Fuja, J. Kliewer, , and Jr. D. J. Costello. Nested codes with multiple interpretations. In *Proc. of Conference on Information Sciences and Systems (CISS)*, pages 1–5, Princeton, NJ, mar 2006.

[88] R. Zamir. Lattices are everywhere. In *Proc. of the 4th Annual Workshop on Information Theory and its Applications (ITA)*, La Jolla, CA, February 2009.

[89] R. Zamir and M. Feder. Information rates of pre/post-filtered dithered quantizers. *IEEE Transactions on Information Theory*, 42(4):1340–1353, September 1996.

[90] R. Zamir and M. Feder. On lattice quantization noise. *IEEE Transactions on Information Theory*, 42(4):1152–1159, July 1996.

[91] R. Zamir, S. Shamai, and U. Erez. Nested linear/lattice codes for structured multiterminal binning. *IEEE Transactions on Information Theory*, 48(6):1250 – 1276, June 2002.

[92] S. Zhang, S. Liew, and P. Lam. Hot topic: Physical layer network coding. In *Proc. of ACM MobiCom*, Los Angeles, USA, 2006.

[93] S. Zhang, S. C. Liew, and L. Lu. Physical layer network coding schemes over finite and infinite fields. In *Proc. of IEEE Global Communications Conference (GLOBECOM)*, New Orleans, Nov 2008.

Résumé des Travaux de la Thèse

Contexte

Au cours des dernières années, le codage réseau a été proposé comme une technique prometteuse qui permet d'améliorer la capacité du réseau [2, 18]. Il peut offrir aussi une meilleure robustesse contre les erreurs et donc une meilleure protection des données. En effet, dans les approches du routage classique, un routeur stocke les informations reçues et les transmet à ses nœuds voisins. Par contre, avec le codage réseau, le routeur peut traiter les données entrantes venant de multiples sources avant de les retransmettre. De cette manière, la quantité d'information transmise à travers le réseau peut être réduite et par conséquent le débit du réseau peut être augmenté.

La topologie réseau sans fil de base qui illustre l'avantage significatif du codage réseau par rapport au routage conventionnel est le canal bidirectionnel à relais [1] (TWRC) c.f. Fig. 7.1.

Dans les scénarios semi-duplex [2] où les nœuds ne peuvent pas transmettre et re-

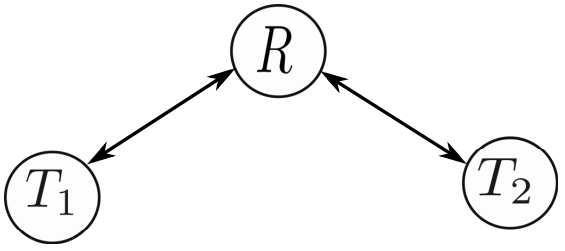

FIGURE 7.1: Canal bidirectionnel à relais

[1] Two-Way Relay Channel

cevoir au même temps, le routage classique nécessite quatre créneaux de transmission. Avec le codage réseau classique, chaque utilisateur transmet son information avec un accès multiple par répartition dans le temps [3]. Puis, le relais calcule le OU-exclusif (XOR) des deux paquets provenant des deux nœuds communicants avant de transmettre le message résultant au cours d'un troisième créneau. Récemment, il y a eu beaucoup d'efforts pour améliorer encore l'efficacité spectrale dans le TWRC. Dans [92], le codage réseau au niveau de la couche physique [4] (PNC) a été proposé où le codage réseau est effectué sur les signaux en bande de base. En particulier, avec PNC, les utilisateurs transmettent simultanément. Le relais décode directement à partir du signal reçu le XOR des paquets transmis qu'il diffuse ensuite au cours du deuxième créneau de temps. Par rapport au routage conventionnel et le codage réseau classique, PNC offre une amélioration significative de l'efficacité spectrale car il nécessite seulement deux temps de transmission.

Cette thèse traite le problème de la communication sur le TWRC. Pour ce problème, différentes stratégies de codage réseau ont été étudiées dans la littérature. Avec certaines stratégies, le relais décode le message de chaque utilisateur séparément, puis crée un nouveau message à partir des deux messages décodés. Avec d'autres, le relais reconstitue une fonction des deux messages directement à partir de la sortie du canal. Nous appelons ces stratégies techniques de codage réseau au niveau de la couche physique. Les schémas PNC profitent des propriétés de diffusion [5] et multi-accès [6] de la liaison radio qui sont considérés généralement comme des nuisibles interférences pour le système. Dans ces schémas, la transmission de bout-en-bout prend deux phases, à savoir une phase d'accès multiple (MAC) et d'une diffusion (BC) phase. Dans le premier intervalle de temps, les nœuds communicants envoient simultanément leurs messages au relais. Ensuite, le relais diffuse son nouveau message reconstruit à partir du mélange des signaux émis à partir de deux nœuds. Cette technique PNC offre une amélioration significative de l'efficacité spectrale par rapport au codage réseau classique appliqué

[2]half-duplex
[3]Time-Division Multiple Access
[4]Physical layer nework coding
[5]Brodcast
[6]Muti-access

au niveau de la couche réseau. Parmi les schémas PNC proposés pour le TWRC, certains ont une haute complexité mais des performances avantageuses tandis que d'autres schémas sacrifient la performance pour une faible complexité. La principale contribution de ce travail est de proposer des schémas PNC qui présentent un compromis entre performance et complexité.

Bibliographie: Schémas de codage réseau au niveau de la couche physique pour le TWRC

Considérant deux phases de transmission pour l'échange des messages dans le TWRC, différents schémas de codage PNC ont été proposés. Une stratégie PNC réfère au processus de calcul de l'information à diffuser par le relais lors de la phase BC sur la base des signaux reçus à partir des deux nœuds au cours de la phase MAC. Dans [92], les auteurs présentent une technique où les signaux en bande de base au relais sont mappés à l'XOR des messages binaires afin d'émuler le codage réseau classique. Une autre stratégie d'émulation de l'XOR a été proposée dans [60] en introduisant le schéma Denoise-and-Forward (DNF). Avec DNF, les relais convertit les signaux reçus en des symboles ou des mots code à partir d'une constellation discrète. Dans [59], une approche théorique a été considérée pour calculer une limite supérieure sur les débits atteignables [7] avec le schéma DNF employé au relais. Dans les références précitées, les signaux sont représentés par des corps finis. Dans [93], les auteurs classent les schémas PNC selon le corps du code réseau adopté: fini ou infini. Nous nous sommes intéressé à des schémas PNC sur le corps des réels. Nous décrivons dans la suite différents schémas PNC que nous regroupons en trois catégories de relayage:

[7] achievable

Décoder-et-Transmettre

Avec la stratégie Décoder-et-Transmettre [8] (DF), le relais décode conjointement les messages avant de les ré-encoder pour la transmission au cours de la phase BC. Ce protocole a été étendu du canal à relais classique [8, 43] au TWRC pour les nœuds semi-duplex dans [63] et dans [64] pour les cas du duplex intégral [9]. Dans ces travaux, le relais, après avoir décoder les deux messages, les ré-encode en utilisant le codage superposé. Dans [56, 55], une région des débits atteignables a été définie pour le TWRC avec la stratégie DF. La même région de débit atteignables a été déterminée de façon indépendante dans [39, 38] où les schémas de codage optimaux basés sur le codage réseau et des techniques de binning aléatoires ont ÃľtÃľ employés au relais après le décodage des deux messages. La région de débits atteingable avec DF est obtenue par l'union des capacités individuelles de les deux canaux à savoir MAC [1, 46] et BC avec informations adjacenbtes [79, 55].

Amplifier-et-Transmettre

Amplifier-et-Transmettre [10] (AF) est un protocole de transmission linéaire pour lequel le signal envoyé par le relais lors la phase BC est une version calibrée du signal reçu pendant la phase MAC. Le signal transmis par le relais est limité par sa contrainte de puissance d'émission. Sachant que les nœuds communicants T_1 et T_2 connaissent leurs propres signaux transmis, ils peuvent les soustraire avant le décodage. Pour le TWRC, ce protocole a été évaluée dans [63, 62, 64]. Le codage réseau analogique (ANC), introduit dans [34], est un schéma PNC basé sur la straégie AF qui fonctionne au niveau signal et représente une mise en œuvre plus simple par rapport au techniques basées sur DF. ANC a été étudié pour différentes modulations et réglages de canal dans de nombreuses références [76, 80, 19, 50].

[8] Decode-and-Forward
[9] full-duplex
[10] Amplify-and-Forward

Comprimer-et-Transmettre

Comprimer-et-Transmettre [11] (CF) a été proposé par Cover et El Gamal dans [8, Theorem 6]. C'est une stratégie de relayage où le relais envoie une version compressée et quantifié de son signal reçu vers la destination. La destination décode en combinant le signal reçu depuis le relais avec son propre signal reçu par le chemin direct avec la source. Le relais utilise le codage source Wyner-Ziv (WZ) [86] pour exploiter les informations adjacentes [12] à la destination. Ce protocole a été étendu pour le TWRC dans [64]. CF pour le TWRC a été largement étudié avec le codage aléatoire dans [64, 65, 36, 26]. Une région de débits atteignables a été dérivé dans [64]. Les débits atteignables dérivés dans [65, 36, 26] présentent que de légères différences liées à un paramètre de partage de temps. Dans [36], une région de débits atteignables pour CF avec codage aléatoire a été présenté en considérant l'optimisation du temps pour les deux phases de transmissions.

Pour le CF avec codage aléatoire, nous avons présenté une évaluation détaillée de la région des débits atteignables CF pour le cas gaussien. Cette évaluation n'a pas été considéré auparavant.

Contributions de la thèse

Dans cette partie, nous présentons un résumé des principaux résultats obtenus dans cette thèse. Nous proposons des schémas PNC pour le TWRC où la transmission de bout-en-bout se produit en deux créneaux horaires. Nous considérons l'optimisation de répartition dans le temps entre les deux phases de transmission, i.e. MAC et BC. Cela permet d'élargir les régions des débits atteignables obtenues tout au long de la thèse.

[11] Compress-and-Forward
[12] side information

Schéma DF avec dimensions finies pour le canal bidirectionnel à relais

Nous considérons la stratégie de relayage DF au relais. L'étude des régions des débits atteignables donne seulement le débit de transmission qui peut être réalisé en utilisant des mots de code de longueurs asymptotiquement grandes. Dans ce cas, il est supposé que les sources ont des données illimitées à envoyer afin d'avoir une erreur probabilité proche de zéro. Cependant, la probabilité d'erreur ne peut être évitée quand un bloc de longueur finie est utilisée. Une approche traditionnelle pour l'étude des taux d'erreur binaire dans un canal point-à-point est l'étude du compromis fiabilité-débit par la métrique de l'exposant d'erreur [22], qui est également connue comme la fonction de fiabilité d'un canal. Dans cette partie, nous considérons la simple extension de ce concept au TWRC. Nous étudions d'abord les probabilités d'erreur individuelles $P_{e,1}$ et $P_{e,2}$ à chaque nœud en fonction de la longueur des mots de code en utilisant la stratégie DF au relais. Ensuite, nous déterminons, pour une longueur de bloc fixe, la région des débits de transmission (R_{12}, R_{21}) lorsque les probabilités d'erreur dérivées sont contraintes. Ainsi, nous considérons le problème d'optimisation suivant pour chaque $\eta \in [0, 1]$:

$$\begin{aligned} \max_{0\leq\alpha\leq 1} \quad & \eta R_{12} + (1-\eta) R_{21} \\ \text{s.c.} \quad & (R_{12}, R_{21}) \in \mathcal{R}_{DF} \\ \text{et} \quad & P_{e,1} \leq c_1 \\ \text{et} \quad & P_{e,2} \leq c_2. \end{aligned} \tag{7.1}$$

où $\mathcal{R}_{DF}$ est la région des débits atteignables pour des mots de code de longueur infinie. c_1 et c_2 sont les deux objectifs fixes pour les probabilité d'erreur à chaque nœud.

Figure 7.2 montre la région asymptotique des débits atteignables (avec des mots de code de taille infinie) et la région des débits de transmission maximum avec des probabilités d'erreur limitées par $c_i = 10^{-6}, i \in \{1, 2\}$ et une taille de bloc $n = 500$. Nous considérons des canaux asymétriques entre le relais et chaque nœud où le rapport signal-à-bruit $RSB_2 = \delta RSB_1$. Nous constatons l'impact de l'asymétrie

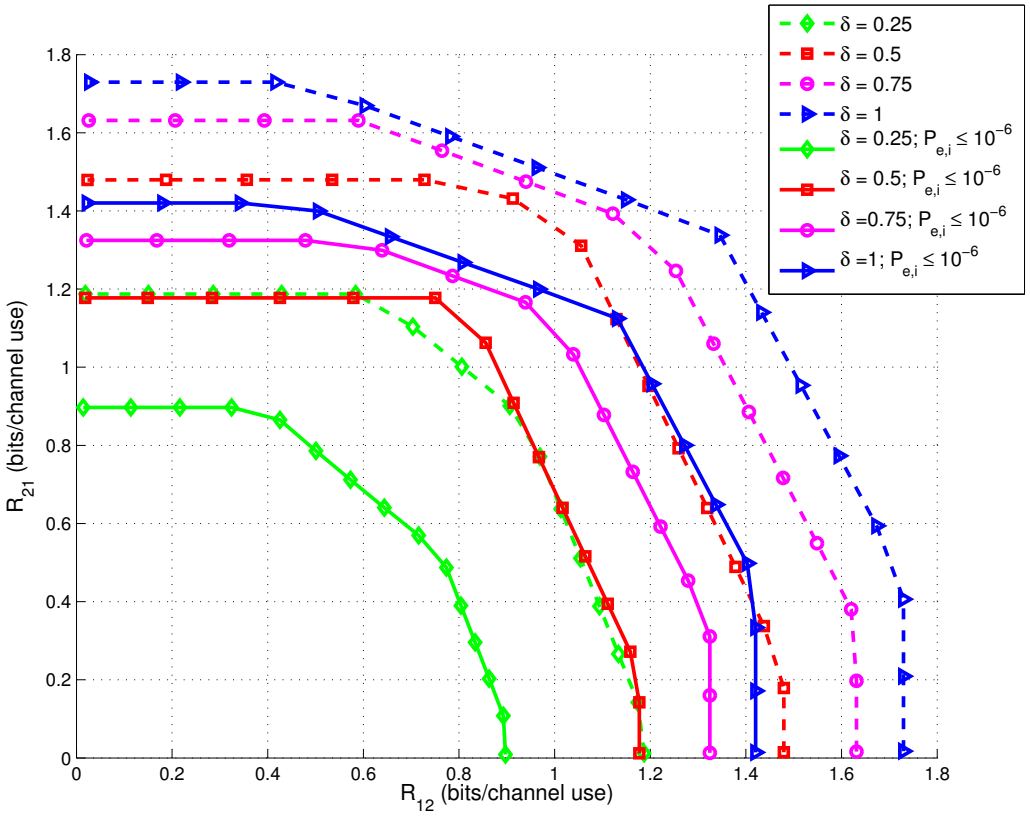

FIGURE 7.2: Régions de débits atteignables maximums pour $P_{e,1}, P_{e,2} \leq 10^{-6}$, n = 500, RSB_1 = 10dB, $\text{RSB}_2 = \delta\ \text{RSB}_1$.

du canal sur les débits de transmission ainsi que le rétrécissement de la région des débits en fonction de la taille de bloc. Nous représentons dans la figure 7.3, deux approches pour l'allocation de la puissance dans les nœuds: fixe et optimale, où la taille de bloc est fixé à 500. Un gain de 30% est constaté par une optimisation de la distribution de la puissance par rapport à une allocation fixe.

Schémas CF pour le canal bidirectionnel à relais

Dans cette partie, nous considérons la stratégie de relayage CF au niveau du relais. Nous dérivons deux régions de débits atteignables pour le TWRC où les schémas PNC proposés sont basés sur le codage en réseau de points [13]. Le relais considère son signal reçu des deux nœuds comme une source à comprimer. Ainsi , il utilise un codage Wyner-Ziv en tenant en compte que chaque nœud a une connaissance

[13]Lattice coding

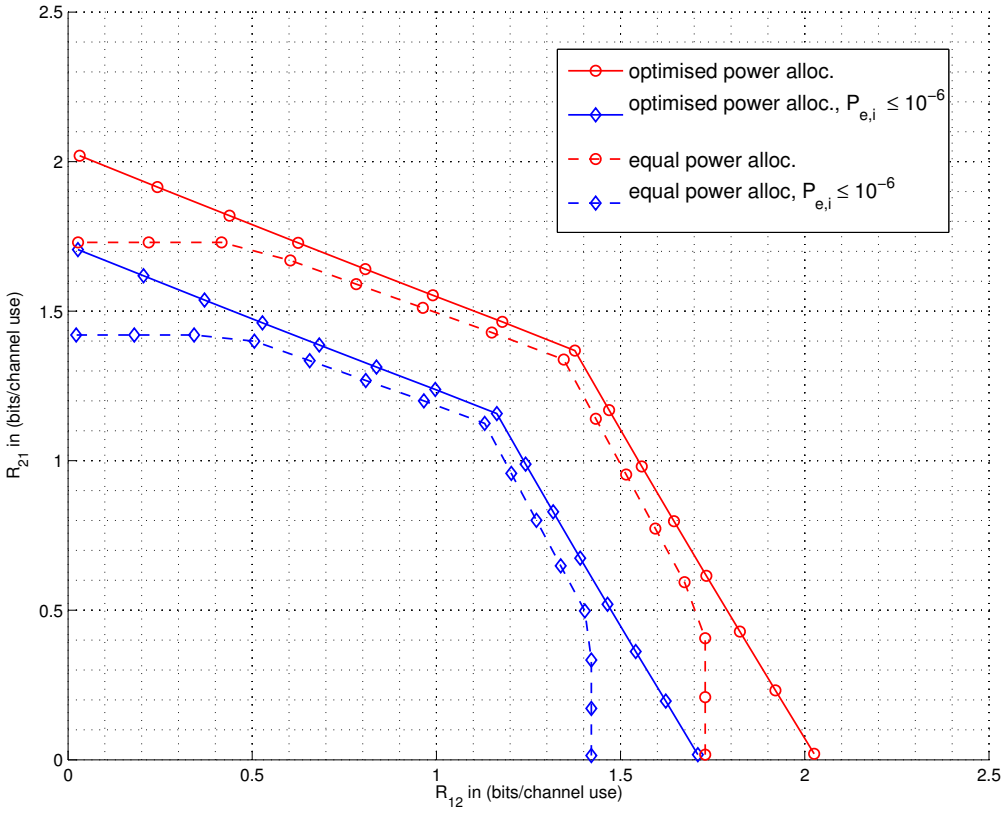

FIGURE 7.3: Région de débits atteignables maximums pour une allocation de puissance fixe et optimisée, RSB = 15 dB, n= 500.

partielle de cette source, appelée information adjacente, qui n'est autre que son propre signal qui a été transmis au cours de la première phase. Dans le premier schéma, le relais diffuse le même signal pour les deux nœuds. La région des débits atteignables pour ce schéma est donnée par le théorème suivant:

Théorème 4.1. *Pour un canal bidirectionnel gaussien à relais, l'enveloppe con-*

vexe des débits de bout-en-bout suivants (R_{12}, R_{21}) *est atteignable:*

$$R_{12} \leq \frac{\alpha}{2}\log_2\left(1+\frac{|h_1|^2P_1}{\sigma_R^2+\frac{|h_1|^2P_1+\sigma_R^2}{\left(1+\min\limits_{i\in\{1,2\}}\frac{|h_i|^2P_R}{\sigma_i^2}\right)^{\frac{1-\alpha}{\alpha}}-1}}\right) \tag{7.2}$$

$$R_{21} \leq \frac{\alpha}{2}\log_2\left(1+\frac{|h_2|^2P_2}{\sigma_R^2+\frac{|h_1|^2P_1+\sigma_R^2}{\left(1+\min\limits_{i\in\{1,2\}}\frac{|h_i|^2P_R}{\sigma_i^2}\right)^{\frac{1-\alpha}{\alpha}}-1}}\right) \tag{7.3}$$

pour $\alpha \in [0,1]$.

avec P_i et h_i, $i \in \{1,2\}$, représentent respectivement la puissance de transmission et le gain de canal au niveau du nœud T_i. P_R est la puissance de transmission au relais. α est le coefficient de division de temps entre les phases de transmission MAC et BC.

Nous montrons que ce schéma offre les mêmes performances que le protocole CF avec codage. Ensuite, nous proposons, et analysons la performance d'un schéma de codage amélioré où le relais envoie non seulement une information commune de son sortie de canal, mais aussi une information individuelle qui ne peut être décodée que par l'utilisateur qui a les meilleures conditions de canal et la meilleure puissance de transmission. La région des débits atteignables par ce schéma est donnée par le théorème suivant:

Théorème 4.2. *Pour un canal bidirectionnel gaussien à relais, l'enveloppe con-*

vexe des débits de bout-en-bout suivants (R_{12}, R_{21}) *est atteignable:*

$$R_{12} \leq \frac{\alpha}{2}\log_2\left(1+\frac{|h_1|^2P_1}{\sigma_R^2+\frac{|h_1|^2P_1+\sigma_R^2}{\left(1+\frac{\nu|h_2|^2P_R}{(1-\nu)|h_2|^2P_R+\sigma_2^2}\right)^{\frac{1-\alpha}{\alpha}}-1}}\right) \tag{7.4}$$

$$R_{21} \leq \frac{\alpha}{2}\log_2\left(1+\frac{|h_2|^2P_2}{\sigma_R^2+\frac{|h_1|^2P_1+\sigma_R^2}{\left(1+\frac{(1-\nu)|h_1|^2P_R}{\sigma_1^2}\right)^{\frac{1-\alpha}{\alpha}}\left[\left(1+\frac{\nu|h_2|^2P_R}{(1-\nu)|h_2|^2P_R+\sigma_2^2}\right)^{\frac{1-\alpha}{\alpha}}-1\right]}}\right) \tag{7.5}$$

pour $\alpha, \nu \in [0, 1]$.

Avec des simulations, nous montrons que le nouveau schéma fournit des gains substantiels qui arrivent jusqu'à 100% par rapport à la région les débits atteignables par le premier schéma pour un régime de RSB moyen et des canaux asymétriques. Il surpasse également la stratégie AF dans tous les régimes de RSB, et DF stratégie pour certains régimes de RSB. Figure 7.4, illustre cet avantage où LCF1 réfère le premier schéma basique et LCF2 le deuxième schéma amélioré.

Schéma CF avec dimensions finies pour le canal bidirectionnel à relais

Dans la partie précédente, des réseaux de points de taille infinie ont été utilisé pour garantir une probabilité d'erreur proche de zéro. Dans cette partie, nous nous intéressons aux réseaux de points de taille finie. Dans ce cas, la probabilité d'erreur de décodage ne peut pas être arbitrairement faible. Partant de ce constat, nous étudions le schéma de codage CF en réseau de points imbriqués proposé avec des réseaux de points de dimension finie. En particulier, nous nous focalisons, dans ce travail, sur le problème de transmission analogique où la distorsion au niveau

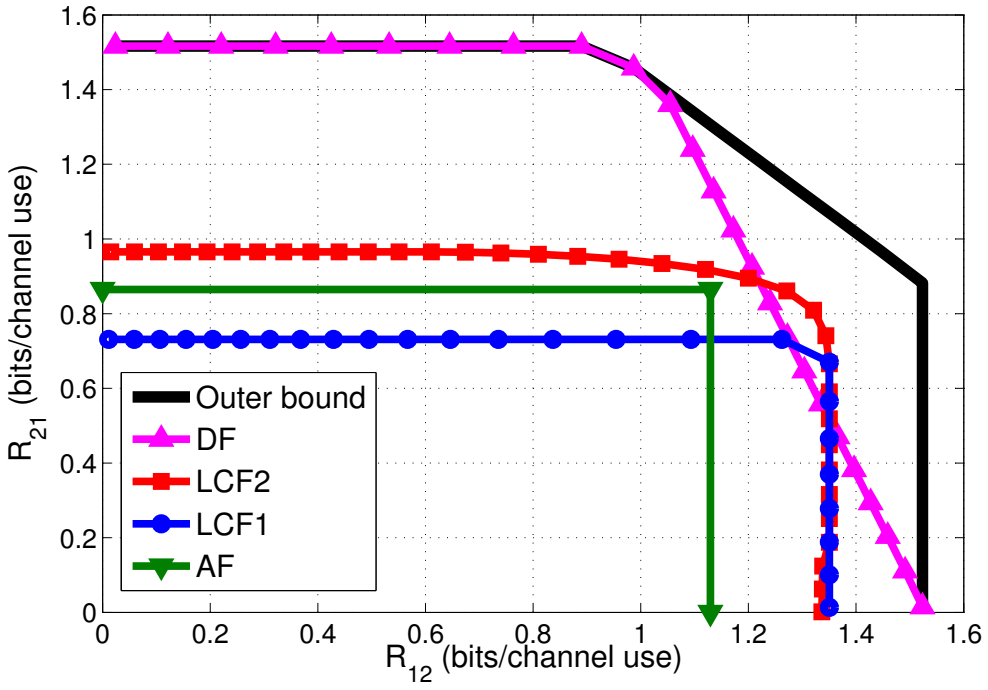

FIGURE 7.4: Régions de débits atteignables de DF, AF, LCF1 et LCF2 pour $\mathrm{P}_1 = 20$ dB, $\mathrm{P}_2 = 18$ dB, $\mathrm{P}_R = 17$ dB, $|h_1|^2 = 4$, $|h_2|^2 = 0.5$

des nœuds de réception est optimisée. La distorsion D_i est définie par:

$$D_i = \frac{1}{n_1}\mathbb{E}\|\mathbf{Y}_R - \hat{\mathbf{Y}}_{Ri}\|^2 \ ; \ i \in \{1,2\}, \tag{7.6}$$

où $\mathbf{Y}_R$ est le signal reçu au relais et $\hat{\mathbf{Y}}_{Ri}$ est le signal reconstitué au niveau de chaque nœud T_i, $i \in \{1,2\}$.

En effet, en choisissant avec soin les facteurs de codage de source, les résultats correspondent au le canal optimal de test avant avec une distorsion minimale. Nous caractérisons les régions des débits de transmission permis par notre système de codage sous des probabilités d'erreur de décodage contraintes. La région des débits est donnée par le théorème suivant:

Théorème 5.1. *Soit (Λ_1, Λ_2), un pair de deux réseaux de points imbriqués de dimension n_1, avec $\Lambda_2 \subset \Lambda_1$. Pour un TWRC Gaussien, l'enveloppe convexe des des débits de bout-en-bout (R_{12}, R_{21}) vérifiant les inégalités suivantes est at-*

teignable.

$$R_{12} \leq \frac{\alpha}{2}\log_2\left(1+\frac{|h_1|^2P_1}{\sigma_R^2+\frac{|h_1|^2P_1+\sigma_R^2}{\left(1+\min\limits_{i\in\{1,2\}}\frac{|h_i|^2P_R}{\sigma_i^2}\right)^{\frac{1-\alpha}{\alpha}}-G(\Lambda_1)\mu(\Lambda_2)}}\right) \tag{7.7}$$

$$R_{21} \leq \frac{\alpha}{2}\log_2\left(1+\frac{|h_2|^2P_2}{\sigma_R^2+\frac{|h_1|^2P_1+\sigma_R^2}{\left(1+\min\limits_{i\in\{1,2\}}\frac{|h_i|^2P_R}{\sigma_i^2}\right)^{\frac{1-\alpha}{\alpha}}-G(\Lambda_1)\mu(\Lambda_2)}}\right) \tag{7.8}$$

où $G(\Lambda_1)$ *est le second moment normalisé de* Λ_1, $\mu(\Lambda_2)$ *est le rapport volume sur bruit de* Λ_2 *[88], et* $\alpha \in [0,1]$.

Après la démonstration de ce théorème, nous discutons les critères de conception du schéma proposé avec des réseaux de points pratique de taille finie.
Sans perte de généralité, nous considérons T_2 l'utilisateur qui a l'information adjacente la plus faible. La région des débits présentée est calculée en supposant que la probabilité d'erreur vérifie

$$Pr(\beta\mathbf{U}_2+\mathbf{E}_q notin\mathcal{V}_2) \leq P_e \tag{7.9}$$

avec $\mathbf{U}_2$ représente l'information inconnue au niveau au terminal T_2, $\mathbf{E}_q$ est l'erreur de quantification et P_e est la probabilité d'erreur maximale fixée.
La dérivation analytique de la probabilité d'erreur pour des réseaux de points pratiques est en général difficile car elle nécessite l'intégration sur la région de Voronoi du réseau de points extérieur. Toutefois, elle peut être calculée numériquement en utilisant Monte Carlo ou l'intégration approchée par une borne supérieure.

En outre, étant donné que la probabilité d'erreur du système est défini par la qualité du réseau de poins extérieur, la performance du système de bout-en-bout dépend plus de ce réseau de points plutôt que le choix de réseau de point intérieur.

Par conséquent, le réseau cubique simple $\mathbb{Z}^{n_1}$ avec le second moment normalisé (NSM) $G(\lambda_1) = \frac{1}{12}$ aura le choix préféré pour le réseau de points intérieur (ou fin). Dans ce cas, pour un bon réseau de points extérieur avec NSM $G(\Lambda_2) = \frac{1}{2\pi e}$, la perte de vitesse par rapport au régime WZ idéal est seulement $\frac{1}{2}\log_2(2\pi E/12) = 0,2546$ bits par dimension. En fait, dans le problème de la quantification, le choix du réseau de points intérieur (resp. supérieur) est équivalent au choix du réseau de points extérieur (resp. inérieur) pour le problème dual de codage canal. Il a été montré dans [33] que pratiquement $\mathbb{Z}^{n_1}$ suffit comme un réseau de points extérieur qui vérifie une probabilité d'erreur arbitrairement petite. Ainsi, un sous-réseau de $\mathbb{Z}^{n_1}$ peut être un choix technique simple pour le réseau de points intérieur. Ainsi nous avons considéré dans nos simulations, Λ_1, le réseau de points intérieur, un sous-réseau de $\mathbb{Z}_1^n$ i.e. $\Lambda_1 = \eta\mathbb{Z}^{n_1}$. Dans ce cas, l'équation (7.10) donne une approximation de la probabilité d'erreur en la borne d'union et la borne de Chernoff:

$$\Pr(\beta\mathbf{U}_2 + \mathbf{E}_q \notin \mathcal{V}_2) \approx K(\Lambda_2)\exp\left(-\frac{1}{8}\gamma_c(\Lambda_2)\mu(\Lambda_2, P_e)\right) \tag{7.10}$$

pour $\mu(\Lambda_2, P_e)$ suffisamment large. $\gamma_c(\Lambda_2) = \dfrac{d_{min}^2(\Lambda_2)}{V(\Lambda_2)^{2/n_1}}$ est le gain de codage de Λ_2 avec $d_{min}(\Lambda_2)$ est la distance minimale entre deux points dans Λ_2. $K(\Lambda_2)$ est le kissing number du lattice Λ_2.

Cette approximation de la probabilité d'erreur permet d'approximer le rapport volume sur bruit de Λ_2, $\mu(\Lambda_2)$, utilisé dans la dé finition des régions de dé bits réalisables dans (7.7) et (7.8). Enfin, nous illustrons nos résultats avec des exemples de réseaux de points de taille finie pratiques.

Schéma CF pour Le canal bidirectionnel à canaux parallèles

Dans ce chapitre, nous examinons notre schéma de codage CF avec des réseaux de points pour des scénarios pratiques rencontrés dans les systèmes modernes tels que les systèmes multi-porteuses, la transmission multi-flux avec plusieurs antennes, étalement de spectre avec des séquences multiples. Dans ce cas, le canal peut être

modélisé par des sous canaux gaussiens parallèles. Pour ces systèmes, le relayage bidirectionnel offre une solution compétitive pour l'extension de la portée de communication. Ainsi, nous considérons, dans cette partie, le TWRC à canaux parallèles où les nœuds communicants échangent leur messages a travers des canaux gaussiens parallèles indépendants. Le relais traite conjointement tous les sous-canaux en même temps. Nous caractérisons la région des débits atteignables par ce schéma de codage.

Théorème 6.1. *Pour un canal gaussien bidirectionnel parallèle à relais, l'enveloppe convexe des débits de bout-en-bout* (R_{12}, R_{21}) *vérifiant les inégalités suivantes est atteignable:*

$$R_{12} \leq \frac{\alpha}{2}\sum_{k=1}^{K}\log_2\left(1+\frac{|h_{1,k}|^2P_{1,k}}{\sigma_{R,k}^2+\frac{\max\limits_{i\in\{1,2\}}\sum\limits_{k=1}^{K}|h_{i,k}|^2P_{i,k}+\sigma_{R,k}^2}{\min\limits_{i\in\{1,2\}}\prod\limits_{k=1}^{K}\left(1+\frac{|h_{i,k}|^2P_{R,k}}{\sigma_{i,k}^2}\right)^{\frac{1-\alpha}{\alpha}}-1}}\right) \tag{7.11}$$

$$R_{21} \leq \frac{\alpha}{2}\sum_{k=1}^{K}\log_2\left(1+\frac{|h_{2,k}|^2P_{2,k}}{\sigma_{R,k}^2+\frac{\max\limits_{i\in\{1,2\}}\sum\limits_{k=1}^{K}|h_{i,k}|^2P_{i,k}+\sigma_{R,k}^2}{\min\limits_{i\in\{1,2\}}\prod\limits_{k=1}^{K}\left(1+\frac{|h_{i,k}|^2P_{R,k}}{\sigma_{i,k}^2}\right)^{\frac{1-\alpha}{\alpha}}-1}}\right) \tag{7.12}$$

avec $\alpha \in [0,1]$.

K est le nombre des sous-canaux parallèles. $P_{i,k}$, $h_{i,k}$, $i \in \{1,2\}$, représentent respectivement la puissance de transmission et le gain de canal au niveau du nœud

T_i sur le sous-canal k. $P_{R,k}$ est la puissance de transmission au relais sur le sous-canal k. $\sigma_{j,k}$, $j \in \{1,2,R\}$ est la variance du bruit gaussien sur le sous-canal k. Après la démonstration de ce théorème, nous comparons ensuite le schéma proposé avec "une approche de traitement distinct sous-canal par sous-canal" qui est le prolongement direct du schéma CF avec codage en réseaux de points où la même stratégie est répétée pour chaque sous-canal. La région de dé bits atteignables de ce schéma est donnée par le théorème suivant:

Théorème 6.2. *Pour un canal gaussien bidirectionnel parallèle à relais, l'enveloppe convexe des débits de bout-en-bout* (R_{12}, R_{21}) *vérifiant les inégalités suivantes est atteignable:*

$$R_{12} \leq \frac{\alpha}{2}\sum_{k=1}^{K}\log_2\left(1+\frac{|h_{1,k}|^2P_{1,k}}{\sigma_{R,k}^2+\frac{\max\limits_{i\in\{1,2\}}|h_{i,k}|^2P_{i,k}+\sigma_{R,k}^2}{\min\limits_{i\in\{1,2\}}\left(1+\frac{|h_{i,k}|^2P_{R,k}}{\sigma_{i,k}^2}\right)^{\frac{1-\alpha}{\alpha}}-1}}\right) \tag{7.13}$$

$$R_{21} \leq \frac{\alpha}{2}\sum_{k=1}^{K}\log_2\left(1+\frac{|h_{2,k}|^2P_{2,k}}{\sigma_{R,k}^2+\frac{\max\limits_{i\in\{1,2\}}|h_{i,k}|^2P_{i,k}+\sigma_{R,k}^2}{\min\limits_{i\in\{1,2\}}\left(1+\frac{|h_{i,k}|^2P_{R,k}}{\sigma_{i,k}^2}\right)^{\frac{1-\alpha}{\alpha}}-1}}\right) \tag{7.14}$$

pour $\alpha \in [0,1]$.

Enfin, nous évaluons à travers des illustrations numériques la performance des deux approches: traitement sous-canal par sous canal et traitement conjoint des sous-canaux. Nous montrons que que le schéma de traitement conjoint permet de réaliser des débits proches du schéma de traitement séparé sur chaque sous-canal comme le montre la figure 7.5. En plus, le schéma proposé basé sur le traitement

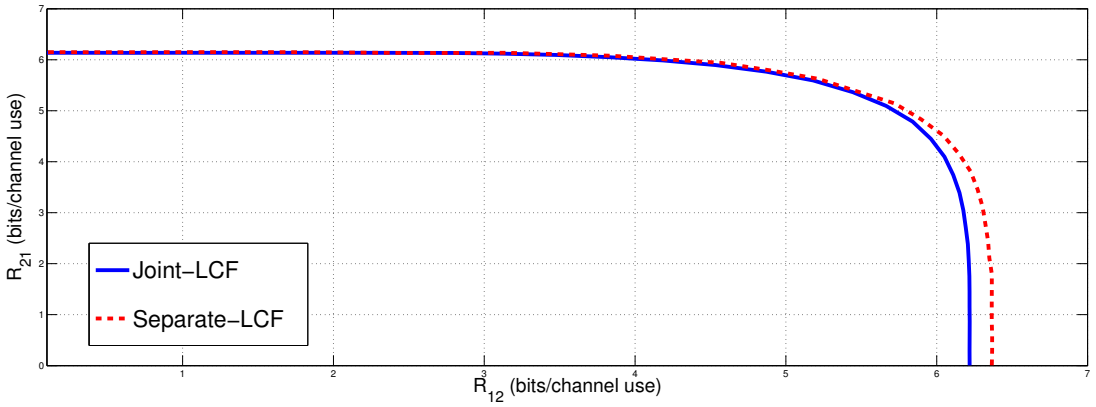

FIGURE 7.5: Régions des débits atteignables pour Joint-LCF and Separate-LCF pour des puissances é gales, $P_1 = P_2 = P_R = 10$ dB

conjoint des signaux reçus de tous les sous-canaux a une complexité réduite par rapport au deuxième schéma basé sur le traitement séparé des sous-canaux. Le relais effectue quatre opérations avec Joint-LCF par contre un total de 4K opérations sont effetuées avec Separate-LCF.

Conclusion et Travaux Futurs

Une meilleure efficacité spectrale représente l'amélioration de la performance clé qui peut être atteinte à travers le codage réseau au niveau de la couche physique (PNC) dans les réseaux coopératifs sans fil. Cette thèse fournit une analyse et une conception de schémas PNC qui permettent d'atteindre de nouveaux débits de transmission pour le canal bidirectionnel à relais (TWRC).

A travers toutes nos études, nous avons considéré un connaissance parfaite de l'état du canal [14] (CSI) au niveau de tous les nœuds. Cependant, nous avons présenté dans le chapitre 4 des réflexions sur la relaxation de cette connaissance parfaite qui permet de s'approcher aux scÁĺnarios plus pratiques pour les schémas de codage proposés. Ces réflexions peuvent être étendues pour étudier en détail le CSI pour les schémas proposés . L'allocation des ressources adaptative peut être aussi prolongée dans la conception des schémas.

[14]Channel State Informaion

Nous avons étudié également le problème de la transmission analogique pour des réseaux de dimension finie uniquement dans le cas d'une seule couche de compression où le relais diffuse un message comprimé commun aux deux nœuds. Cette étude peut être prolongée pour le schéma à deux couches où le relais génère avec la couche commune autre couche de raffinement adressée au meilleur utilisateur. Bien que nos systèmes sont basés sur des codes structurés qui ont une faible complexité par rapport au codage aléatoire, dans ces schémas, les mots de code en réseaux de points sont utilisés uniquement au relais pendant que des mots de code gaussiens sont utilisés dans les deux nœuds communicants. Une extension intéressante de ce travail serait de considérer les codes de réseaux à points dans tous les nœuds ce qui peut être plus approprié pour des systèmes pratiques. Par ailleurs, ce ci nécessite une modification de la construction des livre des codes [15].

Dans ce travail, nous avons examiné le modèle TWRC. Ce canal peut être appliqué pour des réseaux cellulaires, ad-hoc ou hybrides afin d'améliorer la couverture sans fil et augmenter le débit total. Il peut également être intégré dans l'architecture d'un réseau sans fil maillé. Ainsi, une communication bidirectionnelle par l'intermédiaire d'un relais dans un réseau avec plus de deux utilisateurs peut ouvrir de nouvelles possibilités pour des études ultérieures. Pour une mise en œuvre pratique, il faut faire face à de nombreux problèmes.

[15] codebook